

Development of a shoulder musculoskeletal model to assess
the impact of scapular morphology on glenohumeral
biomechanics

by

Marta STRZELCZAK

MANUSCRIPT-BASED THESIS PRESENTED TO ÉCOLE DE
TECHNOLOGIE SUPÉRIEURE IN PARTIAL FULFILLMENT OF THE
REQUIREMENTS FOR THE DEGREE OF DOCTOR OF PHILOSOPHY
PH. D.

MONTREAL, 30 JULY, 2021

ÉCOLE DE TECHNOLOGIE SUPÉRIEURE
UNIVERSITÉ DU QUÉBEC



Marta Strzelczak, 2021



This Creative Commons license allows readers to download this work and share it with others as long as the author is credited. The content of this work can't be modified in any way or used commercially.

BOARD OF EXAMINERS (THESIS PH.D.)
THIS THESIS HAS BEEN EVALUATED
BY THE FOLLOWING BOARD OF EXAMINERS

Mrs. Nicola Hagemeister, Thesis Supervisor
Department of system engineering at École de technologie supérieure

Mr. Mickael Begon, Thesis Co-supervisor
Department of kinesiology and Exercise Science and Institute of biomedical engineering,
Faculty of Medicine at University of Montreal

Mrs. Lauranne Sins, Thesis Co-supervisor
CAE

Mr. Yvan Petit, President of the Board of Examiners
Department of mechanical engineering at École de technologie supérieure

Mr. Rachid Aissaoui, Member of the jury
Department of system engineering at École de technologie supérieure

Mr. Alexandre Terrier, External Evaluator
École Polytechnique Fédérale de Lausanne

THIS THESIS WAS PRESENTED AND DEFENDED
IN THE PRESENCE OF A BOARD OF EXAMINERS AND PUBLIC

JULY 12, 2021

AT ÉCOLE DE TECHNOLOGIE SUPÉRIEURE

ACKNOWLEDGMENT

Foremost, I would like to express my appreciation and thanks to my supervisors Prof. Nicola Hagemester, Prof. Mickael Begon and Lauranne Sins for continuous support, motivation and encouragement. Accomplishing all of this would not have been possible without the assistance and feedback from you. Thank you for believing in me.

My big thanks goes to AnyBody Research Group and Anybody Technology, Aalborg, Denmark, for great support and warm welcome during my research stays.

I would also like to thank all the professors, students and staff at Laboratoire de recherche en imagerie et orthopédie (LIO). Thank you for creating such a great place for research and collaborative work. Working in such a place was a real pleasure.

I would like to thank my parents for the support. Without you, this adventure would not have been possible.

Very special thanks to Maxime. Thank you for your presence and patience.

This thesis is dedicated to Antonina and Helena.

DÉVELOPPEMENT D'UN MODÈLE MUSCULOSQUELETTIQUE DE L'ÉPAULE POUR ÉVALUER L'IMPACT DE LA MORPHOLOGIE SCAPULAIRE SUR LA BIOMÉCANIQUE GLÉNO-HUMÉRALE

Marta STRZELCZAK

RÉSUMÉ

De nombreuses théories, qui visent à expliquer les pathomécanismes des troubles de l'articulation glénohumérale, se concentrent sur la morphologie défavorable de la scapula. Les méthodes *in silico*, telles que la modélisation musculo-squelettique, permettent de mieux comprendre le pathomécanisme sous-jacent. Les méthodes *in silico* ne nécessitent pas de procédures invasives et de spécimens cadavériques coûteux. Cependant, avant d'appliquer le modèle à un problème de recherche, le chercheur doit s'assurer que le modèle est capable de donner la bonne réponse. Le but de cette thèse de doctorat était donc dans une première phase de trouver et d'évaluer une approche pour l'enveloppement du muscle deltoïde, qui représente le comportement physiologique dans toute la gamme des mouvements de l'articulation glénohumérale. Le but de la deuxième phase est d'évaluer les variabilités de la mesure morphologique, appelée angle critique de l'épaule (CSA), sur la biomécanique de l'articulation glénohumérale après NC-TSA et un descellement potentiel du composant glénoïdien.

Dans la première phase, l'avancée dans le développement du modèle musculo-squelettique à grande échelle d'arthroplastie totale de l'épaule non conforme a été démontrée. Une amélioration a été apportée à la représentation géométrique du muscle deltoïde. Deux approches distantes ont été proposées et évaluées, à savoir le modèle à maillage 2D et le modèle d'enveloppement multi ellipsoïde. Les modifications permettent d'étudier l'impact de la morphologie de la scapula sur la biomécanique de l'articulation glénohumérale.

La deuxième phase démontre la faisabilité du modèle ci-dessus à utiliser en application clinique. L'étude présentée visait à évaluer l'impact des variabilités morphologiques de l'omoplate, et plus particulièrement du paramètre morphologique appelé angle critique de l'épaule (eng. critical shoulder angle), comme facteur de risque potentiel de descellement de la composante glénoïdienne.

DEVELOPMENT OF A SHOULDER MUSCULOSKELETAL MODEL TO ASSESS THE IMPACT OF SCAPULAR MORPHOLOGY ON GLENOHUMERAL BIOMECHANICS

Marta STRZELCZAK

ABSTRACT

Many theories, which aim to explain pathomechanisms of glenohumeral joint disorders, focus on unfavorable scapula morphology. *In silico* methods, such as musculoskeletal modeling, give an opportunity to better understand underlying pathomechanism. *In silico* methods do not require invasive procedures and expensive cadaveric specimens. However, before applying the model to a research problem, the researcher must ensure that the model is able to give the correct answer. The purpose of this doctoral thesis was hence in the first phase to find and evaluate an approach for the deltoid muscle wrapping, which represents physiological behavior in full-range of GHJ motion. The purpose of the second phase is to assess the variability of the morphological measurement called the critical shoulder angle (CSA) on the biomechanics of the glenohumeral joint after NC-TSA and potential glenoid component loosening.

In the first phase, the advancement in the development of the large-scale musculoskeletal model of NC total shoulder arthroplasty was demonstrated. Improvement was made in the geometrical representation of the deltoid muscle. Two distanced approaches had been proposed and evaluated, namely *2D-mesh model* and *multi-ellipsoid wrapping model*. The changes allows to study the impact of the scapula morphology on the glenohumeral joint biomechanics

The second phase demonstrates the feasibility of the above model to be used in clinical application. The presented study aimed to evaluate the impact of the morphological variability of the scapula, and more specifically the morphological parameter called the critical shoulder angle, as a potential risk factor in glenoid component loosening.

TABLE OF CONTENTS

	Page
ACKNOWLEDGMENT.....	V
INTRODUCTION	1
CHAPTER 1 LITERATURE REVIEW	3
1.1 Anatomy and physiology of shoulder complex	3
1.1.1 Shoulder complex	3
1.1.2 Static and dynamic stabilizers of glenohumeral joint	5
1.1.3 The deltoid muscle	6
1.1.4 Glenohumeral joint arthritis and total shoulder arthroplasty	7
1.1.5 Scapula morphology	8
1.1.6 Acromion Index	10
1.1.7 Glenoid Inclination	11
1.1.8 Critical Shoulder Angle	11
1.2 Biomechanical modelling of shoulder complex	15
1.2.1 Forward vs Inverse Dynamics	16
1.2.2 Mechanical elements and model kinematics.....	17
1.2.3 Muscle Modeling	18
1.2.4 Stability constraint	22
1.2.5 Musculoskeletal models for NC total shoulder arthroplasty context.....	23
1.2.6 Model validation	25
1.3 Biomechanical impact of shoulder morphology	29
1.3.1 Shoulder simulators	29
1.3.2 Numerical models	30
CHAPTER 2 AIMS AND OUTLINE OF THE THESIS.....	35
2.1 Clinical problem.....	35
2.2 Technical problem	35
2.3 Objectives	36
CHAPTER 3 AN INNOVATIVE 2D-MESH MODEL TO IMPROVE DELTOID MOMENT ARMS, MUSCLE FORCES AND GLENOHUMERAL JOINT REACTION FORCE ESTIMATIONS.....	39
3.1 Abstract	39
3.2 Introduction.....	40
3.3 Methods.....	41
3.4 Results.....	44
3.4.1 Visual analysis of deltoid muscle shape in the scapular plane elevation..	44
3.4.2 Deltoid moment arms estimation and activation patterns.....	45
3.4.3 Contribution of all shoulder muscles to glenohumeral joint moments	46
3.4.4 Contribution of muscle forces and resultant GH-JRF.....	47

3.5	Discussion.....	48
3.6	Conclusion	51
CHAPTER 4 A WRAPPING APPROACH FOR THE DELTOID MUSCLE IN SPRING – BASED MULTIBODY MUSCULOSKELETAL MODELS		
4.1	Abstract.....	53
4.2	Introduction.....	54
4.3	Methods.....	56
	4.3.1 Original model	56
	4.3.2 Multi-Ellipsoid Model	56
	4.3.3 Simulated Movements	58
4.4	Results.....	58
	4.4.1 Muscle Moment Arms	59
	4.4.2 Muscle contributions to net joint moments.....	61
	4.4.3 Muscle Contribution to Glenohumeral Joint Reaction Force	64
4.5	Discussion.....	65
	4.5.1 Anterior Deltoid Moment Arms.....	66
	4.5.2 Lateral Deltoid Moment Arms.....	67
	4.5.3 Joint Moments and Forces	67
CHAPTER 5 A BIOMECHANICAL EXPLANATION OF THE CORRELATION BETWEEN THE CRITICAL SHOULDER ANGLE AND THE GLENOID COMPONENT LOOSENING IN THE NC TOTAL SHOULDER ARTHROPLASTY - MUSCULOSKELETAL MODELLING STUDY		
5.1	Abstract.....	69
5.2	Introduction.....	70
5.3	Methods.....	72
5.4	Results.....	74
	5.4.1 Center of pressure	74
	5.4.2 Contact force.....	75
	5.4.3 Muscle forces.....	76
5.5	Discussion.....	78
5.6	Conclusion	81
CHAPTER 6 GENERAL DISCUSSION		
6.1	Thesis Summary.....	83
6.2	Limitations and Recommendations for Future Research.....	85
CONCLUSION		89
BIBLIOGRAPHY.....		91

LIST OF TABLES

	Page
Table 1-1 A summary of previous research on the influence of the CSA on the biomechanics of the GHJ	33
Table 5-1 Table summarizing five cases of different CSA configurations simulated in this study.....	73

LIST OF FIGURES

	Page
Figure 1-1 Shoulder complex. Photo courtesy of Creative Commons	3
Figure 1-2. The deltoid muscle. Taken from Sakoma et al. (2011) with permission.	6
Figure 1-3. Acromion morphotypes according to Bigliani et al. (1986a).....	9
Figure 1-4 The acromion Index (AI) measured on the anteroposterior radiograph. AI is defined as the ratio between the distance from the glenoid plane to the acromion (GA) and the distance from the glenoid plane to the lateral aspect of the humeral head (GH). Taken from (Nyffeler, Werner, Sukthankar, Schmid, & Gerber, 2006b) with permission.	10
Figure 1-5 The critical shoulder angle (CSA) measured on anteroposterior radiograph. Taken from (Nyffeler & Meyer, 2017) with permission.	12
Figure 1-6. Drawing demonstrating the correlation between the acromion index (AI) and the critical shoulder angle (CSA). Taken from Nyffeler & Meyer (2017) with permission.	13
Figure 1-7. Hypotheses of biomechanical mechanism associated with large acromion extension according to Nyffeler et al. (2006b). Left: A large lateral extension of the acromion is associated with a high ascending force component (Fa) (parallel to the glenoid plane) Right: A small lateral extension of the acromion is associated with a high compressive force component (Fc) (perpendicular to the glenoid plane). Taken from Nyffeler et al. (2006b) with permission.	14
Figure 1-8 A Simplified schema of the modelling workflow in the Anybody Modelling System with integrated FDK algorithm for simulation with determined kinematics.	24
Figure 1-9 Shoulder simulator. Blue cords represent muscles. Taken from Gerber et al., (2014) with permission.	30
Figure 3-1. A Simplified schema of the modelling workflow in the Anybody Modelling System with integrated FDK algorithm: α (FDK) is the humeral head translation; q is a vector containing the position vectors and Euler parameter of all segments; v is a vector containing the linear and angular velocity vectors of all segments; \dot{v} is a vector containing the linear and angular acceleration vectors of all segments; l is a muscle length, $H(f^m)$ is the objective function, which is expressed as a function of the muscle	

forces $f^{(M)}$; $r^{(abduction)}$ is an abduction muscle moment arm; $f^{(FDK)}$ is the FDK residual force for a given $\alpha^{(FDK)}$; $f^{(M)}$ are calculated muscle forces; $f^{(R)}$ are calculated joint reaction forces.43

Figure 3-2. The via-point (up) and the 2D- mesh (down) deltoid models in a) 15°, b) 45° and c) 100° of arm elevation in the scapular plane. Fibres of anterior deltoid are shown in blue, lateral in green and posterior in red. Please notice that other muscles have been hidden to better show changes in the deltoid geometry.44

Figure 3-3. Deltoid moment arms estimation and activation patterns. a) Predicted left- anterior, middle- lateral, right- posterior deltoid moment arms model during an arm elevation in the scapular plane using the via-point (red) and the 2D-mesh (blue) model juxtaposed with literature data. b) Predicted deltoid muscle activation using the via-point (red) and the 2D-mesh (blue) model juxtaposed with normalized EMG (black) with standard deviation (grey area) from Alpert et al., 2000.45

Figure 3-4. Predicted muscles contribution to joint a) abduction, b) rotation and c) flexion moments by the via-point (left) and the 2D-mesh (right) model during an arm elevation in the scapular plane.....46

Figure 3-5. Left – Predicted resultant force for upper limb muscles acting on the GHJ by the via-point (red) and the 2D-mesh (blue) model during an arm elevation in the scapular plane. Right – Glenohumeral joint reaction force (GHJ-RF) for the via-point (red) and the 2D-mesh (blue) model in comparison with in-vivo data from telemetric prosthesis.....47

Figure 4-1. The multi-ellipsoid model: Right–Top view of a) anterior b) lateral c) posterior control surface with tangent lines. Left–Top view of a) anterior b) lateral c) posterior wrapping surfaces (dark blue) fitted to the control surface.57

Figure 4-2. Lateral view of a) via-point model at 90 ° of abduction; b) multi-ellipsoid model at 90 ° of abduction; c) via-point model at 120 ° of scaption; d) multi-ellipsoid model at 120 ° of scaption.....59

Figure 4-3. Predicted average anterior, lateral, posterior deltoid moment arms by the via-point (red) and the multi-ellipsoid (blue) models juxtaposed with literature data during flexion, abduction and scaption.60

Figure 4-4. Predicted muscles contribution to joint 1) abduction, 2) flexion and 3) external rotation moments by the via-point (red) and the 2D-mesh (blue) models during flexion, abduction and scaption.63

- Figure 4-5. Predicted resultant force for upper limb muscles acting on the GHJ by the via-point (red) and the multi-ellipsoid (blue) models during flexion, abduction and scaption.65
- Figure 5-1. The projection of the center of pressure (COP) position on the glenoid component. Normal CSA (case 1) in black; large CSA with extended lateral acromion (case 2) in yellow; red: case 3 – large CSA with upward glenoid tilt; blue: case 4 – normal CSA with extended lateral acromion and downward glenoid tilt; green: case 5 – normal CSA with shorten lateral acromion and upward tilt. The cross correspond to the start of the movement.....74
- Figure 5-2. Glenohumeral joint contact force from 15° to 120° of shoulder abduction, simulated for five different variants of CSA.....76
- Figure 5-3. Supraspinatus, anterior and lateral deltoid shear and compressive forces simulated for the five different variants of CSA.....77

LIST OF ABBREVIATIONS

AC	Acromioclavicular
AI	Acromion Index
ASME	American Society of Mechanical Engineers
COP	Center of pressure
CSA	Critical Shoulder Angle
DoF	Degrees of freedom
EMG	Electromyography
FDK	Force-dependent kinematics
GHJ	Glenohumeral joint
GHJ-RF	Glenohumeral joint reaction force
JRF	Joint reaction forces
SC	Sternoclavicular
TSA	Total shoulder arthroplasty
NC	non-conforming

LIST OF SYMBOLS

cm	centimeter
kg	kilogram
m	meter
N	Newton
N m	Newton-meter
rad	radian

INTRODUCTION

The proper functioning of shoulder complex allows for many everyday activities with the use of upper limbs. The shoulder complex has the greatest mobility of all joints in the human body. It has almost unlimited motions, which cover about 65% of a sphere (Engin and Chen, 1986a). At the same time, it is the seat of many injuries, which are associated with its considerable mobility, low stability and frequent use.

Many theories, which aim to explain pathomechanism of the most frequent shoulder disorders, focus on scapula morphology. Shape of scapula bone is considerably variable among population. Radiological imaging based studies suggest that an unfavorable shape of the scapula bone may foster the development of rotator cuff tear or osteoarthritis (Beat K. Moor, Wieser, Slankamenac, Gerber, & Bouaicha, 2014). Less is known about the impact of scapular morphology on complications in total shoulder arthroplasty (TSA). Arthroplasty is a surgical procedure to restore the function of a joint. A joint can be restored by resurfacing the bones. An artificial joint (called a prosthesis) may also be used.

Several measures have been developed to quantified difference in scapula shape. Currently, one of the most studied measurement is the Critical Shoulder Angle (CSA) (Beat K. Moor et al., 2014). The CSA combines the length of acromion and the glenoid inclination and it is usually measured on an antero-posterior X-Ray. The CSA receives special attention because of its high intra- and inter-observer reliability. Positive correlations have been found between a large CSA and rotator cuff tear, as well as with glenoid component loosening in NC (NC) TSA (Watling et al., 2018). However, the cohort studies based on X-Ray images are unable to establish a causal effect of these disorder developments. Numerical modeling gives an opportunity to better understand underlying pathomechanism. Large-scale musculoskeletal models are gaining in interest in orthopedic application since they do not require invasive procedures or expensive cadaveric specimens, and are convenient for parametric analysis. However, to find clinical problems using a numerical model, the researcher must make sure that the model is suitable for the given applications and that it is able to give a reliable answer.

Therefore, the aim of this thesis is, in a first place, to adapt a large-scale musculoskeletal model (Sins, Tétreault, Hagemeister, & Nuño, 2015) to study the impact of the scapula morphology on glenohumeral joint (GHJ) biomechanics. The current representation of the deltoid muscle in the model leads to non-physiological muscle fibers trajectories. For this purpose, a previously developed musculoskeletal model of NC-TSA (Sins et al., 2015) needs to be improved by changing the geometrical representation of the deltoid muscle. These improvement will allow to use the model to answer a clinical question associated with the CSA. This study aims at understanding the effect of varying the size of the CSA on the biomechanics of the prosthetic GHJ to predict potential risk of glenoid component loosening.

This thesis is divided in five chapters. The **first** chapter describes the state-of-art on anatomy and pathophysiology of the shoulder girdle with a focus on scapula morphology. It also includes information about NC-TSA and glenoid loosening. Subsequently, it presents the state-of art about multibody musculoskeletal modelling with a focus on the inverse-dynamics approach. The **second** chapter highlights the research problem and thesis objectives. Chapters **three** and **four** correspond to the deltoid model development, each of which has been submitted as a full research paper to a scientific journal. Chapter **five** presents a biomechanical evaluation of the clinical measurement called critical shoulder angle on GHJ with NC anatomical TSA, also submitted to a peer-reviewed journal. Chapter **six** provides a general discussion as well as some recommendations for future research on related topics. The thesis ends with the overall conclusion.

CHAPTER 1

LITERATURE REVIEW

1.1 Anatomy and physiology of shoulder complex

1.1.1 Shoulder complex

The shoulder complex connects the upper limb with the thorax. It is composed of three bones, namely the clavicle, scapula and humerus. The main task of the shoulder complex is the proper spatial positioning of the hand during everyday activities. The range of motion of the shoulder complex exceeds that of any other joint mechanism in the human body. Great range of motion is possible due to the simultaneous motions of the several joints composing the shoulder complex: sternoclavicular (SC), acromioclavicular (AC) and GHJ (Figure 1-1)

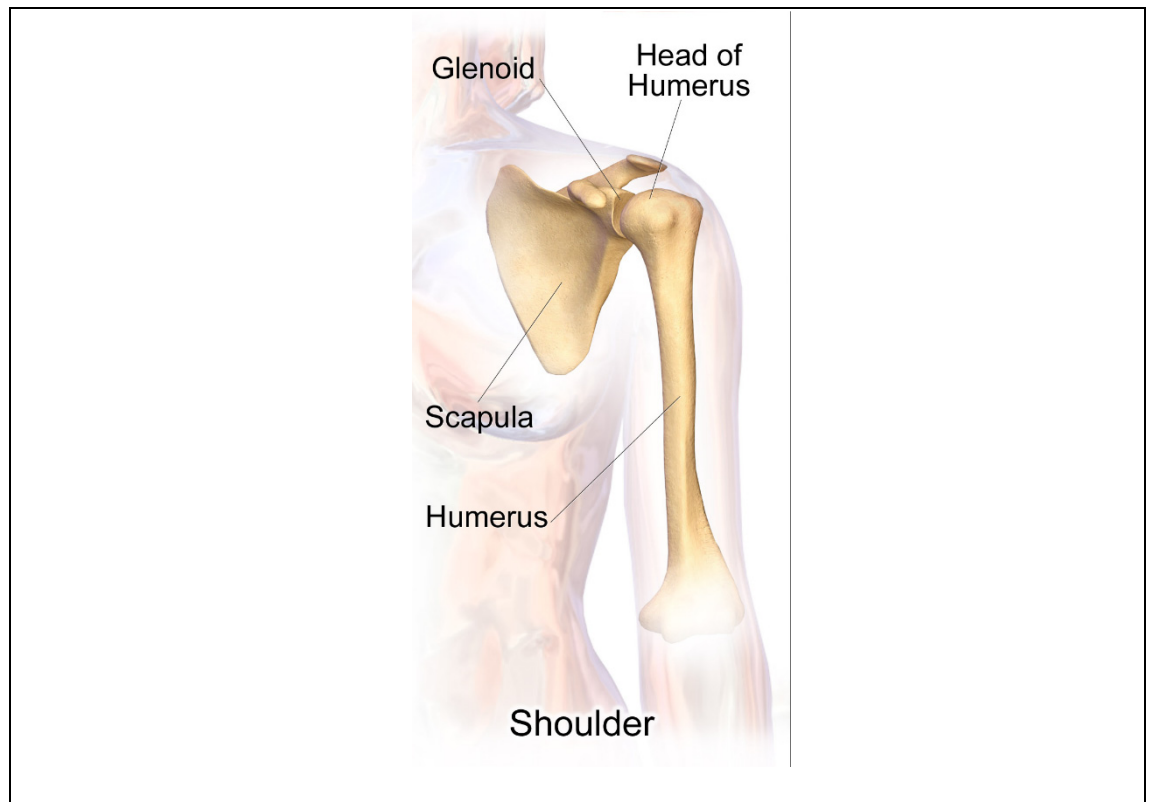


Figure 1-1 Shoulder complex. Photo courtesy of Creative Commons

The SC joint is a saddle-shaped, synovial joint between the proximal clavicle and the manubrium of the sternum. It connects the upper limb with the axial skeleton. Despite its untypical shape, it functions as a ball- and- socket joint and has three degrees of freedom (DoF) (Lee et al., 2014). The AC joint connects the lateral end of the clavicle with the anterior part of the acromion. The AC articulation is the only true synovial joint that attaches the scapula to the thorax through the clavicle bone. It is a plane type joint, which allows only gliding movements (Wong & Kiel, 2018). The shoulder complex is a closed chain and motions of the SC- and AC-joint are coupled (Culham & Peat, 1993; Van der Helm, Veeger, Pronk, Van der Woude, & Rozendal, 1992; Yang, Feng, Xiang, Kim, & Rajulu, 2009). The greatest part of the motion at the shoulder complex comes from rotation of the GHJ often referred to as the shoulder joint. At the GHJ, the humeral head articulates with the glenoid cavity of the scapula. The glenoid cavity is structurally deepened by a fibrocartilaginous rim, the glenoid labrum (Peter Habermeyer, Schuller, & Wiedemann, 1992). The glenoid labrum is attached around the margin of the glenoid cavity. The GHJ is the major articulation of the shoulder complex and the most mobile articulation of the human body (van der Helm, 1994b). Great mobility of the GHJ comes as a consequence of a relatively small and shallow glenoid fossa that is in contact with the large humeral head. Only part of the humerus is in contact with the glenoid at any position of the joint, which comes at the price of low mechanical joint stability. The GHJ is the most commonly dislocated human joint (Rugg et al., 2018).

Considerable mobility of the scapula is also observed in relation to the thorax. The scapula connects the upper limb to the trunk, through the scapulothoracic gliding plane. The scapulothoracic gliding plane is not a true anatomical joint. The thorax and the scapula are connected without any bony or ligamentous attachments one with another. It is a muscle-to-muscle connection between the anterior convex surface of the scapula (subscapularis muscle) and the posterior convex surface of the thoracic cage (serratus anterior). The proper mobility of the scapula is essential for proper shoulder function. The scapulothoracic gliding mechanism allows the scapula to follow the humerus and to position the glenoid cavity correctly. At the same time, in non-pathological conditions, it protects the impingement between the humerus

and the acromion. It provides a stable base from which all shoulder movements start, and its proper positioning determines the effective and strong movements of the shoulder joints.

1.1.2 Static and dynamic stabilizers of glenohumeral joint

Effective performance of upper limb activities depends not only on the mobility but also on the functional stability of the shoulder complex. Because of its high mobility, the GHJ is the least stable synovial joint in the human body. This is due to the anatomy of the shoulder complex, where the GHJ has the least bone stability. The bone stability of the GHJ is increased by the fibrocartilaginous labrum (Peter Habermeyer et al., 1992; Pouliart & Gagey, 2006), which enlarges and deepens the glenoid cavity, while augmenting the articular surfaces' fit. However, shoulder stability is primarily provided by soft tissue structures that intersect with it. The stability of this joint is generally described as the consequence of a passive (static) and active (dynamic) phenomenon.

The passive stability does not require activation of the nervous system. Despite the joint congruity and the glenoid labrum, it comes from following structures: the capsuloligamentar elements (Itoigawa & Itoi, 2016), which are primary passive joint stabilizers, the coracoclavicular ligament (Dawson et al., 2009), and the intra-joint vacuum (Yamamoto et al., 2006). The function of passive stabilizers is to limit the displacement and rotation of the humeral head in the glenoid cavity. The stabilizing function of passive structures is related to the position of the humerus with respect to the glenoid cavity (Felli et al., 2012). The inferior ligament, which is a part of the capsuloligamentar complex, was found to play an important role in anterior stability of GHJ (Turkel, Panio, Marshall, & Girgis, 1981). The active stability comes from the contraction of peri-articular musculotendinous structures that press the joints surfaces together (Blache et al., 2017; Díaz, de Soto, & Uroz, 2020). They include the long head biceps tendon, rotator cuff muscles, peri-scapular muscles, and the deltoid muscle (Billuart, Devun, Skalli, Mitton, & Gagey, 2008; Hsu, Luo, Cofield, & An, 1997).

1.1.3 The deltoid muscle

The deltoid muscle is the muscle forming the rounded contour of the human shoulder (Figure 1-2). The deltoid muscle is the largest shoulder muscle, which envelops the GHJ and determines the silhouette of the shoulder. It consists of three distinct anatomical parts: the anterior (clavicular), the lateral (middle, acromion) and the posterior (spinal) parts. The anterior deltoid originates in the lateral third of the clavicle; the lateral deltoid originates in the lateral margin of the acromion; and the posterior deltoid from the scapular spine. All deltoid fibers coincide and attach on the deltoid tuberosity on the humerus. More detailed description about insertion points of the deltoid muscle can be found in Torpey et al. (1998); Morgan et al. (2006); Rispoli et al. (2009).

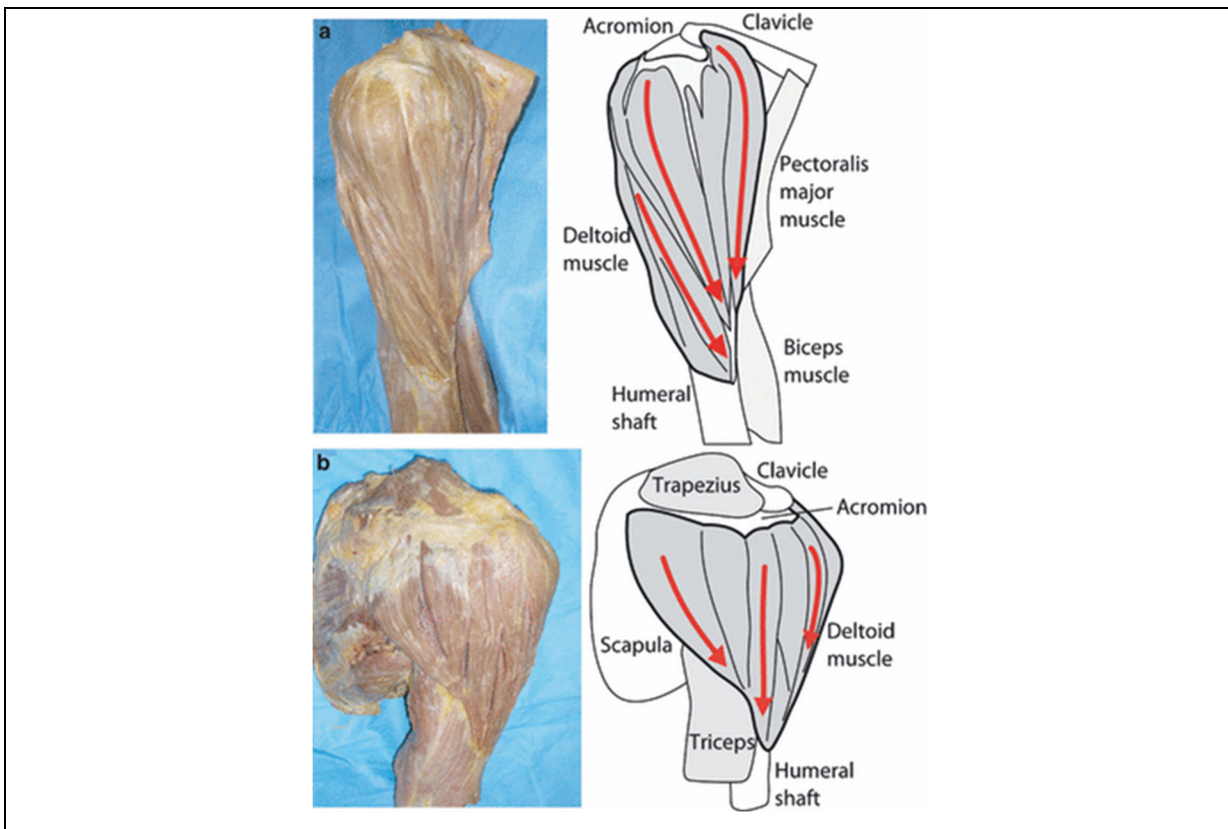


Figure 1-2. The deltoid muscle. Taken from Sakoma et al. (2011) with permission.

The deltoid has a significant role in shoulder function. The deltoid function depends is on the muscle compartment involved. As shown, inter alia, in the article of Reinold et al. (2007) the activation pattern of this muscle during shoulder motion is different according to the three compartments and performed movement. The anterior compartment is responsible for flexion, abduction, and medial rotation of the arm. The largest lateral part provides abduction of the arm, which is also the primary action of the deltoid. The posterior part allows extension, adduction and lateral rotation of the arm. The three parts of the deltoid muscle provide active stabilization of the humeral head during abduction (Billuart et al., 2008; Brown & Wickham, 2006). The deltoid is crucial for shoulder motion and deltoid pathologies can disturb shoulder functioning (Hawkes, Khaiyat, Howard, Kemp, & Frostick, 2019; Hecker et al., 2021).

1.1.4 Glenohumeral joint arthritis and total shoulder arthroplasty

Due to its extensively use, GHJ is often affected by degenerative joint diseases, such as arthritis. The common form of arthritis, also in the case of GHJ is osteoarthritis. Osteoarthritis is characterized by loss of cartilage, and alterations of subchondral bone (Arden & Nevitt, 2006). The most common predisposition factors of osteoarthritis include age, female gender, joint injuries, muscle weakness, anatomical factors and obesity (Ibounig, Simons, Launonen, & Paavola, 2020; Yelin, Weinstein, & King, 2016). Osteoarthritis of the GHJ often causes shoulder pain and stiffness (Weinstein, Bucchieri, Pollock, Flatow, & Bigliani, 2000). Treatment is dictated by patients' age, severity of symptoms, radiographic findings, medical comorbidities, and patient characteristics (Izquierdo et al., 2010). The severe cases and the diagnosis in the late stage of the disease, in which pharmacotherapy is not relieving symptoms, often leads to the surgical interventions, in form of a shoulder arthroplasty. TSA provides significant improvements in pain, function, and quality-of-life (Deshmukh, Koris, Zurakowski, & Thornhill, 2005). Comparative clinical studies found that TSA is a more effective procedure over hemiarthroplasty, mainly due to the progressive glenoid arthritis after hemiarthroplasty (Gartsman, Roddey, & Hammerman, 2000; Lo et al., 2005). Nevertheless, TSA is not recommended for patients who suffer from both arthritis and irreparable rotator cuff tear, because of the eccentric rim loading of the glenoid component which can occur and hence lead to glenoid loosening (Izquierdo et al., 2010). This phenomenon is often called rocking horse

effect (Jackins, Barrett, & Matsen, 1988). However, even in the patients with intact rotator cuff muscles, glenoid loosening remains one of the most common mid- and long-term failure of TSA (Orfaly, Rockwood, Esenyel, & Wirth, 2003). It causes postoperative pain, limited range of motions and often the need for revision surgery (Bohsali, Bois, & Wirth, 2017; Torchia, Cofield, & Settegren, 1997; Wirth & Rockwood, 1996). There is a common agreement that the glenoid component loosening is a multifactorial issue. The reported factors that contribute to the glenoid loosening include radial mismatch, glenoid malpositioning, revision shoulder arthroplasty, glenoid fixation, inadequate glenoid bone stock and rotator cuff tear (Anglin, Wyss, & Pichora, 2000; Cil et al., 2010; Collins, Tencer, Sidles, & Matsen, 1992; Farron, Terrier, & Büchler, 2006; Fox et al., 2009; Franklin, Barrett, Jackins, & Matsen, 1988; Rahme, Mattsson, & Larsson, 2004; Walch et al., 2002). The identification of the factors that contribute to the glenoid loosening is ongoing.

1.1.5 Scapula morphology

The scapula is a flat bone. It is placed on a posterolateral aspect of the thoracic cage and forms the back of the shoulder girdle. The shape of the scapula bone varies among the population. It has been suggested that scapula morphology plays a key role in the development of the most frequent shoulder disorders, such as the rotator cuff tears and the GHJ osteoarthritis (Nyffeler, Werner, Sukthankar, Schmid, & Gerber, 2006a). Special emphasis is put on the morphological differences of the acromion and the glenoid, which have been associated with chronic pain and dysfunctions (Bigliani, Morrison, & April, 1986a; Codman, 1934; Beat K. Moor et al., 2014; Neer, 1972; Watson, 1978). Bigliani et al. (1986b) classified the acromion shape into three types: type I (flat), type II (curved) and type III (hooked) (Figure 1-3).

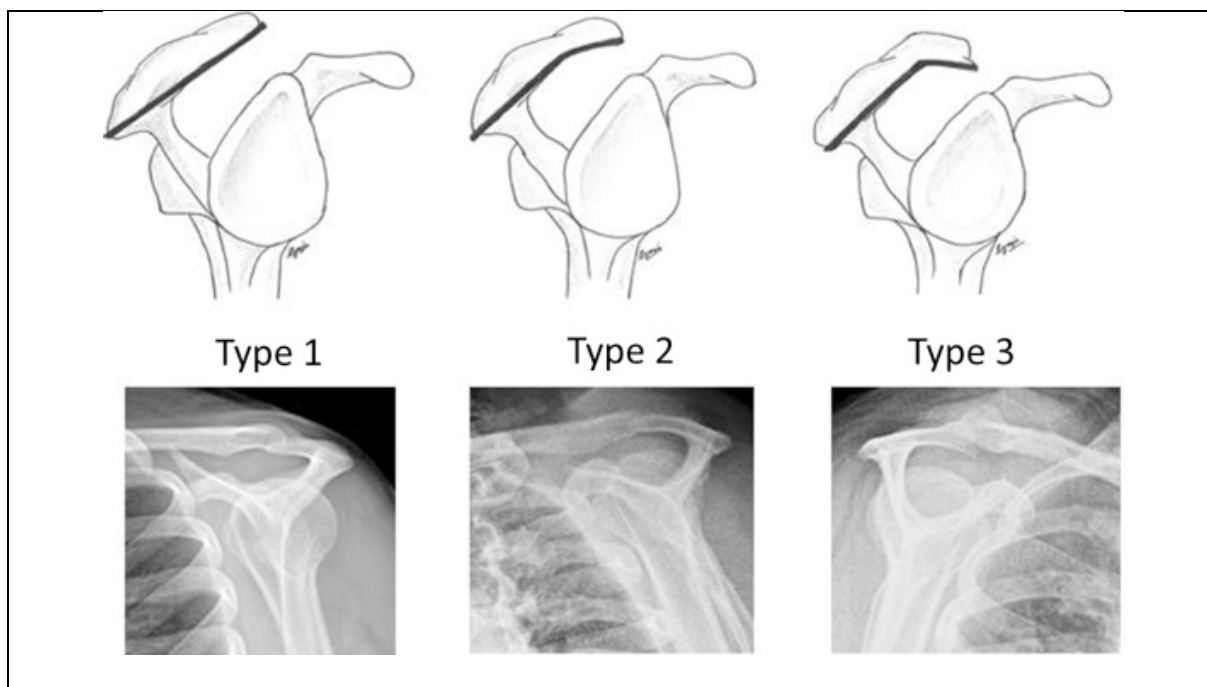


Figure 1-3. Acromion morphotypes according to Bigliani et al. (1986a).
 Taken from Pandey & Jaap Willems (2015) with permission.

They found that a hooked acromion was more prone to rotator cuff tears. Later studies found that rotator cuff tears are correlated with both flat and hooked types (Paraskevas et al., 2008) but others did not find statistically significant correlations (Balke et al., 2013; Beat K. Moor et al., 2014). Further, some of the authors suggested that bone changes are rather the result than the cause of muscle degeneration, as the morphology of the acromion can be affected during the natural progression of rotator cuff disease (Nicholson et al. 1996; Shah et al. 2001). Another disadvantage with this classification is its low inter- and intra-observer reliability (Bright, Torpey, Magid, Codd, & McFarland, 1997). Later studies investigated the scapular morphology in the coronal plane. Especially, the effect of the acromion length and the glenoid orientation were investigated. The acromion length and the glenoid inclination were described quantitatively on true anteroposterior radiographs by many different parameters. True anteroposterior radiographs are often used to determine correlation between shoulder morphology and dysfunction, since they are commonly taken pre- and post-operatively. The

acromion index, glenoid inclination and the critical shoulder angle, described in next section are commonly investigated parameters.

1.1.6 Acromion Index

A lateral extension of the acromion was quantitatively described by the Acromion Index (AI) (Nyffeler et al., 2006a). AI is defined as the ratio between the distance from the glenoid plane to the acromion (GA) and the distance from the glenoid plane to the lateral aspect of the humeral head (GH) (Figure 1-4).

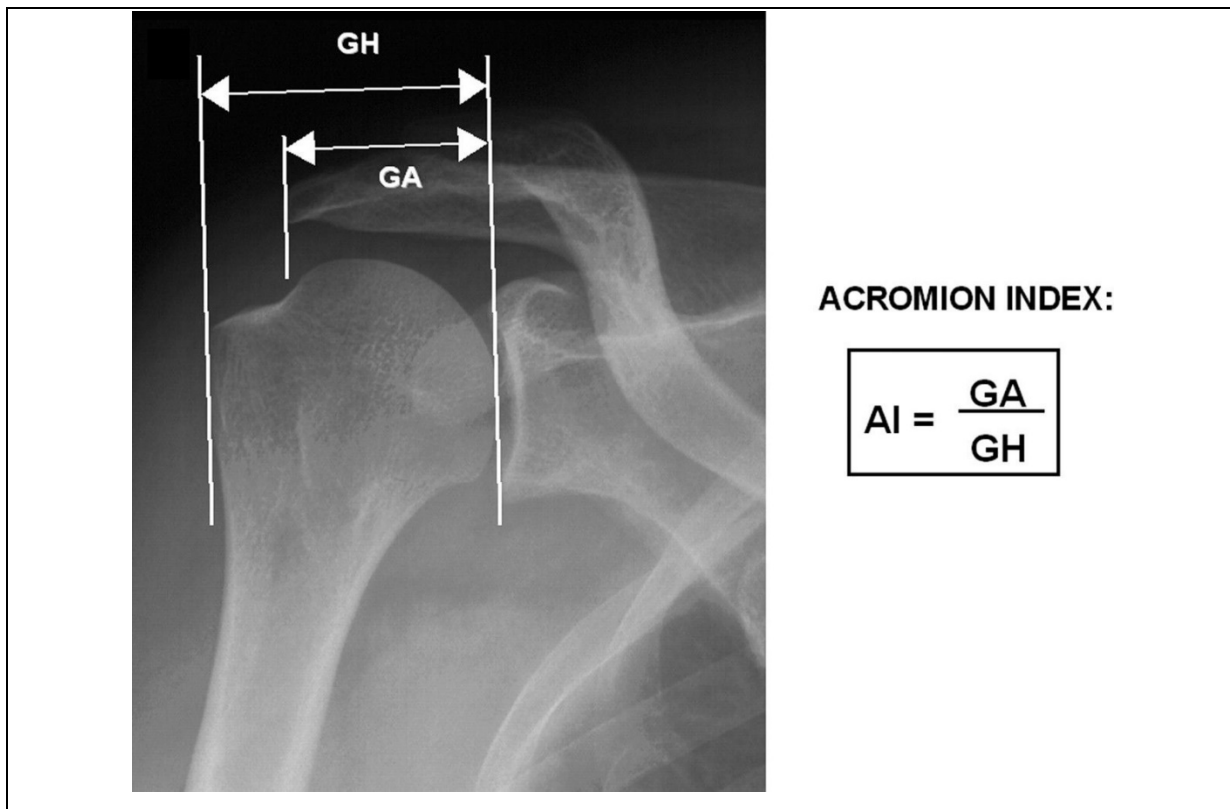


Figure 1-4 The acromion Index (AI) measured on the anteroposterior radiograph. AI is defined as the ratio between the distance from the glenoid plane to the acromion (GA) and the distance from the glenoid plane to the lateral aspect of the humeral head (GH). Taken from (Nyffeler, Werner, Sukthankar, Schmid, & Gerber, 2006b) with permission.

A high AI corresponds to a large lateral extension of the acromion, but it is also influenced by the glenoid inclination. A high AI acromion appears to be associated with full-thickness tear of the rotator cuff. The study of Nyffeler et al. (2006a) patients showed AI values of 0.73 ± 0.06 (n = 102) in shoulders with full thickness rotator cuff tears vs 0.64 ± 0.06 (n = 70) in asymptomatic shoulders. The difference between rotator cuff tear patients and asymptomatic patients was significant ($p < 0.0001$). However, with the small numbers of patients (n = 47), the difference in AI between patients with osteoarthritis (0.60 ± 0.08) and a control group (0.64 ± 0.06) was not significant (Nyffeler et al. 2006)

1.1.7 Glenoid Inclination

Different ways of glenoid inclination measurements are proposed in the literature (Bishop, Kline, Aalderink, Zauel, & Bey, 2009; Churchill, Brems, & Kotschi, 2001; P. Habermeyer, Magosch, Luz, & Lichtenberg, 2006; Hughes et al., 2003; Kandemir, Allaire, Jolly, Debski, & McMahon, 2006). Churchill et al. (2001) described glenoid inclination based on the line that connects the mid-point of the glenoid surface to the transvers axis of the scapula. The transvers axis is defined as a junction of the scapular spin with the vertebral border of the scapula. In their study, based on 176 dried scapula bones, the glenoid inclination varied from -7.0° (downward tilt) to 15.8° (upward tilt).

1.1.8 Critical Shoulder Angle

Later, Moor et al. (2013) introduced the CSA as a morphological parameter which combines the length of the acromion and the inferior-superior tilt of the glenoid. The CSA is determined by the line connecting the inferior and superior margins of the glenoid and the line linking the inferior margin of the glenoid to the lateral aspect of the acromion (Figure 1-5). A high value of CSA corresponds to a large lateral extension of the acromion or superiorly tilted glenoid. An important advantage of the CSA is its excellent inter- and intra- observer reliability (Sankaranarayanan et al., 2020). An averaged CSA of 33.1° (26.8° to 38.6°) was reported in a control group of asymptomatic patients with an intact rotator cuff, 38.0° (29.5° to 43.5°) in patients with a rotator cuff tear and 28.1° (18.6° to 35.8°) in patients with osteoarthritis (Blonna

et al., 2016; Cherchi, Ciornohac, Godet, Clavert, & Kempf, 2016; B. K. Moor et al., 2013). The CSA is also associated with subacromial impingement (Li et al., 2017). According to Nyffeler & Meyer (2017) the CSA is also independent of the orientation of the arm, the width of the glenohumeral joint space and the flatterness of the humeral head, which explains the growing interest in this morphological measurement.

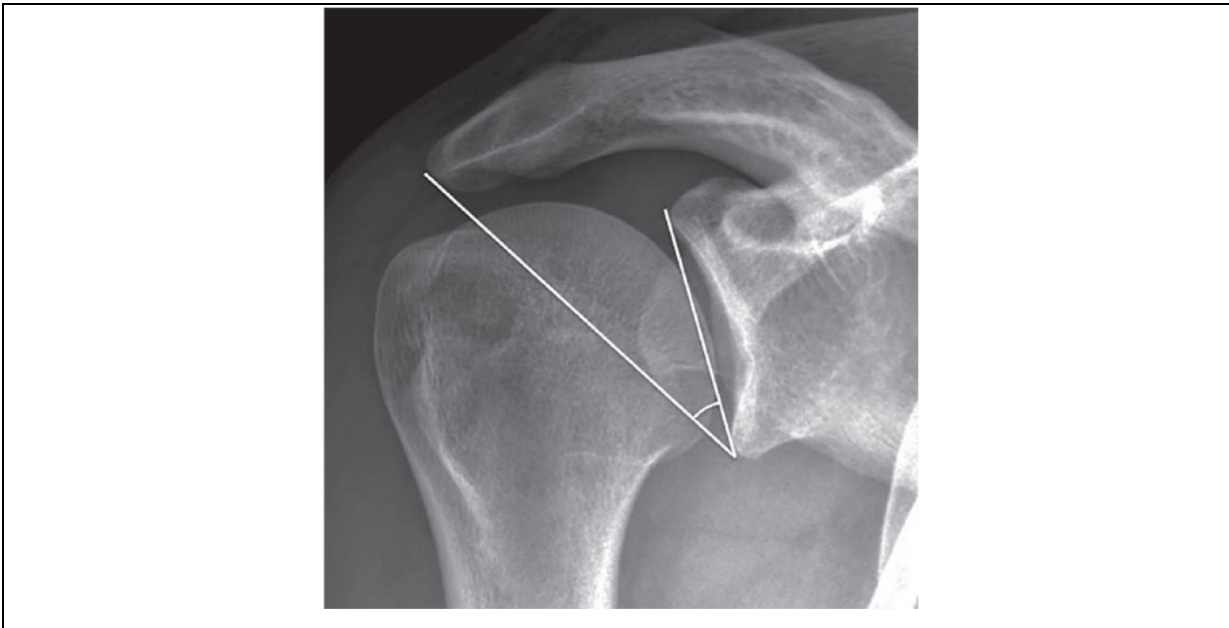


Figure 1-5 The critical shoulder angle (CSA) measured on anteroposterior radiograph. Taken from (Nyffeler & Meyer, 2017) with permission.

It is also important to notice that both AI and CSA depend on the lateral extension of the acromion and on the inclination of glenoid, which was shown in the review of Nyffeler & Meyer (2017) (Figure 1-6). The advantage of the CSA over AI is that the CSA is independent of the size of humeral head, arm orientation and the GHJ space. However, none of these parameters allows quantifying separately lateral extension of the acromion.

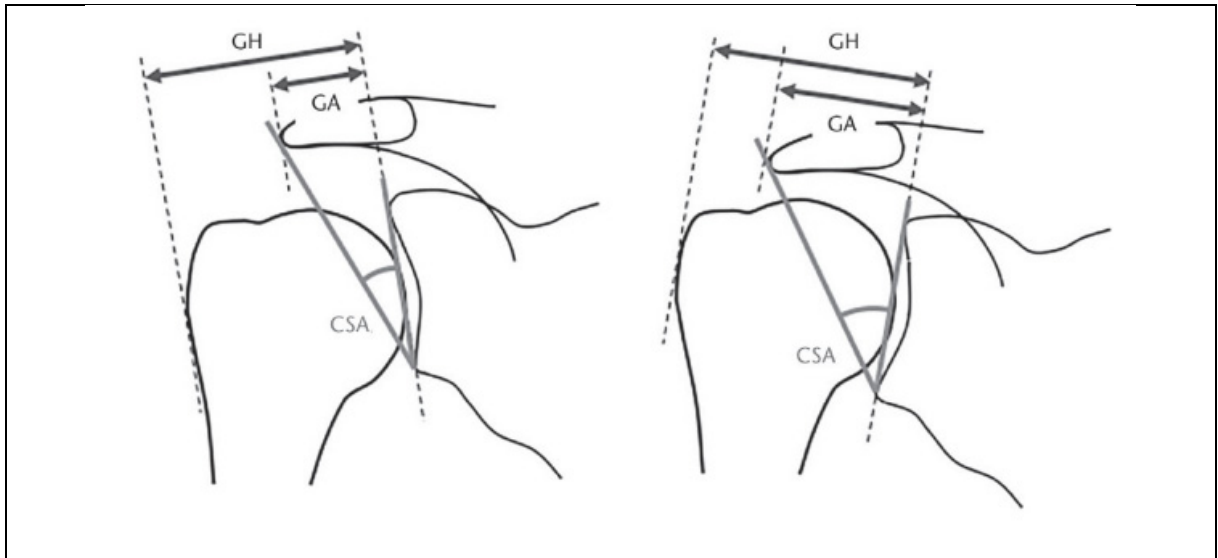


Figure 1-6. Drawing demonstrating the correlation between the acromion index (AI) and the critical shoulder angle (CSA). Taken from Nyffeler & Meyer (2017) with permission.

1.1.8.1 Hypotheses of biomechanical mechanism

Since the lateral deltoid originates from the acromion, Nyffeler et al. (2006b) postulated that a greater lateral extension of the acromion made the direction of the lateral deltoid force vector more vertical. Consequently, the rotator cuff muscles need to provide more force to maintain the centered position of the humeral head on the glenoid, which might result in tears of these muscles. On the other hand, a shorter lateral extension of the acromion can cause more compressive force from the deltoid and hence contribute to higher loads in the GHJ, which may have a joint degenerative effect and lead to arthritis (Figure 1-7).

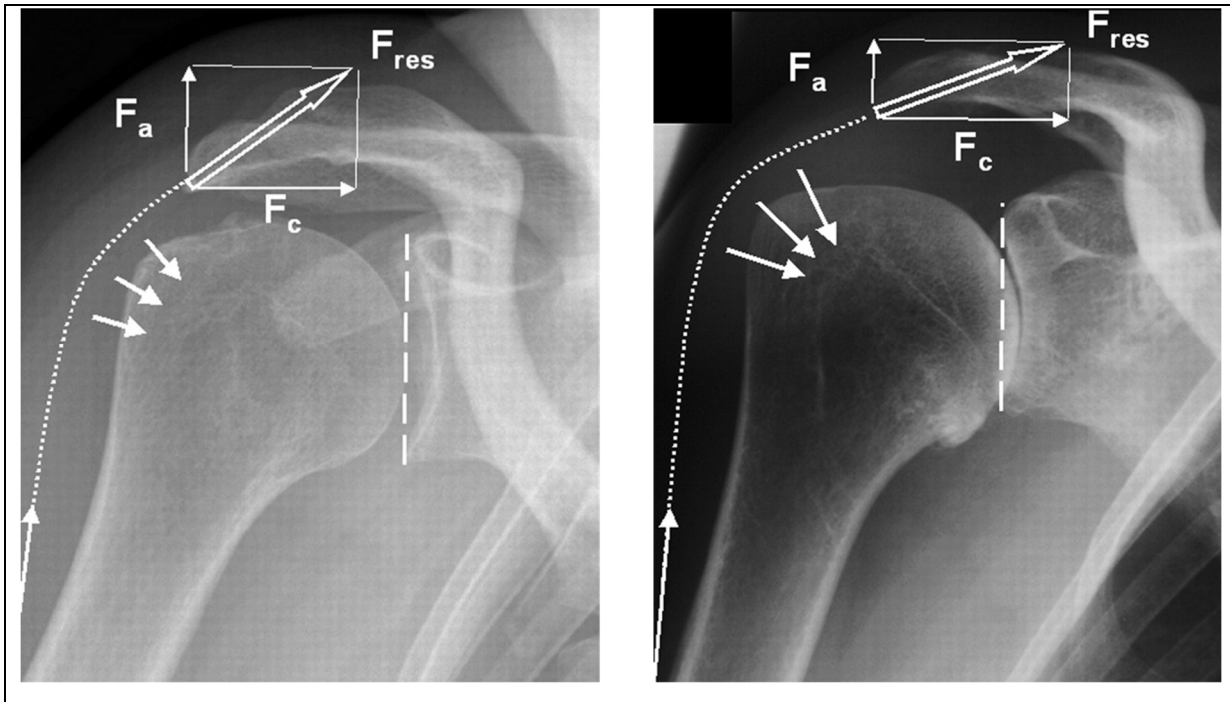


Figure 1-7. Hypotheses of biomechanical mechanism associated with large acromion extension according to Nyffeler et al. (2006b). Left: A large lateral extension of the acromion is associated with a high ascending force component (F_a) (parallel to the glenoid plane) Right: A small lateral extension of the acromion is associated with a high compressive force component (F_c) (perpendicular to the glenoid plane). Taken from Nyffeler et al. (2006b) with permission.

Nonetheless, retrospective studies based on radiographic images are limited in terms of study design and cannot give the direct answer to the pathomechanism behind the unfortunate scapular shape. These studies can only demonstrate a correlation but not a causal relationship between CSA and the rotator cuff tear, osteoarthritis or glenoid loosening. Some biomechanical studies using shoulder simulators (Baumgartner et al., 2014) or numerical models (Bolsterlee, Veeger, & Chadwick, 2013; Favre, Snedeker, & Gerber, 2009) aim at explaining the relationship between CSA and forces distribution around the shoulder.

The great natural variability in the shape of the scapula affects prosthesis design, instrumentation, and intraoperative implantation techniques. Morphological parameters of the scapula that are most commonly considered when designing prostheses include glenoid

height, width, articular surface area, inclination, vault size and shape, and version (Schrumpf, Maak, Hammoud, & Craig, 2011). The study of the CSA in the context of anatomic TSA has received less attention. Watling et al. (2018) found a correlation between large CSA and glenoid component loosening, which remains one of the most common failures after TSA. In addition, Watling et al. (2018) suggested that measuring CSA during TSA may be used as a prognostic factor to counsel patients at risk for glenoid component loosening and may also be a modifiable factor during surgery to improve glenoid component outcomes.

Although, in order to recognize and explain the influence of the scapular morphology on the shoulder functions and TSA failure, in addition to the correlation test, a biomechanical analysis should be carried out.

1.2 Biomechanical modelling of shoulder complex

Numerical models are commonly used as a research approach to understand joints biomechanics and pathologies. They can be beneficial to study musculoskeletal biomechanics when in-vivo experimental techniques are either impractical or impossible. The clinically related questions answered based on numerical models of the shoulder are much less common than those related to a knee or a hip joint. The lower popularity of the numerical shoulder models can be explained by the structural and functional complexity of the shoulder complex itself. Nevertheless, the clinical interest in the numerical models of the shoulder is growing (Bolsterlee et al., 2013).

Numerical shoulder models, which give an insight into joint forces, can be divided into two categories:

- 1) deformable finite element models
- 2) rigid-body musculoskeletal models

The deformable 3D finite element models take into account the distribution of stress and deformations of the bone segments. Musculoskeletal models, unlike finite element models, assume that bones are non-deformable. The choice of the model in a study depends mainly on

the research question that the model aims to answer (Bolsterlee et al., 2013; Favre et al., 2009; Zheng, Zou, Bartolo, Peach, & Ren, 2017).

Musculoskeletal models are developed to estimate muscle forces and joint loadings. They aim at analyzing the musculoskeletal system as a rigid body mechanism together with standard methods of multibody mechanics used to investigate kinematics. Muscle forces estimations usually rely on optimization techniques. The anatomical musculoskeletal system is complex and therefore musculoskeletal models highly simplify reality. Musculoskeletal models have been used in a variety of applications such as ergonomics (Møller et al., 2018), rehabilitation (Castro, Rasmussen, Andersen, & Bai, 2019; E. F. Jensen et al., 2018) sport biomechanics (Kobayashi & Tanaka, 2018; Ohlsson, Danvind, & Joakim Holmberg, 2018) and orthopedics (Hölscher, Weber, Lazarev, Englert, & Dendorfer, 2016; Sins, Tétreault, Nuño, & Hagemeister, 2016). Musculoskeletal models allow to include several segments (multibody models), thus they are appropriate for posture and movements analyses. Hence, in the following chapters of this thesis, the focus will be on multibody musculoskeletal models.

1.2.1 Forward vs Inverse Dynamics

The equations of motion give the relation between forces and motions. Generally, multibody modelling uses two distinct approaches: forward dynamics or inverse dynamics. The approach in which the internal forces (muscle and joint reaction forces) and/or torques are reconstructed from the subjects movements and acting external forces (forces resulting from the interaction between human body and its environment) is called the ‘inverse dynamics approach’, whereas motion prediction from internal forces and/or torques is called the ‘forward dynamics approach’.

Models based on forward dynamics reflect the behavior of the musculoskeletal system, because in the anatomical musculoskeletal system, muscles generate angular acceleration of the bodies. However, muscle forces are difficult to obtain. Thus, the input to forward-dynamics models is typically in the form of muscle excitations and then muscle forces are calculated. Forward

dynamics can be computationally demanding, since it requires a costly optimization in order for the model to achieve the desired movement (Anderson & Pandy, 2001).

Inverse dynamics based models calculate muscle forces based on the description of motions. They require prior knowledge of the model's joint kinematics and external forces to output the internal joint reactions and muscles forces (Silva & Ambrósio, 2002). In inverse approach, the kinematics of joints, muscle and ligaments is solved using inverse kinematics before the kinetics analysis.

In the inverse dynamics approach, usually, the muscle recruitment is a redundant problem. This means that there are more musculotendon units than the total number of equations that describe the dynamic equilibrium of the system. The solution for muscle redundancy is, therefore, often formulated as an optimization problem. This approach is often called a *static optimization*, where optimization problem is solved at each instant of time, by minimizing cost function. In static optimization, a cost function is minimized based on presumed muscle recruitment criteria (e.g., minimum energy, minimum stress, minimum fatigue, minimum activation). The choice of a muscle recruitment criteria should depend on the research question.

Models based on inverse dynamics are computationally efficient (Erdemir, McLean, Herzog, & van den Bogert, 2007). The use of inverse dynamics approach allows building and analyzing full body models with complex muscles representations. Hence, inverse dynamics models are often more suitable to answer clinically related questions.

1.2.2 Mechanical elements and model kinematics

In musculoskeletal models, bones are represented as rigid bodies, often called segments. Segments are characterized by the inertial properties (mass and inertia tensor). Each segment is described by a local fixed coordinated system, usually created from the location of bony landmarks. Segments are constrained by connections between each other or the environment. They are connected by kinematics constraint equations forming idealized mechanical joints, such as spherical or revolute joints. This is also the case of the GHJ, which is generally

modelled as a spherical (ball-and-socket) joint. GH translations are hence neglected, as they are small and difficult to measure.

Models' motions can be described by a set of equations, which are time functions of positions (e.g. locations of specific points in space distance, rotations, angles between segments). Another approach to define model's motion is to use optical motion capture systems or, more recently, inertial sensors. In the motion capture experiments, optical markers are placed on a participant. They are tracked in space by synchronized video cameras. Each marker provides three-dimension Cartesian coordinates (x, y, z), hence adds three kinematics constrains to the model, three markers adding six kinematic constrains to a segment. Markers need to provide as many constraints on the model as there are DoF. The typical situation for the motion capture experiments is that there are more markers than DoF. It creates a situation of kinematic over-determination, which means that, in total, there are more constraint equations than the remaining DoF in the model. The over-determination can be solved as a nonlinear least squares optimization problem (Andersen et al 2009).

1.2.3 Muscle Modeling

Muscles are the actuators in the models and are critical components of a musculoskeletal system. In musculoskeletal models, muscles and tendons are usually defined as one combined element, often called a musculotendon element or musculotendon unit. Each musculotendon element is described by two separate, although computational dependent, models:

- **The geometrical model**, which determines musculotendon element geometry and trajectory
- **The physiological model**, which determines muscle's active force and its passive elastic force related to the kinematic state of muscle.

Both models will be developed in the following sections.

1.2.3.1 Muscle wrapping methods

The geometrical muscle model entails to find the length and contraction velocity of the musculotendon element. A widely used approach in the inverse-dynamics based musculoskeletal models is the so-called spring models (Schultz, Faulkner, & Kadhiresan, 1991). Due to its low complexity and relatively low computational cost, this modelling technique seems to be the most commonly used in the inverse-dynamics musculoskeletal models. In such a model, musculotendon elements are represented as 1-dimensional, massless springs spread between origin and insertion points. The insertion and origin points are rigidly fixed to the bone segments. The shortness path between the origin and the insertion determines the musculotendon element trajectory. Spring models based on the shortest path use different types of geometrical constraints, since a straight line between origin and insertion generally is not sufficient to capture the physiological trajectory of most of the musculotendon elements. Many spring models use constraints such as via-points (Delp & Loan, 1995), or simple geometrical surfaces (Iain W. Charlton & Johnson, 2001; Garner & Pandy, 2000) or a combination of both (Holzbaur, Murray, & Delp, 2005). Via-point algorithms are based on nodes, which are rigidly fixed to a point in the local coordinate systems of given segment. The musculotendon spring is forced to pass through these nodes in any given interval of time. The other method is based on simple geometrical objects such as spheres, cylinders, which are integrated into the shortness path algorithm as obstacles to model the wrapping of muscles over the bones. The spring, that represents a musculotendon element, is supposed to find the shortest path bypassing these obstacles. The friction between muscle fibers and underlying wrapping surface is not taken into account.

For the muscles with broad attachment area and multifunctional compartments, such as deltoid or rotator cuffs, one single line of action is not sufficient. Multi-functionality of such muscles is more accurately described by multiple springs (Carlos Quental, Folgado, Ambrósio, & Monteiro, 2015b). The muscle also has a thickness corresponding to the centroid cross-section, which is linked to the wrapping surface. The muscle thickness can be obtained by the locus of cross-sectional centroids of muscle (Buchanan, Moniz, Dewald, & Rymer, 1993; R. H. Jensen

& Davy, 1975; Tsuang et al., 1993). However, the locus of cross-sectional centroids of muscle are difficult to obtain, especially for multiple joint configurations. (Garner & Pandy, 2000) developed an *obstacle-set* algorithm, which automatically estimates the centroid lines and adjust the radius of the obstacles by integrating geodesic equations. The *obstacle-set method* can accommodate several obstacles, yet additional obstacles augment computational complexity. This method is attractive in the sense that the shortest path can be computed analytically. The advantage of the analytical solution is that it solves quickly. Although, to provide valid muscle moments arms, hence valid forces predictions, the shape, position and orientation of geometrical surfaces has to be determined for each musculotendon unit. The complexity and multiplicity of this method arise in joints with multiple DoF and large range of motion.

In the model of Sins et al. (2015) deltoid is modeled by means of fibers sliding on a sphere representative of the humeral head, and each of which is forced to pass through a rigidly fixed via-point. The consequence is that beyond 90° of abduction, the muscle fibers are forced to follow a V-shape, which affects muscle moment arms. This necessarily influences the results of muscle forces and joint reaction, which can only be viewed with caution beyond this angle of elevation. Thus, this aspect should be considered as an improvement to be prioritized for future developments, in order to obtain more realistic muscle force estimations for elevation angles above 90° .

The wrapping surface models do not exactly represent the bone geometry. Personalized models based on CT-scans resulted in creation of algorithms, which directly use the bone mesh as the wrapping surface. Hence, contact muscle wrapping have been developed, in which springs representing muscle fibers can wrap on arbitrary surface, or directly on the polygonal bone mesh (Desailly, Sardain, Khouri, Yepremian, & Lacouture, 2010; Favre, Gerber, & Snedeker, 2010; Gao, Damsgaard, Rasmussen, & Tørholm Christensen, 2002; Lloyd, Roewer-Despres, & Stavness, 2021). Nevertheless, contact based models also have some limitations. The accuracy of the musculotendon element trajectory depends on the quality of the bones images and segmentation. Calculation time is higher compared to the obstacle-set method. Another

disadvantage of this approach is that it is assumed that the line of action of muscles follows the locus of cross-sectional centroid, which is neglected, is the muscle fibers wrap directly on the bony segment. In addition, direct use of the bone mesh presumes that muscles wrap exclusively on the bony structure. In reality, many muscles, particularly around the GHJ wrap on/interact with the underlying soft tissue structures such as other muscles. This would result in underestimation of muscle moment arms. In theory, it is possible that the algorithm could be extended so it could include also soft tissue constraints, e.g. by including the soft tissue in the bone geometry. However, soft tissue is highly deformable and its distance to the bone surface changes depending on joint position. Nevertheless, careful preparation of the bone surface can lead to significant improvements of the computational efficiency (Gao et al., 2002). The main advantage of using geometrical wrapping objects instead of polygonal bone mesh is the scalability of the first approach.

Geometrical properties of muscles with broad attachment sides, such as the deltoid, are very complex. In fact, there are interactions between muscles fibers as well as interactions between muscles and other soft and hard tissues. A muscle fiber representation as independent, mass- and frictionless springs does not account for these interactions. Hence, the coherence of the muscle with broad attachments is not well represented by such an approach. (Marion Hoffmann, Haering, & Begon, 2017; SP Marsden, 2010) proposed to overcome this problem by creating *2D- muscle mesh*. In this approach, soft tissue passive constraints between muscles fibers are represented by transvers elements connecting together neighboring muscle strings. The muscle is thus represented by 2D-mesh consisting of longitudinal and transverse elements. Intersection points of the transverse and longitudinal elements are defined by wrapping nodes. These wrapping nodes are preventing from penetrating the wrapping object. The limitation of this approach is that the 2D-mesh model is computationally less stable and that the computational time increased with each wrapping node added to the model. The 2D-mesh model is also not suitable for the analytical solution.

1.2.3.2 Physiological muscle model

To account for the force-length and force-velocity relationship in the musculotendon actuators, the most commonly adapted model is a three-element phenomenological model described by Hill (1938), often referred as Hill-type model. The current concept for this model is described by Zajac (1989). This model neglects physical phenomena of cross bridge dynamics and describes the musculotendon unit as a contractile element in combination with elastic elements. The model includes an active contractile element, which functions as an actuator. The contractile element is connected to a parallel passive elastic element and a serial elastic element. Elastic elements account for the elasticity of the tendon tissue and the connective tissue surrounding the muscle. This model requires several physiological parameters that might be difficult to obtain or even to estimate for individuals. The force produced by the active element relies on four parameters, namely peak isometric muscle force, optimal muscle fiber length, optimal muscle-fiber pennation angle and the maximum shortening velocity of the muscle. The force in the passive elements is dependent on the tendon slack length and its stiffness. The muscle force estimated from this element is highly sensitive to these parameters especially to the tendon slack length (Ackland, Lin, & Pandy, 2012). In order to attenuate this effect, these values are often calibrated according to the positions of the joints that correspond to the optimal lengths of the fibers (Heinen, Lund, Rasmussen, & de Zee, 2016).

1.2.4 Stability constraint

In addition to the kinematic constraints, which forms the idealized joints, many shoulder models contain stability constraints. The GHJ is believed to be stable when the resultant force vector is pointing within the glenoid cavity. Thus, glenohumeral stability constraint is formed that the joint reaction force points into the glenoid surface, otherwise the model calculates the additional muscle forces required to redirect the resultant vector into the glenoid cavity (van der Helm, 1994a). GHJ reaction force is then calculated as the sum of the forces required to ensure the stability. Thus, the presence of such a stability constraint does not allow to simulate glenohumeral instability.

1.2.5 Musculoskeletal models for NC total shoulder arthroplasty context

1.2.5.1 Contact modeling

Numerical analysis of prosthetic joint requires an analysis of the contact mechanics prosthetics components in order to estimate resistance of the implant. For example, a small and concenter center of pressure (COP) displacement may reduce the risk of glenoid loosening. Additionally, a vast contact surface may reduce the risk of wear by decreasing stress concentrations (F. Liu, Galvin, Jin, & Fisher, 2011). Contact analysis is usually associated with finite elements models, which allows studying pressure distribution, materials stress and contact mechanics area. Yet the contact analysis can also to some extent be included in the rigid multibody models. Sins et al. (2015) implemented contact-modelling algorithm available in AnyBody modelling system (Damsgaard, Rasmussen, Christensen, Surma, & de Zee, 2006) to the TSA musculoskeletal model. The contact-modelling algorithm in AnyBody modelling system is based on the penalty formulation (Lin & Otaduy, 2008), which allows to compute the contact force between two rigid bodies. In the article of Sins et al. (2015) contact was defined between two rigid STL prosthetics' components, in which polyethylene glenoid component was considered as a slave surface. The contact- modelling algorithm is also used to estimate the magnitude of the contact force and contact force distribution, namely contact area and center of pressure, based on elasticity theory (Sins et al., 2015). The algorithm does not allow estimating surface stress.

1.2.5.2 Force dependent kinematics

Most musculoskeletal models represent GHJ as an idealized ball-and-socket joint. Idealized joint representation might be interesting when studying general kinematics and dynamics of the musculoskeletal system. However, the anatomical GHJ is NC and many prosthesis are design to include this non-conformity. The non-conformity influences joint kinematics and joints' internal force equilibrium. The possibility of capturing this effect simply using kinematic constraints and stability constrains is limited. (Favre et al., 2012; Alexandre Terrier,

Vogel, Capezzali, & Farron, 2008) developed a finite elements model which represents GHJ with 6-DoF, hence allowing for non-conformity of the joint. Quental et al. (2016) proposed to model the GHJ as a spherical joint with clearance in the multibody musculoskeletal model, meaning that some displacement is allowed. (Sins et al., 2015) introduced the GH translations into the TSA model using the force-dependent kinematics (FDK) approach (Figure 1-8), developed by (Andersen, De Zee, Damsgaard, Nolte, & Rasmussen, 2017). The FDK extend an inverse dynamics approach by allowing computation of joint translations based on joint geometry, contact force and enclosing soft tissues elasticity. The FDK method is based on the assumption of quasi-static force equilibrium between all acting forces in the model in same the directions as displacements. In the FDK approach, a kinematic driver equation (Figure 1-8) is added in a standard inverse dynamic analysis approach to obtain a kinematically determinate system. A similar approach is used for reaction forces computation. Thus, the FDK approach computes the muscle and reaction forces required to balance the model for a given DoF.

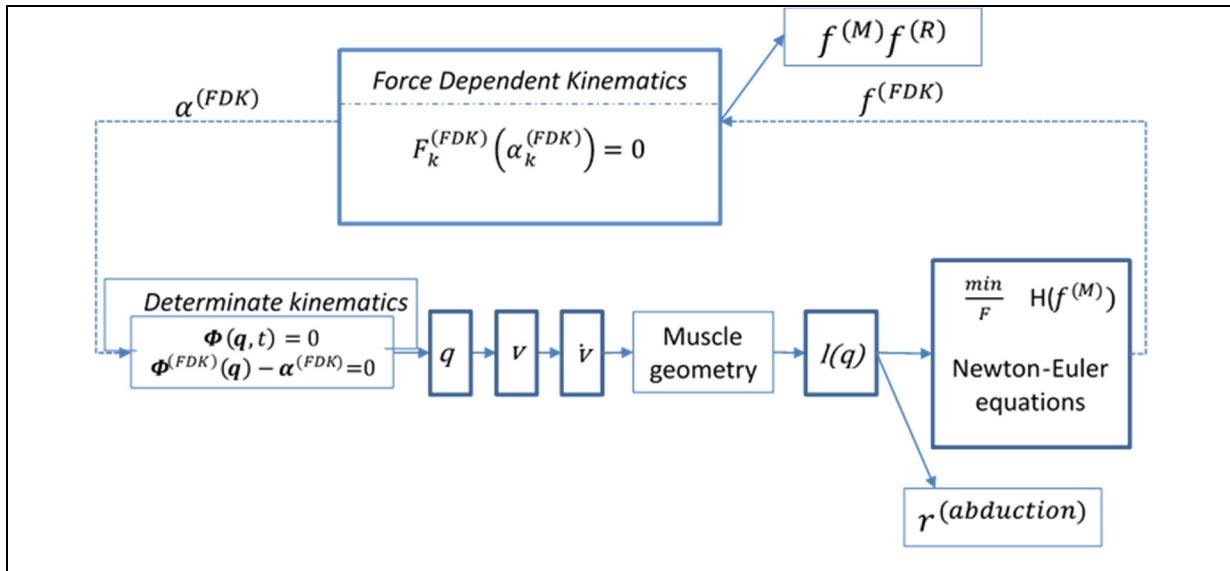


Figure 1-8 A Simplified schema of the modelling workflow in the Anybody Modelling System with integrated FDK algorithm for simulation with determined kinematics.

1.2.6 Model validation

Critical evaluation of models is necessary to justify the credibility of an *in-silico* study. Verification and validation procedures assess the reliability and accuracy of the computer model and simulation results. Verification and validation are two independent procedures. Lund et al. (2012) defined that model verification deals with the question of how the model is implemented and the numerical accuracy of the solution, while model validation is the process of determining how accurately the model represents the system. The verification process should always be performed in prior to validation to eliminate errors due to model implementation. Many musculoskeletal model based studies use established software, where the verification process has already been completed. The validation process determines reliability of the model's predictions by comparison with experimental data. The level of required accuracy depends on the specific application of the model and not on the model itself. Therefore, Lund et al. (2012) and; Hicks et al. (2015) claimed that the validation process should be suitable to the intended use of the model and should always follow the formulation of the research question. Because validation experiments can be costly, invasive and time consuming, musculoskeletal models are often validated based on experimental data from literature. Hicks et al. (2015) postulated that in this case, the validation of musculoskeletal model usually requires comparing results to as many independent datasets as possible. Some of the common validations of musculoskeletal model-based studies of the shoulder are presented below:

Muscle moment arms

The data to construct and validate model geometry in musculoskeletal models comes from imaging and cadaver studies. One method reported in the literature to validate muscle geometry is a comparison of muscle moment arms from experimental studies to the ones calculated by the model. In classical mechanics, the moment arm is defined as the perpendicular distance between the force line of action and the axis of rotation. In the biomechanical context, it represents the capacity of the muscle to produce muscle torque (Pandy, 1999). Thus, moment arm validation also leads to partial and indirect muscle force validation. Two techniques are used to determine the moment arm of muscles: the geometrical method and the tendon excursion

method (Pandy, 1999). The geometrical method is based on the classical definition of moment arms and relies on the estimation of the joint center and muscle lines of actions from medical images. The tendon excursion method is based on the assumption that the moment arm is the rate of tendon length change with respect to the movement of the joint. The moment arm is then calculated from the sum of the derivatives of muscle length with respect to each kinematic DoF. This method gains in popularity because it allows obtaining effective muscle moment arms during motion (Hik & Ackland, 2019). The fact that it is not a direct geometrical measurement is indicated as an advantage of this method as muscle path and geometry are complex and a lot of muscles contribute to more than one DoF (Ackland, Pak, Richardson, & Pandy, 2008). Most of the experimental studies which reported muscle moment arms for the deltoid muscle have looked at very simple motions such as flexion, scaption and abduction. These studies derived data from cadaver specimens, mostly from elderly cadavers, and are based on the tendon excursion method (Hik & Ackland, 2019). Many studies do not normalize moment arms to subject size. Hik & Ackland (2019) found that the validation of muscles in musculoskeletal models remains difficult also due to variability in reported values between different studies.

Electromyography

The inability to measure muscle forces directly confronts researchers with the question on how to validate muscle forces in a model. A commonly chosen option is to use electromyography (EMG) signal to obtain information about the active state of the muscles and compare it with the predicted activity obtained from the simulation. Muscle activity patterns are typically compared to EMG activity patterns. Favorably, EMG data should be collected with synchronized optical markers or inertial sensors to detect motions from which joint angles are computed and used to drive the motion in the model. Generally, simulations should reproduce the most important features of muscle coordination set up in experimental studies. This process leads to the indirect and qualitative validation of muscles forces (Lund et al., 2012). Many of the limitations while using EMG signal for musculoskeletal model validation are coming from EMG data registration itself. EMG signal is difficult to normalize, it is burdened with measurement errors and it is difficult to compare predicted activity by the model with EMG

for dynamic trials as during recording dynamics trials the innervation zones can move under the electrodes and may be misinterpreted as changes of muscle activation level (Lund et al., 2012). In addition, if EMG electrodes are placed over the innervation zone, the activity is remarkably lower. It is also difficult to reach deeply located muscles with surface electrodes. A safe and reliable way to reach muscles which are deeply located between the scapula and the thoracic cage as supraspinatus, infraspinatus, teres minor, lower subscapularis is to use bipolar finewire intramuscular electrodes (Kelly et al., 2005; Waite, Brookham, & Dickerson, 2010). Further, the electromechanical delays between EMG and predicted muscle activation have to be taken into account (Hicks et al., 2015).

In-vivo glenohumeral joint reaction forces

One of the possible direct validation of musculoskeletal models is the comparison of joint reaction forces (JRF) between data collected from instrumented prostheses with model the one predicted by the model. As noticed by Lund et al. (2012) the JRF is mainly influenced by muscle forces; hence, it is also an indirect validation of muscle force pattern estimated by the model. Bergmann et al. (2011) reported glenohumeral joint reaction force (GHJ-RF) measured with an instrumented hemiarthroplasty joint in the right arm. The data was collected 7-months postoperatively for various simple movements. The study was intended for validation of computational models. It is especially useful for the validation of the models that aim for evaluation of the prosthetic joints, since reaction force might differ for an intact joint force. Even if this method is considered as a gold standard in terms of musculoskeletal model validation, it brings several drawbacks that need to be pointed out. Three patients from Bergmann study had minor damages of rotator cuff muscles caused during the surgery, which could influence GH-JRF. Models are generally built based on the data collected from subjects who are different from those used in the experiment. In the Bergmann's experiment, kinematics data was not collected. In addition, in terms of validating prosthetic models, it is important to mention that the technique, implant design and implementation differ. All these elements can influence joint reaction force predictions.

Sensitivity analysis

The part of validation process when there is no sufficient experimental data available or when the data is limited is called sensitivity analysis. Sensitivity analysis refers to modification of model inputs by changing one or several particular variables in order to better understand their impact on model predictions (Hicks et al., 2015). The simulation results are most credible when they are insensitive to variables with high uncertainty. The guide from the American Society of Mechanical Engineers (ASME) proposes to perform sensitivity studies before validating a model to clarify the model characteristics that will be important to monitor during experimental testing, but the whole process should be execute again after a validation step (ASME, 2006).

1.3 Biomechanical impact of shoulder morphology

1.3.1 Shoulder simulators

A pathomechanism associated with the lateral acromion extension and the glenoid inclination was firstly investigated using mechanical shoulder simulators (Baumgartner et al., 2014). In these mechanical models the polyethylene glenoid was articulated with a dummy (Gerber, Snedeker, Baumgartner, & Viehöfer, 2014; Viehöfer, Snedeker, Baumgartner, & Gerber, 2016) or a cadaveric (B. K. Moor et al., 2016) humerus, depending on the configuration. They also include mechanical actuators with a cord and pulley to mimic musculotendon elements. Using such a simulator Gerber et al. (2014) analyzed a CSA of 38° which was previously reported as a mean CSA value with a risk of rotator cuff tear (B. K. Moor et al., 2013). In this model, glenoid component was tilted 5° superiorly and remained in a fixed position. Only the lateral acromion extension was varied to reproduce a large (38°) and a normal (33°) CSA. This was done by adjusting the medial/lateral position of the pulley carrying the deltoid cord. The model was configured to apply increasing tension on the deltoid and supraspinatus cord until reaching a maximum thoracohumeral abduction angle of at least 82° . As a result, the GHJ reaction forces were calculated. The study analyzed the relationship between the lateral extension of the acromion and the stability of the shoulder joint. The joint stability was defined as an *instability ratio* between compressive and shear force. The instability ratio was higher in the model with the lateralized acromion. In order to stabilize the arm in space, the authors had to increase the supraspinatus force from 13% to 33%. Therefore, the conclusion was that large CSA could induce supraspinatus overload. With the same shoulder simulator Viehöfer, Snedeker, et al. (2016) investigated a shoulder with a small CSA of 28° , which was previously reported to be the one at risk of osteoarthritis. They found that the GHJ reaction force increased with the decrease of the CSA. Moor et al. (2016) used a shoulder simulator and changed the CSA by varying only the glenoid superior-inferior tilt. The varied inclination by 5° increments allowed simulation of a critical shoulder angle ranging from 20° to 45° . Thoracohumeral abduction from 0° to 60° were investigated. They found that tilting glenoid superiorly increased the shear force component and therefore the instability ratio. In addition, increasing

the force in the supraspinatus cord helped to decrease the shear force component and to avoid superior subluxation of the humeral head. They suggested that the increased activity of the rotator cuff may foster rotator cuff tears.

The in-vitro studies helped to understand the biomechanical impact of CSA, however they have several limitations. The anatomy of shoulder complex is significantly simplified. The geometry of the shoulder girdle is limited to mimic only the GHJ, hence neglecting the effect of other inter-playing joints and bi-articular muscle actions. The deltoid and rotator cuff muscles are represented by single-unit motorized linear actuators (cords and pulleys) (Figure 1-9Figure 1-9).

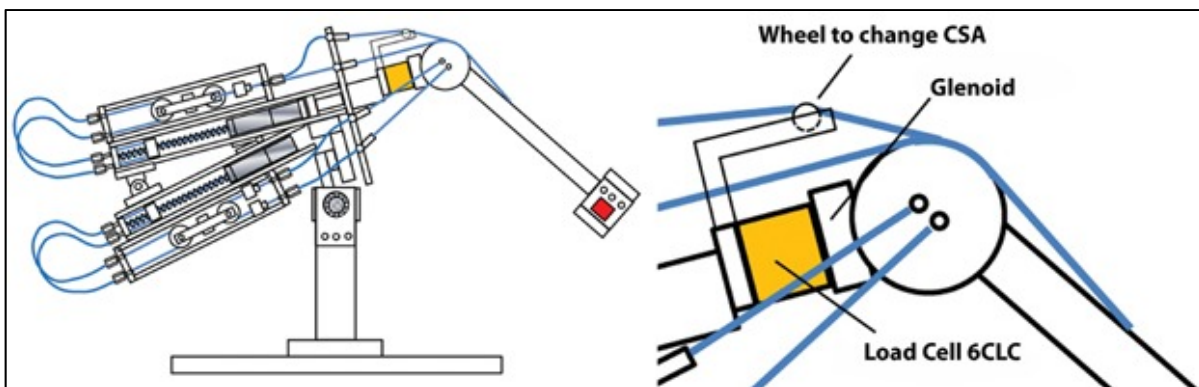


Figure 1-9 Shoulder simulator. Blue cords represent muscles. Taken from Gerber et al., (2014) with permission.

Such muscles representation does not allow estimating muscles force distribution and co-contraction. Finally, simulator based studies investigated the effect of only simple abduction movements up to 82° , while the GHJ has much larger range of motion.

1.3.2 Numerical models

Another approach to study a pathomechanism related to the scapular morphology is numerical modeling. To date few studies used numerical models to study an impact of the CSA on GHJ biomechanics. Terrier et al.(2006) conducted a 3D finite element study, where the bones were considered non-deformable. They found that large lateral extension of the acromion increases

superior translation of the humeral head during elevation of the arm. Viehöfer, Gerber, et al. (2016) conducted a numerical study using 3D finite element shoulder model in which impact of the laterally extended acromion was examined. The model included the non-deformable representation of the scapula and humerus as well as 152 musculotendon units. The arm abduction was performed around the center of the GHJ, which makes a GHJ to behave as a perfect ball-and-socket joint. The study shows that GHJ compressive force decreased and inferior-superior shear force increased with extended CSA, which required an additional supraspinatus force to stabilize GHJ. In another study, Engelhardt et al. (2017) used a multibody musculoskeletal model based on MRI images combined with a 3D finite element model. The study investigated the effect of the CSA on the humeral head translation and the articular cartilage strain. The choice of investigated parameters in this study is based on the assumption that humeral head superior translation is related to the rotator cuff tear and increased cartilage strain can cause osteoarthritis. In this study, a large CSA caused the increase of superior glenoid head translation and shorter acromion or an upward glenoid tilt caused increased cartilage strain. Villatte et al. (2020) used the UK National Shoulder Model (I. W. Charlton & Johnson, 2006) to quantify muscle forces and GHJ-RF. In this study, the GHJ was modelled as a ball-and-socket joint, with stability constraints. The CSA in this study was varied by modifying attachment points of the lateral deltoid. The authors found that increased CSA produced higher superior shear forces and lower compressive force compared to a normal CSA. Table 1-1 presents the main findings of studies on the influence of the CSA on the biomechanics of the GHJ.

Table 1-1 A summary of previous research on the influence of the CSA on the biomechanics of the GHJ

Study	Methods	Movement	Modification of Glenoid inclination	Modification of Acromion Length	Measured Values	Main Findings
Gerber et al. (2014)	shoulder simulator	abduction (6-82°)		+	GHJ compressive and shear force, instability ratio	The instability ratio is higher in the model with the lateralized acromion.
Moor et al. (2016)	shoulder simulator	abduction (0-60°)	+		GHJ compressive and shear force	Tilting glenoid superiorly increased the shear force.
Terrier et al. (2006)	FEM	scaption		+	GHJ-RF, humeral head translation	Large lateral extension of the acromion increases superior translation of the humeral head.
Viehöfer, Gerber, et al. 2016	FEM	abduction (0-100°)		+	muscle moment arms, muscle forces, GHJ-RF(instability ratio)	GHJ compressive force decreased and inferior-superior shear force increased with extended CSA.
Engelhardt et al. 2017	MRI MS model (boundary conditions) + FEM	abduction (60°)	+	+	cartilage strain, humeral head translation	Large CSA caused the increase of superior glenoid head translation and shorter acromion or an upward glenoid tilt caused increased cartilage strain
Villatte et al. 2020	MS model (UKNSM)	scaption + flexion from motion capture (slow and fast)		+	GHJ compressive and shear force	Increased CSA produced higher superior shear forces and lower compressive force

CHAPTER 2

AIMS AND OUTLINE OF THE THESIS

2.1 Clinical problem

As described in the review of the literature, scapula morphology presents certain variability among population. This variability are hypothesized to influence the function of GHJ. Different morphological measurements are used in clinical practice to quantify morphological variability of scapula. One of the most studied measures is the CSA, which combines the length of the acromion and the glenoid inclination. Correlation between the large CSA and the rotator cuff tear and the small CSA and the osteoarthritis has been found. However, little is known about an impact of the CSA on the glenoid component loosening after NC TSA and biomechanics of the prosthetic joint.

2.2 Technical problem

Computer simulation methods have been developed to study shoulder biomechanics and to estimate internal loads that are either impractical or impossible to obtain using in-vitro or in-vivo experiments. When choosing or developing a numerical model to answer specific research question, researcher must ensure that the model is able to give the valuable insight. Consequently, a model has to be adapted to the specific application and then validated. Sins et al. (2015) adapted the musculoskeletal shoulder model from Anybody Modeling System (Damsgaard et al., 2006) by adding translation in inferior- superior and anterior-posterior directions using a FDK algorithm (Andersen et al., 2017) as well as contact calculation between the glenoid component and the humeral head (Sins et al., 2015). This makes the model suitable for evaluation of joints after NC TSA. Starting from this model, several shortcuts still have to be addressed to evaluate different scapular morphotypes. As it was empathies in the literature review, one of the remaining issues in multibody shoulder models is a geometrical representation of the deltoid muscle. Lateral and posterior compartments of the deltoid are attached to the scapula; hence, physiologically correct deltoid representation is key to evaluate

the impact of scapula morphology. However, appropriate deltoid muscle geometry is challenging due to the anatomical complexity of this muscle and large range of motion at the GHJ. In the model of Sins et al. (2015) deltoid is modeled by means of fibers sliding on a sphere representative of the humeral head, and each of which is forced to pass through a rigidly fixed via-point. The consequence is that beyond 90° of abduction, the muscle fibers are forced to follow a V-shape, which affects muscle moment arms. This necessarily influences the results of muscle forces and joint reaction, which can only be viewed with caution beyond this angle of elevation. Thus, this aspect should be considered as an improvement to be prioritized for future developments, in order to obtain more realistic muscle force estimations for elevation angles above 90° .

2.3 Objectives

The objective to this thesis is to find and evaluate an approach for the deltoid muscle wrapping, which represents physiological behavior in full-range of GHJ motion and to implement this approach to the multibody musculoskeletal model of the upper extremity. Consequently, the second objective is to apply this model to answer a clinical question, which aims to investigate the CSA. More specifically the previously developed model is used. to assess the influence of the size of the CSA on the GHJ biomechanics after NC TSA and potential glenoid component loosening.

The above-mentioned objectives are reflected by the chapter subdivision of this thesis, which is presented as follows:

The **chapter 3** presents the implementation and the evaluation of the 2D-mesh deltoid model to the LIO-shoulder model (Sins et al., 2016) which is built in the Anybody modelling system. The 2D-mesh model consists in transvers constraints between muscle fibers. The aim of this investigation was to overcome the issue of the non-anatomical shape of deltoid muscle fibers over 90° of abduction, which leads to changes in the force distribution around the GHJ. The 2D mesh model replaced previous solution, commonly used to define fibers trajectories in

musculoskeletal models, in which each muscle fiber was rigidly fixed to the bone segment by so-called via-points. In this chapter, we present quantitative and qualitative comparison between two models: one developed in this thesis with 2D-mesh and the previous one with a via-point deltoid muscle representation (Sins et al., 2016) as well as validation against data from the literature.

The **chapter 4** presents a new approach for deltoid muscle wrapping for spring-based multibody musculoskeletal models, which is based on the use of multiple ellipsoids allowing for wrapping. This approach was also created to overcome difficulties of the deltoid muscle geometrical representation. However, it demonstrates several advantages compared to the 2D-mesh method. It is simple and easily implementable, computationally efficient, and it is suitable for contact and analytical muscles representation. In addition, according to our knowledge, there is no evidence in the literature about optimal obstacle shape and placement to reproduce deltoid muscle geometry in multibody shoulder models.

In the **chapter 5**, the clinical problem of the biomechanical impact of shoulder morphology is addressed. An evaluation of this problem using a musculoskeletal shoulder model is proposed. More specifically, it presents a biomechanical evaluation of the clinical measurement called the CSA on the GHJ with NC anatomical total shoulder arthroplasty, using the previously developed multibody shoulder model. The results of the analysis are discussed in the context of surgical correction of the CSA to prevent glenoid component loosening.

Chapter 6 summarizes main findings presented in this thesis and presents a general discussion. In addition, in this chapter are presented limitations of this work and remaining problems of the clinical use of musculoskeletal shoulder models. Finally, the chapter proposes ideas and directions for future research.

CHAPTER 3

AN INNOVATIVE 2D-MESH MODEL TO IMPROVE DELTOID MOMENT ARMS, MUSCLE FORCES AND GLENOHUMERAL JOINT REACTION FORCE ESTIMATIONS

Marta Strzelczak (1, 2), Lauranne Sins (2), Mickaël Begon (3, 4), Nicola Hagemeister (2, 5)

(1) École de technologie supérieure, Montréal, Canada

(2) Laboratoire de recherche en imagerie et orthopédie, Centre de recherche du CHUM,
Montréal, Canada

(3) School of kinesiology and Exercise Science and Institute of biomedical engineering,
Faculty of Medicine, University of Montreal, Montreal, Canada

(4) Research Centre, Sainte-Justine Hospital

(5) Département de génie des systèmes, École de technologie supérieure, Montréal, Canada

Paper submitted for publication, July 2018

3.1 Abstract

We proposed a 2D-mesh representation of the deltoid muscle to improve a realism of forces and moments predictions in a multibody shoulder model. Our 2D-mesh model was qualitatively compared to a commonly used via-point model during an arm elevation in the scapular plane and to previous in-vitro studies in terms of deltoid moment arms. The most notable improvement was observed for the moment arms of the anterior deltoid, which shows better agreement with in-vitro studies. Consequently, joint reaction force above 90° of arm elevation was more consistent with in-vivo data, validating the 2D-mesh representation of the deltoid muscle.

Keywords: musculoskeletal modelling, shoulder model, muscle geometry, deltoid

3.2 Introduction

Multibody musculoskeletal models are commonly used to estimate muscle forces. In musculoskeletal models, muscle fibers are typically modelled as elastic strings from origin to insertion points to estimate their trajectories. The trajectories can be constrained by wrapping objects, i.e. by geometrical surfaces representing underlying bone structures. Muscles with broad attachment sites, such as the deltoid, are the most challenging to represent in musculoskeletal models. The deltoid muscle is usually represented by 3 to 12 independent elastic strings (Carlos Quental, Folgado, Ambrósio, & Monteiro, 2015a; Van der Helm et al., 1992). Via-points (fixed nodes in a local coordinate system) are commonly used to prevent deltoid fibers sliding down the wrapping object that represents the humeral head. However, presence of the via-points may lead to non-anatomical deltoid fiber trajectories (Sins et al., 2015), especially in overhead movements (e.g. high arm elevation). In addition, most of the models assume that all fibers within a muscle deform independently of their neighboring fibers, therefore losing the muscle integrity. To reproduce muscle geometry and to account for interaction between fibers other researchers have introduced a 2D-mesh muscle model with transverse constraints between muscle fibers. The 2D-mesh muscle model was previously implemented to the deltoid (Stuart Marsden, 2010) and the rotator cuff muscles (Marion Hoffmann et al., 2017) to better predict muscle length and moment arms. The 2D-mesh representation of rotator cuff muscles presents advantages over the independent lines model in terms muscles length and moment arm estimations (Marion Hoffmann et al., 2017). Yet the above-mentioned studies implemented the 2D-mesh model in shoulder models that considered the shoulder as a ball and socket joint. Moreover, they did not investigate the effects of 2D-mesh representation on model dynamics. The objective of this study is to reproduce the complex deltoid geometry by incorporating a 2D-mesh representation of the muscle (Fig.2 - down) into an existing multibody musculoskeletal model from Sins et al. (2015) that allows from small glenohumeral translations during arm elevation. In complement to previous publications, besides differences in muscle geometry and moment arms, we aim to report

changes in model dynamics (muscle activation patterns, muscles' contribution to joint force and moments and GHJ-RF. We hypothesized that the addition of transverse constraints to the deltoid model would lead to more consistent estimations of these parameters compared to the original via-point model.

3.3 Methods

A multibody musculoskeletal upper-limb model was previously developed using the Anybody Modelling System (Anybody Technology, Aalborg, DK) (Sins et al., 2015). The upper-limb is modelled with 12 degrees-of-freedom (DoF) namely: sternoclavicular (3-DoF), glenohumeral (3-DoF in rotation and 2-DoF in translation), elbow (2-DoF), and wrist (2-DoF) joints. Elbow and wrist joints are locked in extended position. The GHJ is replaced by a NC prosthesis where the anteroposterior (AP) and the inferior-superior (IS) joint translations ($\alpha^{(FDK)}$) are modelled using the force-dependent kinematics (FDK) (Andersen et al., 2017). Briefly, the FDK takes into account the joint elasticity and geometry and is based on quasi-static equilibrium between forces ($F^{(FDK)}$) in the IS and AP directions $\alpha^{(FDK)}$ (Andersen et al., 2017; Sins et al., 2015). Therefore, this shoulder model is no longer a ball and socket representation of the GHJ. The model contains 118 Hill-type muscle-fiber elements including intact rotator cuff and deltoid muscle. The original deltoid model is composed of 12 independent lines of action (5 for the anterior, 5 for the medial, and 2 for the posterior deltoid) (Fig. 3-2- up). A spherical wrapping object (36-mm radius), centered in the humeral head, is used to prevent penetration of the fibers into the bone and thus to reproduce the curved deltoid fibers' trajectory. The muscle path is computed as the shortest path from the origin to the insertion. Additionally, 12 via-points, one for each muscle fiber element, are rigidly fixed to a supplementary phantom segment. Via-points are defined to maintain muscle fibers trajectories and to prevent their uncontrolled sliding on both sides of the humeral head when searching for the shortest path.

In the proposed 2D-mesh model, the inbuilt sheet muscles from the Anybody Modelling System (Damsgaard et al., 2006) is used to represent the deltoid muscle (Fig. 3-2- down). The via-points from the original model are removed and each muscle-fiber element is composed of

a series of 21 longitudinal linear springs connected by nodes. Each node is also connected with transverse linear spring with a node located on the neighboring muscle fiber, altogether forming a 2D-mesh. The stiffness of longitudinal and transverse springs is defined by a longitudinal : transverse ratio of 10:1 for all compartments, which is in line with the Young modulus of Morrow, Haut Donahue, Odegard, & Kaufman (2010). The ratio is confirmed using a sensitivity analysis (unpublished data). To maintain the bulky shape of the deltoid muscle longitudinal stiffness has to be at least 10 times higher than transverse stiffness. The nodes and longitudinal springs are in contact with the same glenohumeral wrapping sphere as described in the original model. The contact between each node and the wrapping sphere is governed by a static equilibrium of minimum potential elastic energy of the mesh.

An arm elevation in the scapular plane is simulated from 15° to 120° for one male subject (84 kg) using a Fourier sine expansion as a driver function in abduction (Eq. (1)), where θ is a position (rad) of the humerus relative to the thorax. The hand is constrained to stay in the scapular plane. Scapular and clavicular movements are simulated based on linear regression equations proposed by (De Groot & Brand, 2001).

$$\theta(t) = \frac{3\pi}{8} \sin\left(\frac{\pi}{8}t - \frac{\pi}{2}\right) + \frac{7\pi}{24} \quad (1)$$

Both models are based on the inverse dynamics approach (Figure 3-1).

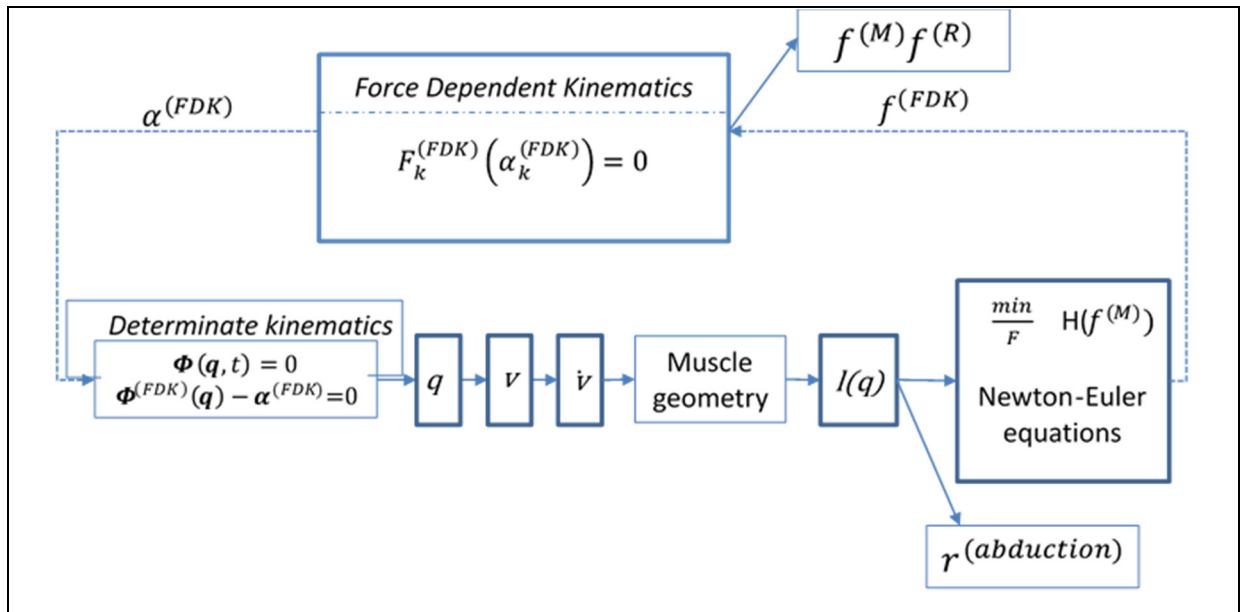


Figure 3-1. A Simplified schema of the modelling workflow in the Anybody Modelling System with integrated FDK algorithm: α (FDK) is the humeral head translation; q is a vector containing the position vectors and Euler parameter of all segments; v is a vector containing the linear and angular velocity vectors of all segments; \dot{v} is a vector containing the linear and angular acceleration vectors of all segments; l is a muscle length, $H(f^m)$ is the objective function, which is expressed as a function of the muscle forces $f^{(M)}$; $r^{(abduction)}$ is an abduction muscle moment arm; $f^{(FDK)}$ is the FDK residual force for a given $\alpha^{(FDK)}$; $f^{(M)}$ are calculated muscle forces; $f^{(R)}$ are calculated joint reaction forces.

The solution of muscle recruitment is formulated as an optimization problem, where a cost function has been defined as the second-order polynomial criterion, in which a square sum of muscle strength is minimized (Damsgaard et al., 2006). Anterior, lateral and posterior deltoid moment arms, activation patterns, contribution of all shoulder muscles to GHJ moments and to GHJ-RF as well as resultant GHJ-RF are estimated using 1) the original via-point model and 2) the 2D-mesh model for qualitative comparison.

3.4 Results

3.4.1 Visual analysis of deltoid muscle shape in the scapular plane elevation

In the original via-point model, the anterior fibers adopt a V-shape around 45° of arm elevation. The lateral fibers adopt a V-shape around 90° of arm elevation. In the 2D-mesh model this V-shape is no longer present (Figure 3-2).

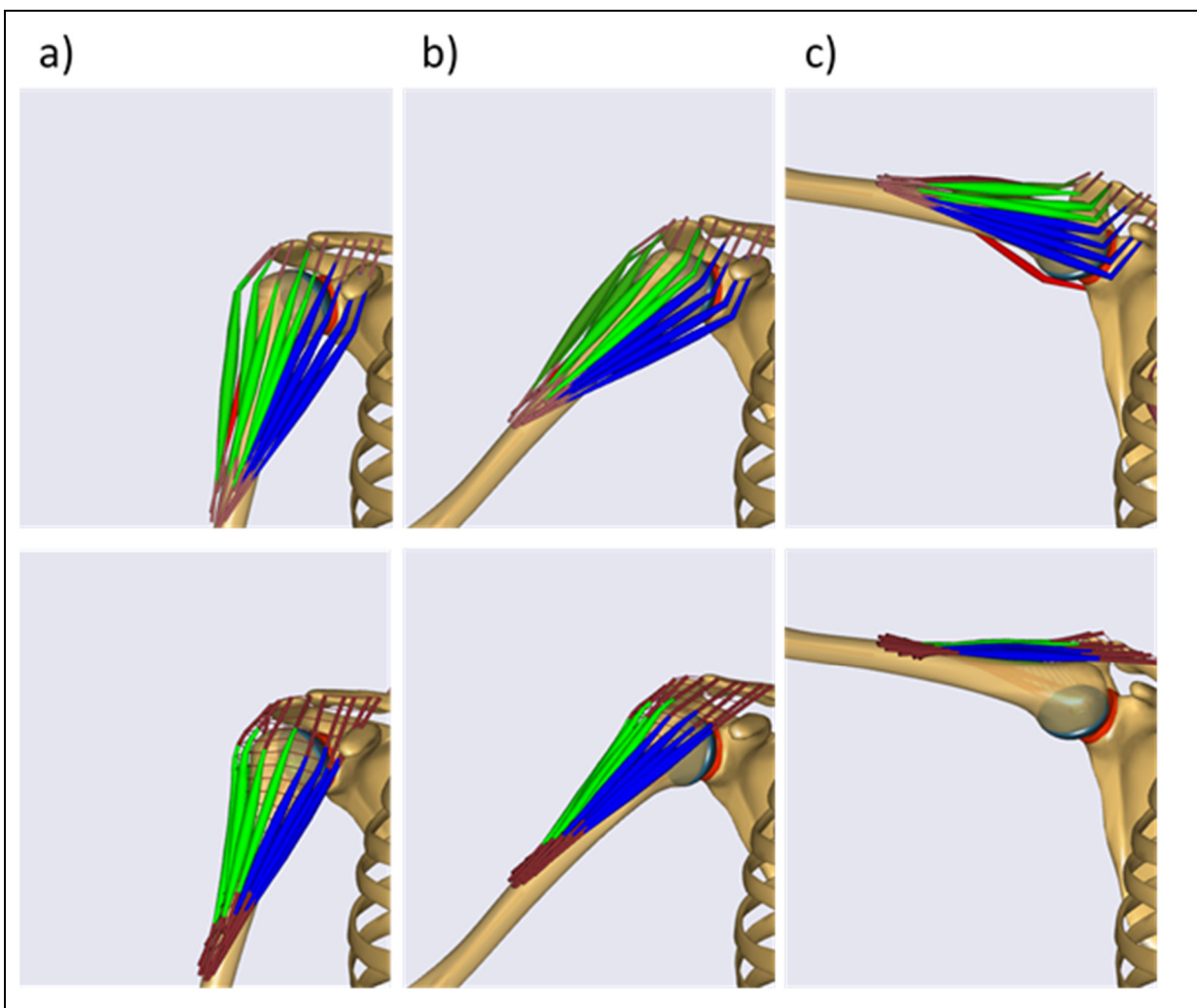


Figure 3-2. The via-point (up) and the 2D- mesh (down) deltoid models in a) 15°, b) 45° and c) 100° of arm elevation in the scapular plane. Fibres of anterior deltoid are shown in blue, lateral in green and posterior in red. Please notice that other muscles have been hidden to better show changes in the deltoid geometry.

3.4.2 Deltoid moment arms estimation and activation patterns.

The most notable differences in terms of muscle moment arms and muscle activation are observed for the anterior deltoid (Figure 3-3).

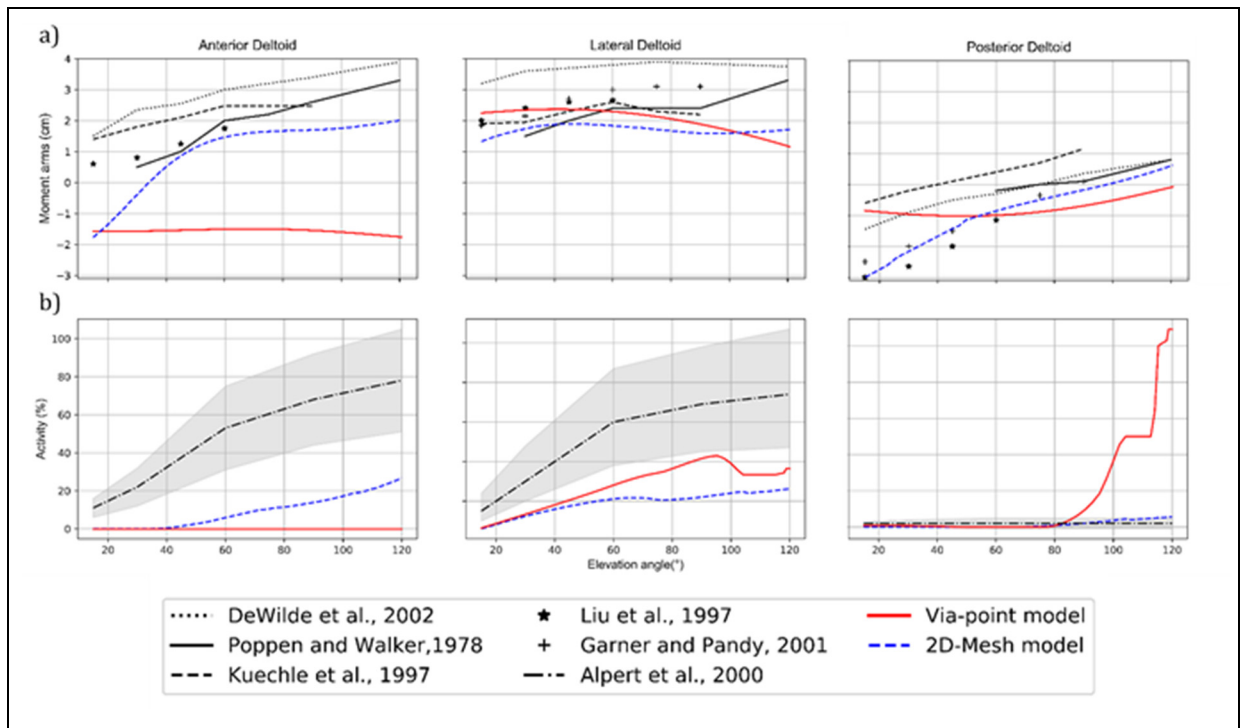


Figure 3-3. Deltoid moment arms estimation and activation patterns. a) Predicted left-anterior, middle- lateral, right- posterior deltoid moment arms model during an arm elevation in the scapular plane using the via-point (red) and the 2D-mesh (blue) model juxtaposed with literature data. b) Predicted deltoid muscle activation using the via-point (red) and the 2D-mesh (blue) model juxtaposed with normalized EMG (black) with standard deviation (grey area) from Alpert et al., 2000.

In the via-point model, the anterior deltoid indicates adduction function (negative moment arm). On the contrary, in the 2D mesh model, the anterior deltoid indicates abduction function (positive moment arm) (Figure 3-3). Consequently, in the via-point model, the anterior deltoid remains inactive during the entire elevation movement, which explains the lack of muscle force

produced by the anterior deltoid. In the 2D-mesh model, the anterior deltoid is activated around 40° of elevation (Figure 3-3)

3.4.3 Contribution of all shoulder muscles to glenohumeral joint moments

In the via-point model, mainly the lateral deltoid and the infraspinatus contribute to the joint abduction moment above 90° of arm elevation (Figure 3-4).

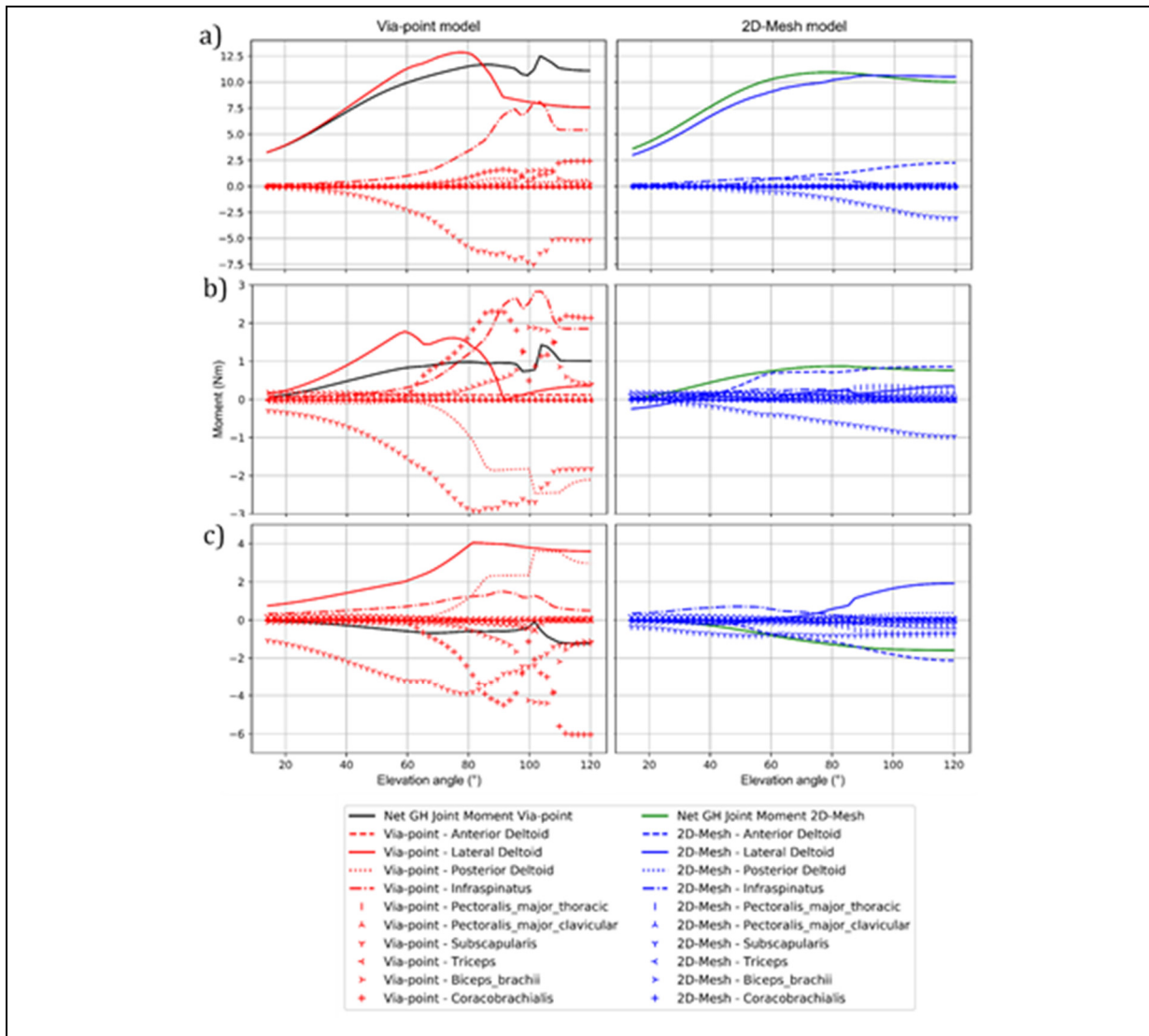


Figure 3-4. Predicted muscles contribution to joint a) abduction, b) rotation and c) flexion moments by the via-point (left) and the 2D-mesh (right) model during an arm elevation in the scapular plane.

The lateral and the posterior chiefs of the deltoid as well as the infraspinatus generate the moment in external rotation. High external rotation moment is compensated by the subscapularis and the coracobrachialis (Figure 3-4). Further, the subscapularis activation results in undesired adduction moment that resists the arm elevation (Figure 3-4). In the 2D-mesh model, the lateral deltoid contributes to the abduction moment arm throughout the entire elevation movement with the help of the anterior deltoid at higher elevation angles (Fig. 4a - right). The infraspinatus is much less involved, meaning that the subscapularis does not counterbalance in rotation and does not produce resistance in abduction.

3.4.4 Contribution of muscle forces and resultant GH-JRF

In the via-point model more muscles with higher force magnitude contribute to GH-JRF than in the 2D-mesh model. The biggest differences between models are observed for the infraspinatus (Figure 3-5).

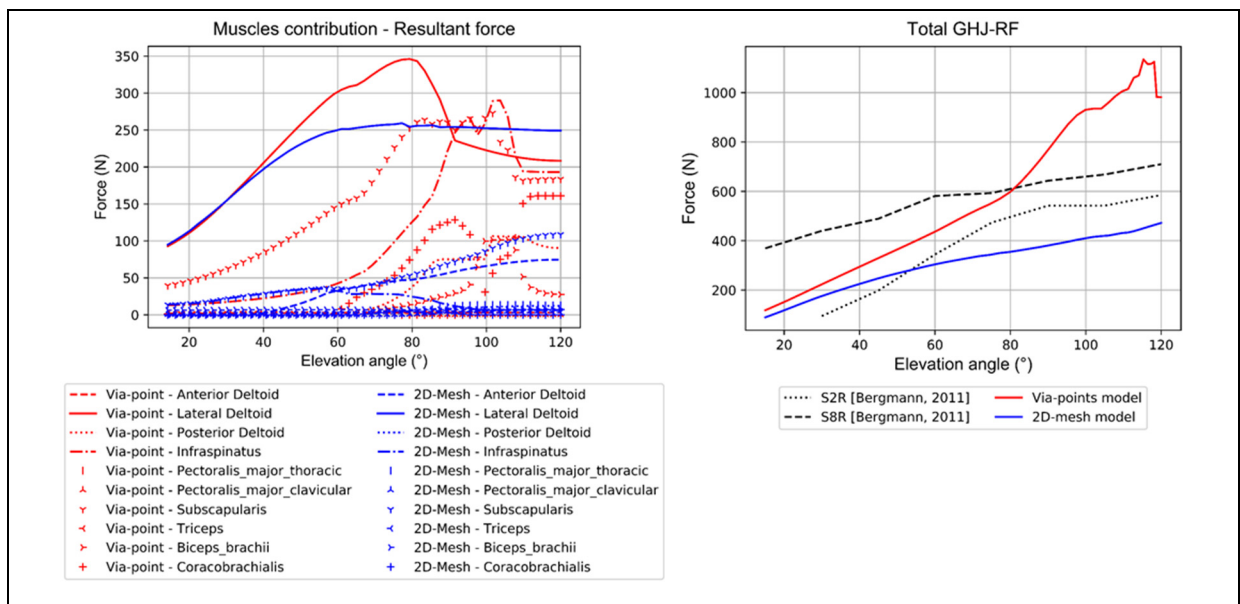


Figure 3-5. Left – Predicted resultant force for upper limb muscles acting on the GHJ by the via-point (red) and the 2D-mesh (blue) model during an arm elevation in the scapular plane. Right – Glenohumeral joint reaction force (GHJ-RF) for the via-point (red) and the 2D-mesh (blue) model in comparison with in-vivo data from telemetric prosthesis.

Consequently, changes in the individual muscle contributions lead to differences in predicted GHJ-RF between models at high elevation angle (Fig. 5 - right). In the via-point model, the GHJ-RF is in line with in vivo GHJ-RF from a telemetric prosthesis study non-physiological until 80° of arm elevation. Above 80° , GHJ-RF suddenly increases reaching 1134 N around 105° . In the 2D-mesh model, the predicted GHJ-RF follows the trend reported in the (Bergmann et al., 2011) during the entire arm elevation.

3.5 Discussion

In the present study, we modelled the deltoid muscle as a 2D-mesh in the multibody musculoskeletal shoulder model to improve its geometry and assess the effect on model dynamics. The 2D-mesh representation was successfully implemented to shoulder muscles with broad attachment sites (Marion Hoffmann et al., 2017; Stuart Marsden, 2010). Nevertheless, to our knowledge, we are the first to examine impact of 2D-mesh representation on deltoid muscle activation, individual muscle contribution to GHJ-RF and moments and resultant GHJ-RF. Additionally, previous models represented the glenohumeral articulation as a simplified ball-and-socket joint with 3-DoF. In the present study the glenohumeral articulation was modelled with 5-DoF, which more accurately reflects the anatomical joint. Moreover, unlike in the previous studies, the multibody shoulder model (Sins et al., 2015) is accessible to the modelling community via the Anybody Modelling System (Damsgaard et al. 2006).

As expected, the 2D-mesh model showed improvements in reproducing the muscle geometry. In fact, by integrating transverse constrains into the deltoid model, the rounded contour of deltoid muscle fibers overlying humeral head was maintained, whereas in the via-point model anterior fibers adopt a non-physiological V-shape around 45° of arm elevation and lateral fibers adopt a non-physiological V-shape around 90° . The V-shape has occurred due to the presence of rigidly fixed via-points, which constrain the fibers' path. Simply removing the via-points would result in sliding of the fibers anteriorly or posteriorly because of the shortest path algorithm that is used.

Tendon excursion studies using cadaveric models indicated abduction moment arms for the anterior deltoid, which increase progressively with increasing elevation (Kuechle, Newman, Itoi, Morrey, & An, 1997; J. Liu, Hughes, Smutz, Niebur, & Nan-An, 1997). The via-point model showed adduction moment arms during whole elevation movement, meaning that in the original model, the anterior deltoid acted solely as an adductor. The 2D-mesh model correctly predicted an abduction moment arms with a similar trend as experimental studies above 35° (Kuechle et al., 1997; J. Liu et al., 1997). However, below 35°, the 2D-mesh model predicted adduction moment arms and at these low elevation angles, we observed a penetration of anterior fibers into the coracoid process. Bone penetration might indicate that the model would need an extra constraint such as an additional wrapping surface.

The 2D-mesh solved the problem of non-anatomical fibers trajectories and misleading anterior deltoid function related to predicted moment arms. However, discrepancies in the existing literature (De Wilde, Audenaert, Barbaix, Audenaert, & Soudan, 2002; Kuechle et al., 1997; J. Liu et al., 1997) suggest that more subject specific validation should be used to assess further development of 2D-mesh model. Geometrical representation of the deltoid muscle affected muscle activation and muscle force predictions. Important differences, especially in anterior deltoid activation, have been found between numerical and experimental (based on electromyography (EMG)) studies. Only onset and offset of muscles activation as well as trends could be compared between models prediction and EMG data (van der Helm, 1994a). Indeed, some musculoskeletal models predict no substantial activation of the anterior deltoid during the arm abduction in the scapular plane (Dickerson, Hughes, & Chaffin, 2008; Sins et al., 2015) while experimental studies reported muscle activation up to 78 % of maximum muscle contraction (Alpert, Pink, Jobe, McMahon, & Mathiyakom, 2000) in high elevation angles. The 2D-mesh largely solved the problem of lack of activation in the anterior deltoid.

Changes in deltoid muscle geometry affected not only deltoid activation, but also the overall muscles' recruitment pattern. In the via-point model, several shoulder muscles generated high moments, which were above or opposite to the net joint moment. Additionally, in the via-point

model, other muscles, especially the infraspinatus, compensated for the lack of abduction moment capacity produced by the anterior deltoid. This results in a series of muscle activation to ensure the balance of moments in all three planes. Indeed, the contraction of infraspinatus together with the lateral and the posterior deltoid generated an external rotation moment. This external rotation moment needed to be balanced by other muscles to produce a small internal rotation moment to elevate shoulder in the scapular plane. EMG studies (Alpert et al., 2000; Reddy, Mohr, Pink, & Jobe, 2000; Townsend, Jobe, Pink, & Perry, 1991) reported only co-activation of the infraspinatus and the subscapularis muscles, which is in line with activation patterns of the 2D-mesh model.

Consequently, the additional activation of these muscles generated forces that affected GHJ-RF. The biggest difference in the muscles' contribution between two models appeared above 90° of arm elevation, where the V-shape caused by the via-points is present for all deltoid fibers in the original via-point model. Therefore, the contribution of individual muscles explained differences in predicted total GHJ-RF between models. Predicted GHJ-RF by both models were compared to in vivo data obtained using telemetric prostheses from Bergmann et al. (2011). The via-point model followed the trend from Bergmann et al. (2011) study only until 90° of arm elevation. Above 90°, non-physiologically high loads in GHJ were observed. Prediction of GHJ-RF improved significantly with the 2D-mesh model. The 2D-mesh model followed the trend from Bergmann et al. (2011) study during entire elevation movement. Even so, differences in the force magnitude was observed between 2D-mesh model and the experimental study (Bergmann et al. 2011). The underestimation may come from the contribution of the rotator cuffs muscles – intact in the model and often deficient in arthroplasty patients (Sanchez-Sotelo, Cofield, & Rowland, 2001), differences in joint kinematics which was not recorded in Bergmann et al. (2011) and, above all, the cost function in the static optimization. Least quadratic activation function is known to underestimate muscles forces and co-contraction especially in the shoulder (Forster, Simon, Augat, & Claes, 2004) resulting in lower joint contact forces.

There is still space for improvement in the development of a 2D-mesh model. We evaluated 2D-mesh model only for scapular plane elevation, since it is the most commonly reported movement in the literature. To assess further the finding of this study, model needs to be evaluated during the full range of motion. However, there is a lack of experimental data to validate musculoskeletal models of the shoulder during more complex movements and larger ranges of motion.

3.6 Conclusion

The 2D-mesh deltoid model presents more consistent predictions in terms of shoulder dynamics than the model with independent lines of action and rigidly fixed via-points. The 2D-mesh shows the ability to maintaining correct muscle shape even at high elevation. Besides that, the 2D-mesh deltoid model demonstrates more realistic estimations of deltoid muscle activation, more realistic muscle recruitment patterns and better prediction of GHJ-RF when compared with the literature. This study shows that the geometrical representation of the deltoid considerably affects model predictions. Incorrect representation of deltoid muscle geometry can lead to misleading predictions of muscle recruitment as well as joint forces and consequently, limits model applications or leads to wrong interpretations

CHAPTER 4

A WRAPPING APPROACH FOR THE DELTOID MUSCLE IN SPRING –BASED MULTIBODY MUSCULOSKELETAL MODELS

Marta Strzelczak (1, 2), Morten Enemark Lund (3), Nicola Hagemeister (2, 4), Mickael Begon (5, 6)

- (1) École de technologie supérieure, 1100, rue Notre-Dame Ouest. Montréal QC H3C 1K3, Canada
- (2) Laboratoire de recherche en imagerie et orthopédie, Centre de recherche du CHUM, Tour Viger 900, rue St-Denis, Montréal QC H2X 0A9, Canada
- (3) AnyBody Technology A/S, Niels Jernes Vej 10, 9220 Aalborg, Denmark
- (4) Département de génie des systèmes, École de technologie supérieure, 1100, rue Notre-Dame Ouest, Montréal QC H3C 1K3, Canada
- (5) Laboratoire de Simulation et Modélisation du Mouvement, Campus de Laval CP 6128, Succursale Centre-ville Montréal, QC H3C 3J7, Canada,
- (6) Department of kinesiology, University of Montreal, 2100 Edouard Montpetit Blvd, Montreal, QC H3T 1J4, Canada

Paper submitted for publication, January 2020

4.1 Abstract

We propose a multi-ellipsoid wrapping approach for the deltoid muscle to improve muscle fiber trajectories in the multibody musculoskeletal model. Predicted deltoid muscle moment arms from the model with implemented multi-ellipsoid wrapping was qualitatively compared to the moment arms from the via-point model and experimental data from the literature.

Additionally, we evaluated muscle contribution to the glenohumeral net joint moments and to the glenohumeral joint reaction force. The multi-ellipsoid wrapping approach improved muscle fibers geometry during abduction and scaption movements. The most notable improvement is noticed in the muscle moment arms of the anterior deltoid. The improvement in the muscle geometry influences overall joint moments and forces predictions. The multi-ellipsoid wrapping approach can successfully replace via-points in the deltoid muscle modelling.

Keywords: musculoskeletal modelling, shoulder model, muscle geometry, deltoid

4.2 Introduction

In most musculoskeletal models, muscles are represented by elastic, one-dimensional, massless strings from origin to the insertion. The advantage of this technique is its simplicity and low computational costs as compared with 2D-mesh (Marion Hoffmann et al., 2017) and 3D-volumetric models (Blemker & Delp, 2005; Webb, Blemker, & Delp, 2014). Strings based models rely on shortest path algorithms to determine trajectories of the muscle lines of action. To avoid penetration inside bony structures, via-points and/or wrapping objects are defined. This strategy is especially well established for the knee models (Marra et al., 2015) which are characterized by relatively simple morphology in comparison to the shoulder. Indeed, in knee models, simple geometrical shapes, such as spheres and cylinders, can accurately describe bones contours.

When modelling muscles that contribute to shoulder motions, the choice of wrapping objects is more challenging. This is mainly due to the morphology of the shoulder girdle leading muscles to wrap around not only rigid, but also elastic structures, like deep muscles. Moreover, many of the shoulder muscles, such as the deltoid and rotator cuff muscles have broad attachment sites. Thus, one single line of action is not sufficient to represent the function of such muscles. In fact, the deltoid muscle is usually represented by 3 to 12 fibers (Carlos Qental et al., 2015a; Van der Helm et al., 1992). Modelling a deltoid muscle as a series of independent lines of action makes it difficult to find one single wrapping geometry, which

controls to all fibers composing the muscle. The common technique for determining deltoid lines of action trajectories is to use a single sphere or an ellipsoid, which is fixed to the GHJ center of rotation. It prevents fibers from penetrating into the humeral head. To avoid the fibers sliding from the rounded obstacle via-points are added in some models (Damsgaard et al., 2006). However, the presence of rigidly fixed via-points lead to non-anatomical fibers trajectories in high elevation angles.

One solution to improve the deltoid muscle trajectory is to use multiple wrapping surfaces. Marsden et al. 2008 proposed an analytical double-wrapping algorithm. This method meant to model the humerus bone surface as a sphere-cylinder composite with the sphere representing the humeral head and the cylinder representing the humeral shaft (S. P. Marsden, Swailes, & Johnson, 2008). However, in some joint positions, deltoid fibers' trajectories are also constrained by other bones such as scapula or other muscles such as rotator cuff muscles. Noticing this limitation, Scholz et al. 2016 developed a more computationally efficient multi-wrapping algorithm, which could be applied to multiple obstacles with different shapes (Scholz, Sherman, Stavness, Delp, & Kecskeméthy, 2016). To our knowledge, this algorithm has not yet been implemented in a shoulder model. Moreover, it is difficult to adapt manually several wrapping objects to a complex geometry such as the scapular girdle. There is no evidence in the literature about optimal obstacle shape and placement to reproduce deltoid muscle geometry in multibody shoulder models.

The objective of this study was to develop a systematized wrapping approach for the deltoid muscle, in which each muscle fiber wraps around one unique ellipsoid. We hypothesized that this technique would lead to more realistic fibers trajectories, and thus it would improve estimation of muscle moment arms as well as leads to more realistic moment and force predictions. We also hypothesized that implementation of this wrapping technique into the model would not increase simulation time.

4.3 Methods

4.3.1 Original model

A multibody musculoskeletal shoulder model was previously developed using the Anybody Modelling System (Anybody Technology, Aalborg, DK) (Damsgaard et al., 2006). The upper-limb is modelled with 10-degrees-of-freedom (DoF) namely: sternoclavicular (3-DoF), glenohumeral (3-DoF), elbow (2-DoF), and wrist (2-DoF) joints. The model contains 118 muscle-fiber elements. The deltoid model contains 12 independent lines of action: five for the anterior, five for the lateral and two for the posterior compartment. In this model, a spherical wrapping object centered on the humeral head with a 36 mm radius is used to avoid penetration of lines of action into the humeral head. The muscle path is computed based on the shortest path algorithm from origin to the insertion. Additionally, via-points, rigidly fixed to a supplementary phantom segment, prevent uncontrolled sliding of muscle fibers on the humeral head.

4.3.2 Multi-Ellipsoid Model

In the multi-ellipsoid model, the deltoid wrapping has been modified in the following way. Each muscle compartment (anterior, lateral and posterior) contains now four muscle fibers. To determine fibers' trajectories and to prevent muscle penetration into bony structures, the original sphere plus via-points were replaced by a set of elliptical wrapping objects combined with a so-called "control ellipsoid" for each compartment (Figure 4-1).

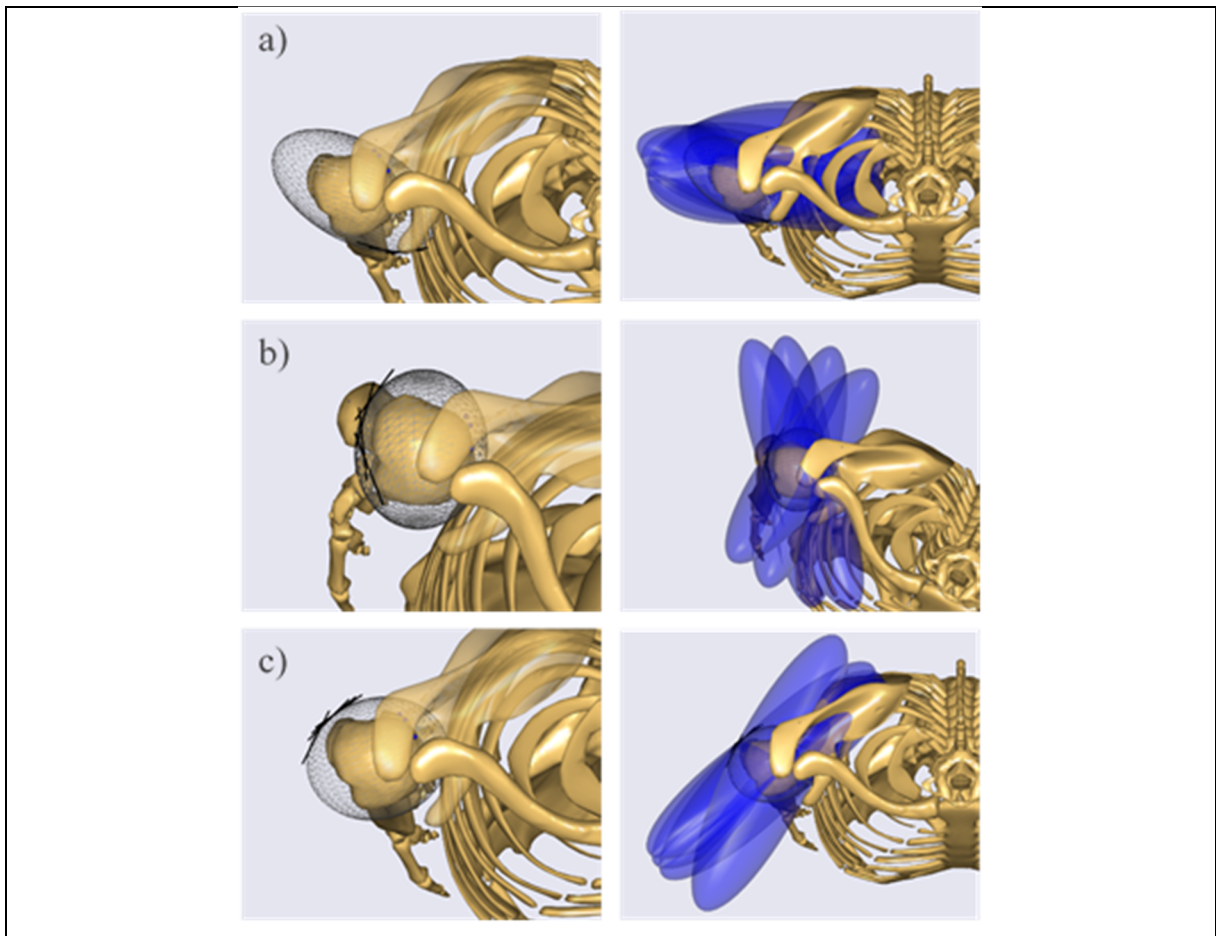


Figure 4-1. The multi-ellipsoid model: Right–Top view of a) anterior b) lateral c) posterior control surface with tangent lines. Left–Top view of a) anterior b) lateral c) posterior wrapping surfaces (dark blue) fitted to the control surface.

The “control ellipsoids” are manually fitted to nodes representing bony landmarks on the scapula (Figure 4-1). For the control surface of the anterior compartment, the coronoid process, the GHJ center of rotation, the glenoid center, and the acromioclavicular joint center of rotation are used. For the lateral and the posterior control surfaces, we used the acromion angle, the GHJ center of rotation, the acromioclavicular joint center of rotation and the glenoid center. From each control ellipsoid, an ellipse defined in the axial plane is extracted and then, tangents to this ellipse are calculated in intervals that vary from 5° to 15° depending on each muscle fiber trajectory. The interval was chosen such that the middle of the tangent line lies between

the origin and insertion points in the anatomical position for each muscle fiber. Each tangent line thus defines the actual position and orientation of the wrapping ellipsoid, one for each muscle fiber (Figure 4-1).

4.3.3 Simulated Movements

Three arm movements are simulated, namely flexion, abduction and scapular plane elevation (scaption) from 0° to 120° , using the via-point and the multi-ellipsoid models. We compare abduction and flexion moment arms of the anterior, lateral and posterior deltoid between both models. We also compare those values to previous studies from literature (Hik & Ackland, 2019). We then compare muscles contribution to joint moments and muscle contribution to GHJ-RF estimated by both models.

4.4 Results

Movements were successfully simulated in 1.3-1.7 minutes for the via-point model and 1.4-1.6 minutes for the multi-ellipsoid model. In the via-point model, deltoid fibers take a V-form above 90° of arm elevation during abduction and scaption motions (Figure 4-2). In the multi-ellipsoid model, the deltoid takes on a round-shape in anatomical position (Video 1). In high elevation, a V-form is not present while using this model. (Figure 4-2).

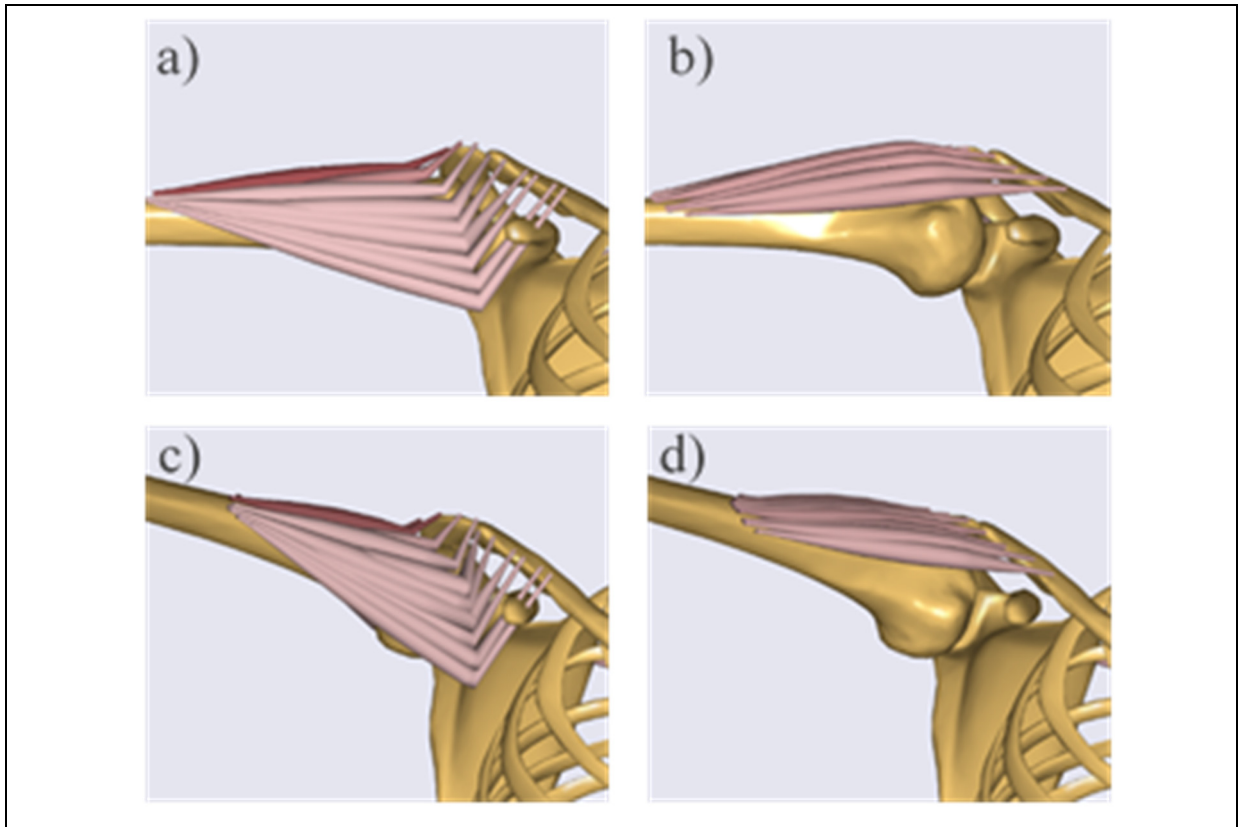


Figure 4-2. Lateral view of a) via-point model at 90 ° of abduction; b) multi-ellipsoid model at 90 ° of abduction; c) via-point model at 120 ° of scaption; d) multi-ellipsoid model at 120 ° of scaption.

4.4.1 Muscle Moment Arms

Figure 4-3 shows moment arms of the deltoid during flexion, abduction and scapular plane elevation (scaption). In flexion, both models follow the trend from experimental studies. However, moment arms of all three muscles compartments calculated by the multi-ellipsoid model are higher (up to 2.7 cm) than those estimated by experimental studies between 60 ° and 120 (Ackland et al., 2008) (Figure 4-3).

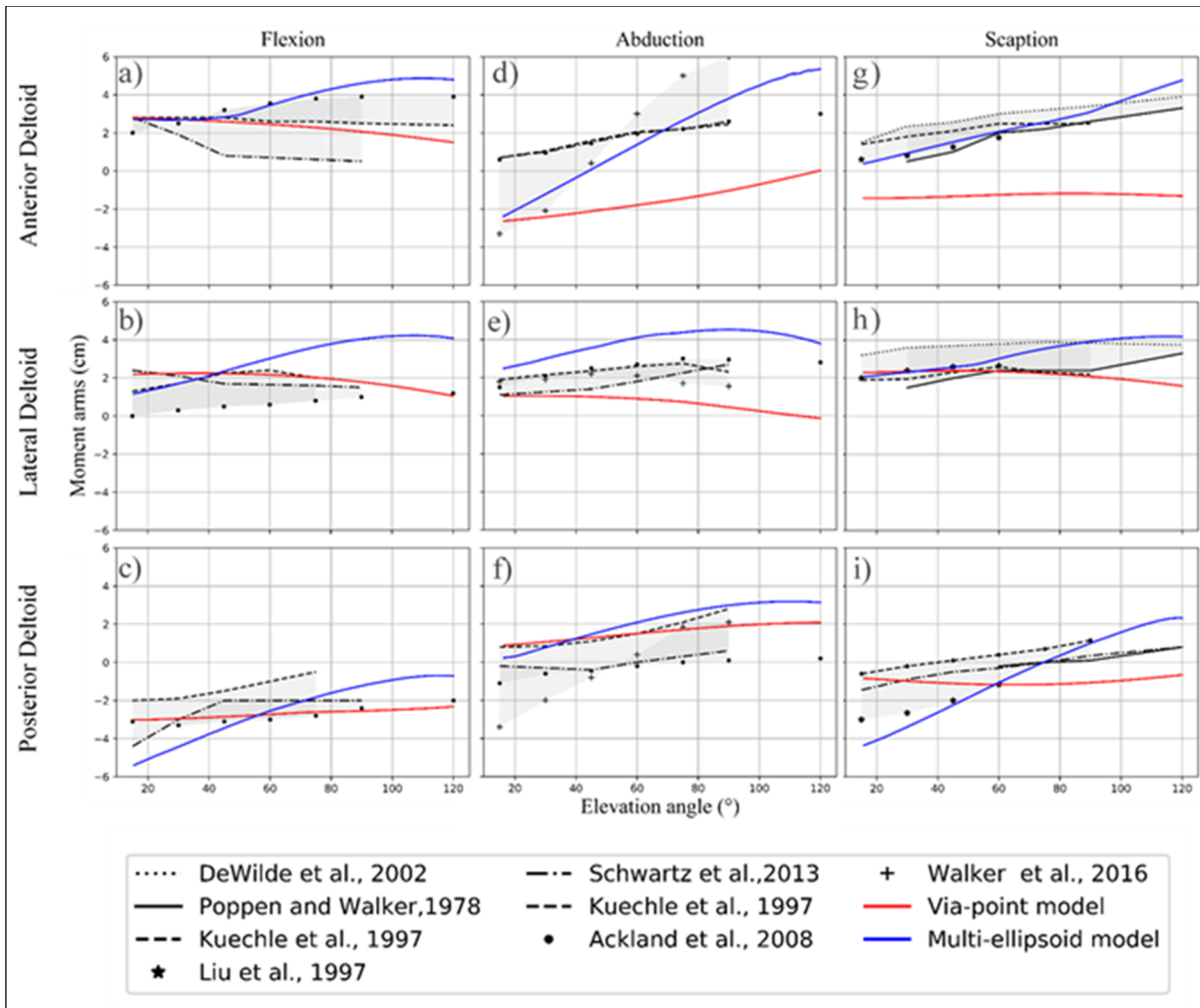


Figure 4-3. Predicted average anterior, lateral, posterior deltoid moment arms by the via-point (red) and the multi-ellipsoid (blue) models juxtaposed with literature data during flexion, abduction and scaption.

During the abduction movement, the biggest difference between the two models is observed in the anterior deltoid moment arms. In the via-point model, the anterior deltoid shows only adduction moment arms which vary from -2.83 cm (at 15 °) to -0.02 cm (at 120 °). In the multi-ellipsoid model, moment arms of the anterior deltoid change from adduction to abduction around 45 ° and vary from -2.38 cm (at 15 °) to 5.35 cm (at 120 °), which fits the experimental corridor (Figure 4-3). In the abduction, noticeable differences occur also in the moment arm prediction of the lateral deltoid. In the via-point model, abduction moment arm of the lateral

deltoid is underestimated compared to experimental data and varies from -0.13 cm (at 120 °) to 1.05 cm (at 15 °) vs 1.80 cm (at 15 °) to 2.20 cm (at 120 °) (Ackland et al., 2008). In the multi-ellipsoid model, abduction moment arms of the lateral deltoid is slightly overestimated and varies from 2.48 cm (at 15 °) to 4.51 cm (at 90 °) (Figure 4-3). In scaption, the anterior deltoid in the via-point model again shows exclusively adduction moment arms, from -1.42 cm (at 15 °) to -1.19 cm (at 120 °). The multi-ellipsoid model shows solely abduction moment arms of the anterior deltoid, which varies from -2.38 cm (at 15 °) to 5.35 cm (at 120 °) (Figure 4-3).

4.4.2 Muscle contributions to net joint moments

4.4.2.1 Flexion

During flexion, the main contribution to abduction, flexion and external rotation net joint moments comes from the anterior deltoid in both the via-point and the multi-ellipsoid model (Figure 4-4).

4.4.2.2 Abduction

During abduction, the biggest differences between the two models are observed for the abduction and external rotation joint moments. In the via-point model, mainly the lateral deltoid provides an abduction moment. To counterbalance this abduction moment, the subscapularis provides an adduction moment. In the multi-ellipsoid model, mainly the anterior and the lateral deltoids provide an abduction moment. In the via-point model, the net rotation moment varies from -17.88 Nm at 84 ° to -0.11 Nm at 0 °. Mainly the subscapularis and the lateral deltoid provide a moment in internal rotation. In the multi-ellipsoid model, the net rotation moment varies from -5.08 Nm at 120° to -0.05 Nm at 0°. Mainly the anterior deltoid provides internal rotation moment (Figure 4-4).

4.4.2.3 Scaption

During scaption, both models provide similar net abduction moments (max: 9.42 Nm—the via point model vs 9.62 Nm—the multi-ellipsoid model). However, in the via point model, mainly the lateral deltoid provides this abduction moment. The subscapularis provides an adduction moment. In the multi-ellipsoid model, mainly the lateral deltoid and the anterior deltoid provide the abduction moment (Figure 4-4).

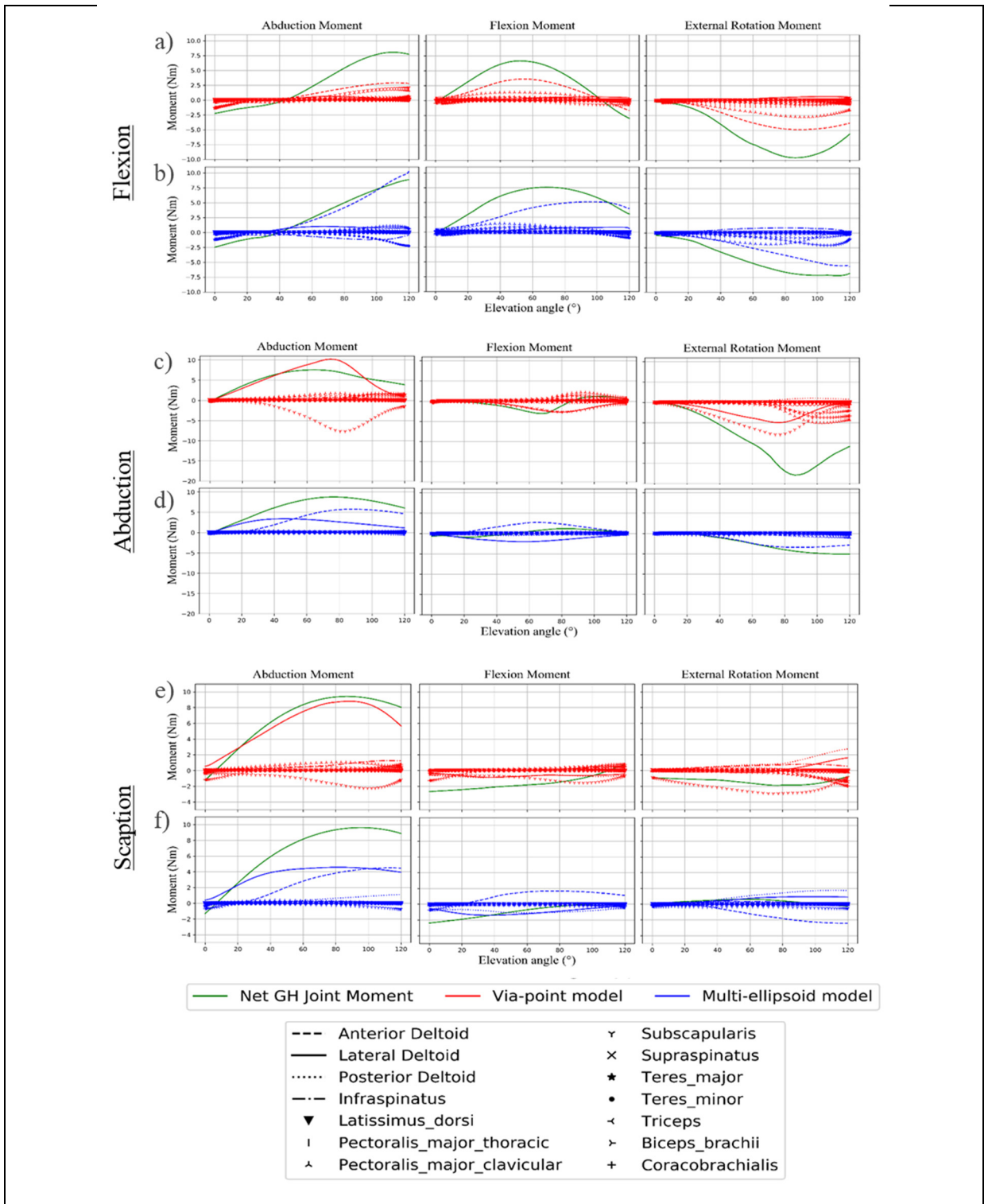


Figure 4-4. Predicted muscles contribution to joint 1) abduction, 2) flexion and 3) external rotation moments by the via-point (red) and the 2D-mesh (blue) models during flexion, abduction and scaption.

4.4.3 Muscle Contribution to Glenohumeral Joint Reaction Force

4.4.3.1 Flexion

In both models, the contribution to GHJ-RF comes mainly from the anterior deltoid. We observe similar trends in mediolateral, inferosuperior, anteroposterior forces (Figure 4-5).

4.4.3.2 Abduction

During abduction, we observe notable differences in the muscle contribution to GHJ-RF. In the via-point model, the anterior deltoid does not contribute to GHJ-RF (Figure 4-5). The lateral deltoid (max. 322 N) and the subscapularis (max. 191 N) are the main contributors to compressive (medial) force. The supraspinatus also provides notable shears, superior (max. 227 N) and posterior (max. 243 N) forces (Figure 4-5 f, h). In the multi-ellipsoid model, mainly the anterior (max. 168 N) and the lateral deltoid (max. 110 N) contribute to the compressive force (Figure 4-5).

4.4.3.3 Scaption

During scaption, important differences were observed between the two models in terms of muscle contribution to GHJ-RF. In the via-point model, the lateral deltoid mainly provides compressive force (max. 259 N) (Figure 4-5) with the support of the subscapularis (max. 80 N) and the posterior deltoid (max. 69 N) (Figure 4-5). Likewise, the subscapularis provides shear forces in the superior (max. 57 N) and posterior (max. 82 N) direction. In the multi-ellipsoid model, compressive force comes from the anterior deltoid (max. 141 N) and the lateral deltoid (max. 122 N) (Figure 4-5) with the support of the posterior deltoid (max. 43 N) (Figure 4-5).

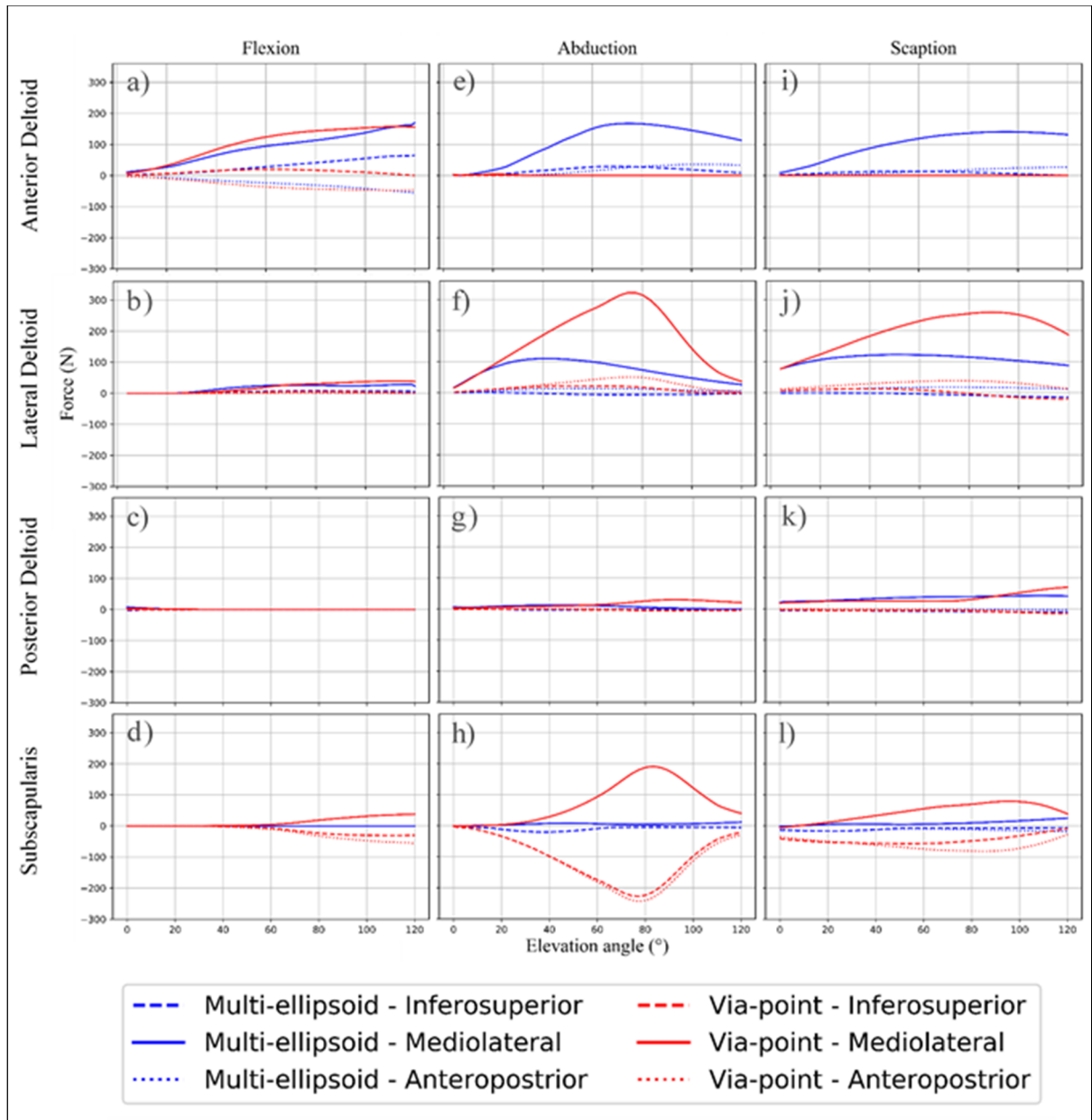


Figure 4-5. Predicted resultant force for upper limb muscles acting on the GHJ by the via-point (red) and the multi-ellipsoid (blue) models during flexion, abduction and scaption.

4.5 Discussion

In the present study, we developed a muscle wrapping approach called multi-ellipsoid wrapping to estimate the deltoid muscle trajectory in a multibody musculoskeletal shoulder

model. The approach is implemented in the AnyBody Managed Model Repository (AMMR) (Version 2.2.0) (Lund, Tørholm, Dzialo, & Jensen, 2019). We show that our model improves muscle fibers geometry during abduction and scaption movements; hence, it allows obtaining more realistic joint moments and muscle forces prediction compared to a model with rigidly fixed via-points.

The multi-ellipsoid model visually improves muscle fibers' geometry. Indeed, the rounded shape of the deltoid is reproduced while in the via-point model deltoid fibers adapt a V-shape. This is especially visible for the anterior deltoid, where the V-shape in the via-point model occurred above 45° (Figure 4-2). The most notable improvement in moment arms is found for abduction and scaption movements.

4.5.1 Anterior Deltoid Moment Arms

Cadaveric-based studies indicate that the anterior deltoid has abduction moment arms during the entire abduction movement (Ackland et al., 2008; Kuechle et al., 1997; Schwartz et al., 2013). Walker et al. 2016 found that the anterior deltoid works as an adductor below 40° of abduction and then above 40° it changes its function to abduction (Walker, Struk, Matsuki, Wright, & Banks, 2016). In the via-point model, the anterior deltoid shows only adduction moment arms during the entire abduction. This means that in this model the anterior deltoid acts as an antagonist, which is contrary to the literature findings (Hik & Ackland, 2019). The multi-ellipsoid model shows adduction moment arms below 45° of abduction. Above 45° , the anterior deltoid changes to abduction moment arms, which is in line with the findings of Walker et al. 2016 (Walker et al., 2016).

An improvement is also noticed during scaption motion. All cadaveric-based and numerical studies indicate abduction moment arms in the anterior deltoid (De Wilde et al., 2002; Kuechle et al., 1997; J. Liu et al., 1997; Poppen & Walker, 1978). In the via-point model, the anterior deltoid works solely as an adductor (antagonist) during scaption. In the multi-ellipsoid model, the anterior deltoid shows an abduction moment arm during the entire scaption.

4.5.2 Lateral Deltoid Moment Arms

Previously cited cadaveric-based studies show abduction moment arms for the lateral deltoid during the entire abduction movement (Ackland et al., 2008; Kuechle et al., 1997; Schwartz et al., 2013). In the via-point model, above 100° of abduction, the lateral deltoid moment arms changes to adduction. In the multi-ellipsoid model, the lateral deltoid shows abduction moment arms during entire movement, but its magnitude is slightly overestimated compared to the literature findings (Hik & Ackland, 2019).

4.5.3 Joint Moments and Forces

The biggest differences in the joint moment predictions are observed for the abduction. In the via-point model, the lateral deltoid almost exclusively contributes to the abduction moment. The antagonist muscle—the subscapularis, counteracted the extensive moment provided by the lateral deltoid. Consequently, the subscapularis muscle provides an internal rotation moment, which with the contribution of other muscles leads to a large internal rotation moment. Extensive joint abduction moment also results in high compressive loads in GHJ. Additionally, large rotation moment contributes to high shear forces provided by the subscapularis muscle. In the multi-ellipsoid model, both - the lateral and the anterior deltoid provides abduction moment. Therefore, mostly the lateral and the anterior deltoid contributes to compressive force in the GHJ. Important differences in terms of joint moments are also observed for the scaption movement. In the via-point model, mainly the lateral deltoid provides an abduction moment. The subscapularis provides an adduction moment to balance the joint moment provided by the lateral deltoid. Consequently, the subscapularis muscle also produces an extensive internal rotation moment. In the multi-ellipsoid model, the lateral deltoid provides abduction moments during the entire scaption motion and above 25° of arm elevation in conjunction with the anterior deltoid. However, the anterior deltoid provides the opposed flexion and rotation moments that need to be balanced by other muscles.

In brief, the multi-ellipsoid model solves the problem of non-anatomical fibers' trajectories and misleading anterior deltoid muscle function especially for abduction and scaption

movements. This approach is also reasonable in terms of computational time compared to the 3D-volumetric mesh representation (Blemker & Delp, 2005; Webb et al., 2014), that are known to be computationally expensive.

Some limitations of this modeling study need to be noticed. Firstly, we used a simple muscle model that neglects the force-length-velocity relationship. The use of a three elements Hill-type muscle model might improve muscle forces predictions (Zajac, 1989). However, this Hill-type muscle model requires careful calibration of muscle-tendon length and muscles physiological parameters as an input. Nevertheless, the aim of this study was to present an approach for deltoid muscle geometry modelling, not to evaluate the validity of muscles force prediction. Secondly, control ellipsoids are fitted manually to the bone geometry in the anatomical position. We believe that we can get better fit of control surfaces e.g. by using reconstructed muscle images. Especially, when it comes to the model scaling. This is considered as a next step in development of the multi-ellipsoid model. Finally, discrepancies in the existing literature about muscle moments arms (Hik & Ackland, 2019) suggest that subject specific validation needs to be performed to assess further development of the multi-ellipsoid model.

CHAPTER 5

A BIOMECHANICAL EXPLANATION OF THE CORRELATION BETWEEN THE CRITICAL SHOULDER ANGLE AND THE GLENOID COMPONENT LOOSENING IN THE NC TOTAL SHOULDER ARTHROPLASTY - MUSCULOSKELETAL MODELLING STUDY

Marta Strzelczak (1, 2), Lauranne Sins (2), Mickaël Begon (3, 4), Nicola Hagemeister (2, 5)

(1) École de technologie supérieure, Montréal, Canada

(2) Laboratoire de recherche en imagerie et orthopédie, Centre de recherche du CHUM, Montréal, Canada

(3) School of kinesiology and Exercise Science and Institute of biomedical engineering, Faculty of Medicine, University of Montreal, Montreal, Canada

(4) Research Centre, Sainte-Justine Hospital

(5) Département de génie des systèmes, École de technologie supérieure, Montréal, Canada

Paper submitted for publication, June 2021

5.1 Abstract

Background The glenoid loosening is the one of the most common complication in total shoulder arthroplasty. The correlation between the critical shoulder angle and glenoid loosening has been found (Watling et al. 2018). The critical shoulder angle is a morphological measurement connecting the line between the inferior and superior margins of the glenoid to the lateral aspect of the acromion.

Methods A large-scale musculoskeletal shoulder model was previously developed using the Anybody modelling platform (Anybody Technology, Aalborg, DK). An anatomical NC total shoulder prosthesis was integrated into the model.

Results The large CSA causes more superior position of the center of pressure. Reducing lateral acromion extension while maintaining superiorly tilted glenoid lowers the COP position. GHJ contact force and muscle forces increase with superior glenoid inclination and decrease with lateral extension of acromion.

Conclusion The superior position of COP caused by large critical shoulder angle might cause extensive superior edge loading, which can support glenoid component loosening. Additionally, more superior position of the humeral head can cause subacromial impingement and contribute to rotator cuff tear. Further studies are required to quantify the effect of the CSA on the glenoid loosening and answer the role of the CSA corrections before this measurement can be included in the surgical procedures

Keywords: musculoskeletal model, shoulder model, scapula, critical shoulder angle, glenoid loosening

5.2 Introduction

In the total shoulder arthroplasty (TSA), the glenoid loosening is one of the most common complications (Fox et al. 2009), which often leads to a revision surgery (Melis et al. 2012; Bonneville et al. 2013). It is commonly accepted that the glenoid loosening is a complex and multifactorial problem (Schumpf et al. 2011). Several risk factors have been identified as potential contributors to glenoid loosening. The most frequently identified factors are: rotator cuff tear (Franklin et al. 1988; Collins et al. 1992; Anglin et al. 2000), prosthetic mismatch (Walch et al. 2002), component fixation (Rahme et al. 2004), insufficient bony support (Cil et al. 2010), and glenoid component malpositioning (Farron et al. 2006). Recently, a correlation between the critical shoulder angle (CSA) and glenoid loosening was also highlighted (Watling et al., 2018).

The CSA is a morphological measurement determined usually on anteroposterior radiographs. This measurement was introduced by Moor et al. (2013) as the line connecting the inferior and superior margins of the glenoid to the lateral aspect of the acromion. This definition means that

a large CSA can be the result of either an increased lateral extension of the acromion, or a superiorly tilted glenoid. The excellent inter and intra-observer reliability was found in CSA measurement (Sankaranarayanan et al. 2020) - an undoubted asset in clinical practice. Several studies about the CSA focused on its correlation with rotator cuff tears and/or osteoarthritis. A large CSA ($\geq 35^\circ$) correlated with rotator cuff tear (Moor et al. 2013; Docter et al. 2019), while a small CSA ($\leq 28^\circ$) correlated with osteoarthritis (Moor et al. 2013; Moor et al. 2014; Spiegl et al. 2016; Bjarnison et al. 2017; Heuberger et al. 2017). However, less emphasis was devoted to assessing the impact of different CSA in the context of anatomical TSA. Watling et al. (2018) found the correlation between glenoid loosening and an increased CSA in midterm follow-up after TSA based on anteroposterior radiographs. They suggested that large CSA could cause extended superior loading on the glenoid component, and hence foster glenoid loosening. However, a causal link between the CSA and glenoid loosening cannot be explained due to the retrospective nature of this study. Several cadaveric and modelling studies quantified correlations between CSA and shoulder degeneration, however they employed intact GHJs (Engelhardt et al., 2017; Gerber et al., 2014; B. K. Moor et al., 2016; Villatte et al., 2020). According to our knowledge, there is no biomechanical study that specifically looked at the CSA in the context of anatomical TSA and glenoid loosening. In addition, it remains unclear whether a glenoid tilt has the same effect as an acromion length in the force distribution around the prosthetic shoulder joint.

The aim of this study was, therefore, to explore the effect of alterations of the CSA on the main factors of prosthetic glenoid component loosening, i.e. the position of the center of pressure (COP), glenohumeral joint (GHJ) contact force, and the deltoid and supraspinatus shear and compressive forces using a musculoskeletal model of the NC total shoulder arthroplasty during scapular plane abduction. The CSA was studied by varying acromion length and glenoid tilt independently to better understand their respective role in glenoid loosening process. In addition, we studied the combination of the short acromion with superior glenoid tilt and long acromion with inferior glenoid tilt, which lead to a normal CSA to account for the effect of surgical correction of the CSA.

5.3 Methods

An inverse dynamics multibody musculoskeletal model of the right upper-limb was previously developed in the Anybody Modelling System (Anybody Technology, Aalborg, DK) (Sins et al. 2015). An anatomical NC total shoulder prosthesis was integrated into the model as in Sins et al. (2015). The humeral head component has 51 mm in diameter. The mismatch between the humeral head and glenoid components was 6.4 mm as suggested in previous studies (Walch, 2002; Sins, 2016). The upper-limb was modelled with 11 degrees-of-freedom (DoF) namely: sternoclavicular (3-DoF), acromioclavicular (3-DoF), glenohumeral (3-DoF in rotation and 2-DoF in translation). More precisely, clavicle, scapula and glenohumeral kinematics were calculated from thoraco-humeral Eulerian angles using linear regressions of the scapulohumeral rhythm (De Groot & Brand, 2001). The anteroposterior and the inferior-superior joint translations were simulated using a force-dependent kinematic model (Andersen et al. 2017). Briefly, this model takes into account the joint elasticity and geometry and is based on a quasi-static equilibrium between forces in the inferior-superior and anteroposterior directions (Sins et al. 2015; Andersen et al. 2017). Therefore, this shoulder model is no longer a ball and socket representation of the GHJ. Elbow and wrist joints were locked in extended position. The model comprises 118 Hill-type muscle bundles, including intact rotator cuff and deltoid muscle. In contrast to the original model from Sins et al. (2015) the deltoid fiber trajectories were modelled with multi-ellipsoid approach.

The lateral acromion extension

A parametric representation of the acromion was imported into the musculoskeletal model. This representation contained all lateral deltoid insertion points so that it was possible to vary the lateral extension of the acromion by scaling it in the mediolateral direction in relation to the scapula coordinate system. The attachments of the other muscles were kept unchanged.

The glenoid inclination

The glenoid component was rotated around the anteroposterior axis within the anatomical range (Churchill et al., 2001). Sphere fitting function was used to find a new GHJ center after a superior and inferior tilt of glenoid.

Simulations

We simulated abduction from 15° to 120° in the scapular plane. The effect of the lateral acromion extension and the glenoid inclination were simulated independently. Specifically, we performed five simulations by changing CSA: 1) Normal CSA of 30° with 4° of glenoid superior inclination, which according to Moor et al. (2013) is not associated with GHJ pathologies. 2) Large CSA of 40° with 4° of glenoid inclination and extended lateral acromion. 3) Large CSA of 40° with 10° of glenoid component superior inclination (upward tilt) and unchanged lateral acromion. 4) Normal CSA of 30° with inferior glenoid inclination (downward tilt) and extended lateral acromion. 5) Normal CSA of 30° with superior glenoid inclination and shortened lateral acromion (Table 5-1). The output of the simulations for analysis were the displacement of the center of pressure, the GHJ contact force, and the deltoid and supraspinatus shear and compressive forces.

Table 5-1 Table summarizing five cases of CSA configurations simulated in the study.

	CSA	Glenoid inclination	Lateral acromion length
Case 1	30°	4°	Normal
Case 2	40°	4°	Extended
Case 3	40°	10°	Normal
Case 4	30°	-6°	Extended
Case 5	30°	10°	Shorten

5.4 Results

5.4.1 Center of pressure

The two large CSA configurations (cases 2 and 3) caused more superior glenoid component loading (Figure 5-1).

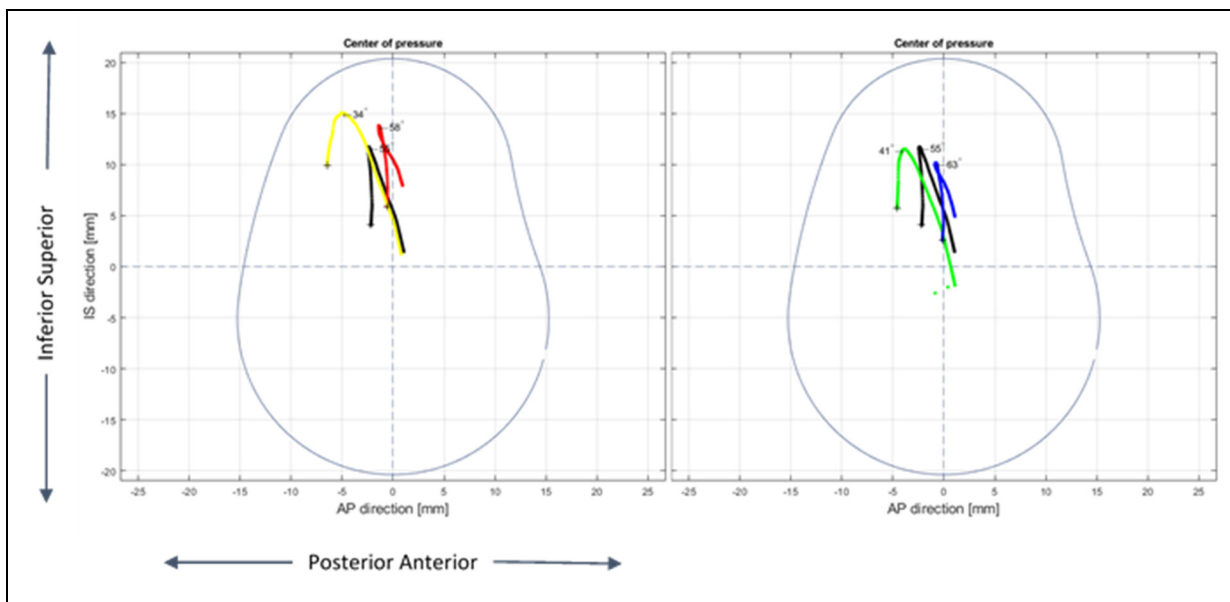


Figure 5-1. The projection of the center of pressure (COP) position on the glenoid component. Normal CSA (case 1) in black; large CSA with extended lateral acromion (case 2) in yellow; red: case 3 – large CSA with upward glenoid tilt; blue: case 4 – normal CSA with extended lateral acromion and downward glenoid tilt; green: case 5 – normal CSA with shorten lateral acromion and upward tilt. The cross correspond to the start of the movement.

For the large CSA with higher lateral acromion extension, the position of the COP shifted posteriorly for about 4 mm and superiorly between 6 mm to 3 mm at lower abduction angle. After 60° of abduction, the position of COP nearly follows the position COP of normal CSA. For the large CSA with upward glenoid tilt, the position of COP shifted anteriorly and

superiorly during the entire movement. Superior shift was about 3 mm and anterior shift was about 2 mm compared to normal CSA. The reduction of the acromion length moved the COP more inferiorly even with superiorly tilted glenoid. The same effect was observed for the glenoid inferior tilt and long acromion extension.

5.4.2 Contact force

Later extension of the acromion reduced GHJ contact force (Figure 5-2) despite the greater size of the CSA compared to the normal CSA (case 1). Correction of the CSA by an inferior tilt of the glenoid component (case 4) led to a decreased GHJ contact force but the value is still inferior to the normal CSA.

The opposite effect was observed for glenoid inclination. Despite the greater CSA, the upward glenoid inclination (case 3) increased GHJ contact force compared to the normal CSA (case 1). Short acromion (case 5) increases GHJ contact force, but the value is superior to one observed in the case 1.

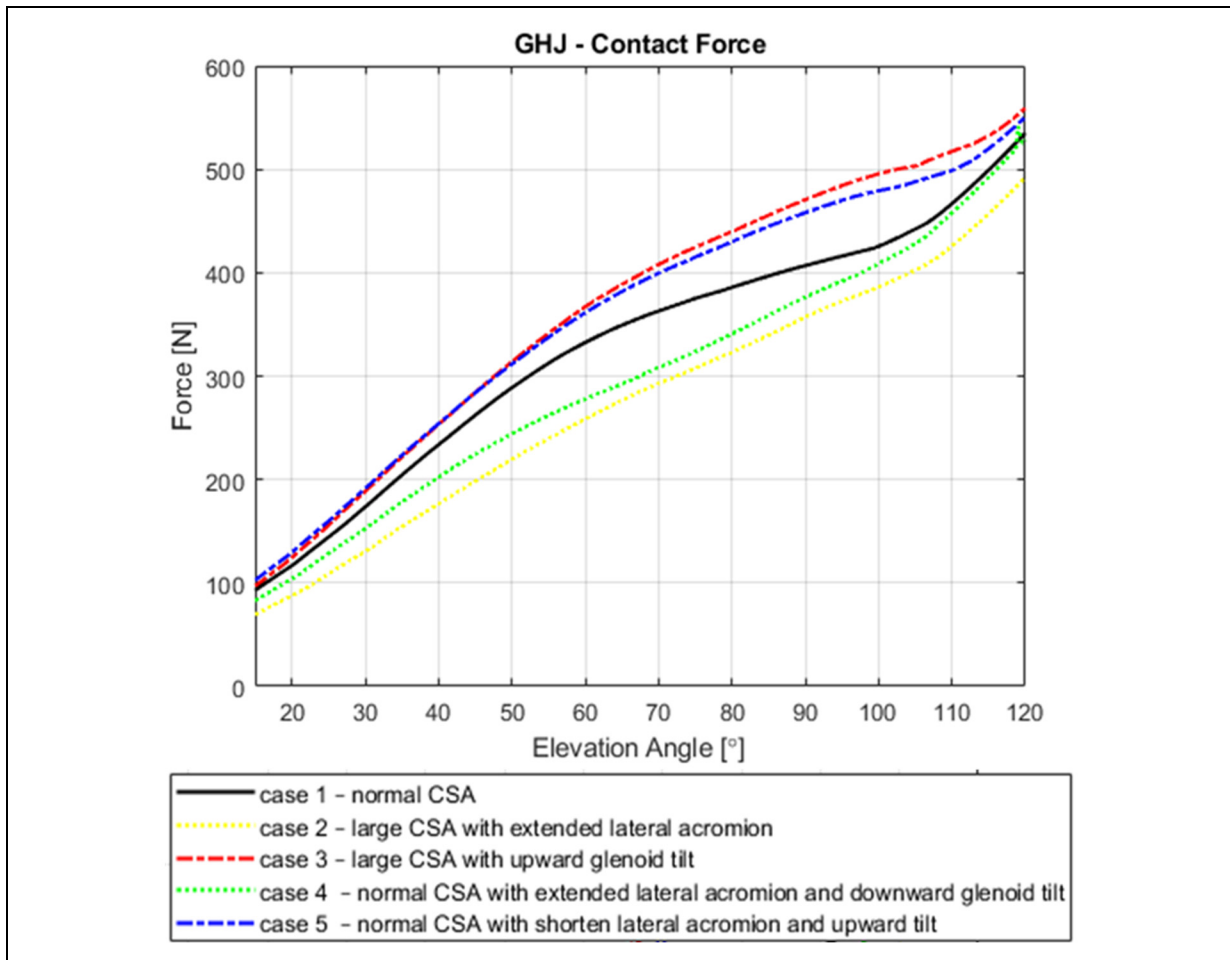


Figure 5-2. Glenohumeral joint contact force from 15° to 120° of shoulder abduction, simulated for five different variants of CSA.

5.4.3 Muscle forces.

Analogous effect to GHJ contact force was observed in muscle forces (Figure 5-3).

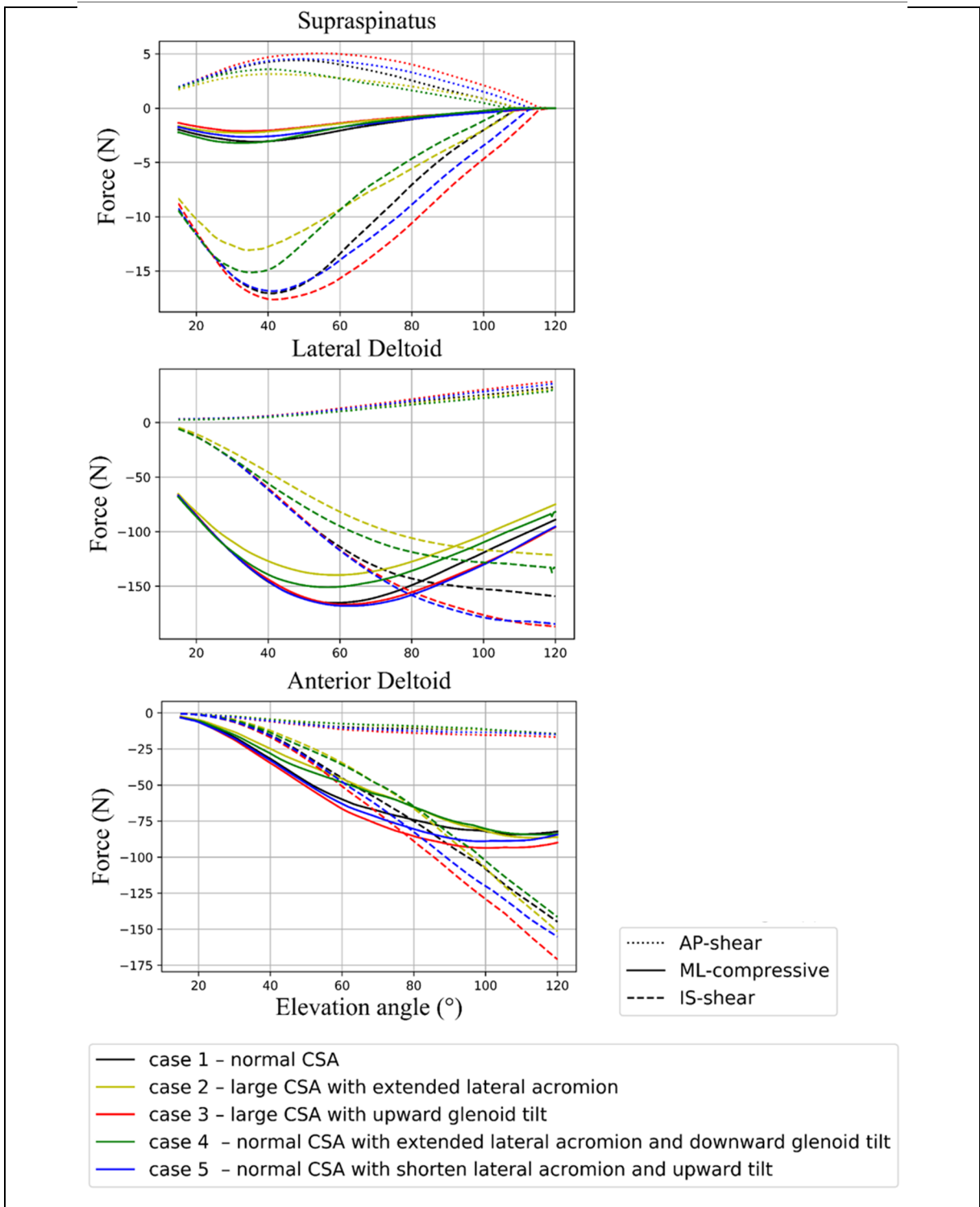


Figure 5-3. Supraspinatus, anterior and lateral deltoid shear and compressive forces simulated for the five different variants of CSA.

Anterior and lateral deltoid mean compressive force decreased for the extended lateral acromion with increased CSA (case 2). Likewise, both deltoid and supraspinatus mean inferior-superior shear forces decreased in the case 2. The highest relative difference was observed in lateral deltoid inferior-superior shear force (24% at 81° of abduction) and in anterior deltoid compressive force (31% at 63° of abduction). Correcting CSA by tilting the glenoid component inferiorly (case 4) caused an increase in the inferior-superior shear and compressive force of lateral deltoid, but these forces still remained higher than in the case 1. The opposite effect on muscles forces was observed in the case of large CSA with inferiorly tilted glenoid (case 3), where mean muscle inferior-superior shear and compressive forces increased compared to a normal CSA from the case 1. The highest relative difference was observed in anterior deltoid inferior-superior shear force (18% at 115° of abduction) and anterior deltoid compressive force (12% at 101° of abduction). After shortening the acromion to correct the CSA (case 5), shear and compressive forces of anterior deltoid and supraspinatus inferior-superior shear force decreased, but remained higher than in the normal CSA from case 1.

5.5 Discussion

In the present study, we evaluated the effect of an alteration of the CSA on GHJ biomechanics in NC TSA using a musculoskeletal shoulder model. In addition, we evaluated two cases, which aim at replicating a correction of the CSA to normal values by either acromion reduction or glenoid inferior tilt. Their respective impact on the main biomechanical parameters responsible for prosthetic glenoid loosening were quantified: COP position, GHJ contact force, deltoid and supraspinatus shear and compressive forces during scapular plane abduction. The present study leads to two main findings. Firstly, a large CSA leads to a more superiorly placed COP, which hypothetically can be moved more inferiorly by correcting the CSA by either acromion reduction or glenoid tilting. Secondly, large acromion extension shows different force patterns around the GHJ compared to superiorly tilted glenoid regardless of the size of CSA.

Several studies quantified correlations between CSA and shoulder degeneration. Two studies used shoulder simulators to analyze the effect of acromion length (Gerber et al. 2014) and glenoid tilt (Moor et al. 2016) during scapular plane abduction. Moor et al. (2016) found that, for the superiorly tilted glenoid, shear joint reaction force increased for the whole movement and compressive joint reaction force increased above 40°. These results are consistent with our findings since we observed increased superior shear force for both deltoid and supraspinatus as well as increased joint contact force. Gerber et al. (2014) found that increased lateral acromion extension decreased the compressive component of the joint reaction force for the whole motion and increased superior shear force in the low and middle range of abduction movement. Our results also show the reduction of GHJ contact force with increased lateral acromion extension. However, in our simulations, muscles superior shear force decreased in the low and middle range of abduction, which certainly affects total shear force at the GHJ. Studies using biomechanical models also investigated the effects of variations of the CSA on GHJ biomechanics. Villatte et al. (2020) used a musculoskeletal model to evaluate muscle forces and GHJ reaction force for several values of the CSA by modifying the attachment points of the lateral deltoid. They found that increased CSA produced higher superior shear forces and lower compressive force compared to the normal CSA. However, their three-DoF ball and socket joint model neglects joint translations which is a key factor in the mechanism of glenoid loosening. Engelhardt et al. (2017) combined a musculoskeletal model and a finite element model to assess effect of lateral acromion extension, glenoid inclination and the CSA on the glenohumeral translations and cartilage strain at 60° of scapular plane abduction. They found a positive correlation between CSA and humeral head migration, which is consistent with our results.

Watling et al. (2018) proposed that CSA measurement during anatomical TSA could be used as a prognostic factor to identify patients at risk for glenoid component loosening and maybe a modifiable factor during surgery to improve surgical outcomes. The most relevant choice for CSA correction in TSA would be to place the glenoid component in a more favorable inclination, if remaining bone stock allows for it. However, as it was mentioned before, large CSA may also be the result of more laterally extended acromion. Should the surgeon tilt the

glenoid more inferiorly in this case? Our results show that placing glenoid more inferiorly lowers the COP position, even if the lateral acromion remains extended. Thus, it allows reducing the loads at the superior edge and wider subacromial space. Yet, based on our simulations, this will not completely restore the forces balance around the GHJ. Another, surgical procedure that allows the CSA correction is a reduction of the acromion extension through acromioplasty. It has been shown that carefully performed arthroscopic acromioplasty, can reduce the CSA without deltoid attachment damage (Katthagen et al. 2016; Gerber et al. 2018). However, the study of Olmos et al. (2020) has shown that lateral acromioplasty cannot sufficiently reduce the CSA over 40°. In addition, it remains unclear whether the correction of the CSA through lateral acromioplasty would bring the desired effect, namely minimizing the risk of developing rotator cuff tear and preventing a re-tear (MacDonald, McRae, Leiter, Mascarenhas, & Lapner, 2011). According to our knowledge, there is no evidence if lateral acromioplasty can prevent glenoid loosening. However, it should be emphasized that rotator cuff tear is often associated with glenoid loosening (Franklin et al. 1988; Collins et al. 1992; Anglin et al. 2000). Our results show that reducing lateral acromion extension while maintaining superiorly tilted glenoid lowers the COP position, thereby releasing edge loads and potentially preventing subacromial impingement, but has a minimal effect on the distribution of the forces around GHJ. Based on our simulations, we can draw the general conclusions that the COP position is sensitive to the CSA. Force distribution around the GHJ would rather be sensitive to superior glenoid inclination and lateral acromion extension alone. Our results suggest that measurement of the CSA in some cases might be insufficient to recommend its correction and choose the most appropriate surgical procedure.

The novelty of our study is the use of musculoskeletal model of the shoulder, which allows for the glenohumeral head translations, in contrast to other models used to evaluate the CSA, which includes stability constraints at GHJ. The generic morphology with modifiable parameters such as glenoid tilt and acromion length, allows a controlled investigation. Yet, the use of generic model is undoubtedly a simplification. Model personification based on the anatomy of patients with morphological variability and evaluation of more complex movements would be a great insight to this study. Additional finite element analysis would

also be beneficial for a more detailed examination of the CSA impact on GHJ biomechanics. The other limitation is that our study focused only on the scapula morphology and more specifically the CSA. Glenoid loosening is known as a multifactorial problem. It is also important to determine the importance of shoulder morphology and the CSA among other risk factors for the glenoid loosening.

Further clinical and biomechanical studies are required to quantify the effect of the CSA on the glenoid loosening and answer the role of the CSA corrections before this measurement can be included in the surgical procedures. We believe that our study brings important understanding to the biomechanical impact of shoulder morphology and more specifically the CSA in the context of TSA. Nevertheless, our results should be treated as exploratory.

5.6 Conclusion

In this study, the large scale musculoskeletal shoulder model was used to discover the effect of the CSA on GHJ biomechanics and potential glenoid loosening. The CSA was studied by varying acromion length and glenoid tilt independently to better understand their respective role on glenoid loosening process. The large CSA causes more superior position of the COP. The reduction of the CSA lower the COP position. GHJ contact force and muscle forces are not particularly sensitive to the size of the CSA. GHJ contact force and muscle forces increase with superior glenoid and decrease with lateral extension of acromion.

CHAPTER 6

GENERAL DISCUSSION

6.1 Thesis Summary

The primary aim of this thesis was to create a biomechanical tool to better understand the effect of scapular morphology changes on GHJ biomechanics in the context of NC-TSA. The first phase, related to the technical problem, aimed to improve an existing musculoskeletal shoulder model (Sins et al., 2015) and make it suitable to investigate movements above 90° of thoracohumeral abduction. Two methodological approaches were developed, the first one by using a 2D-mesh approach and the second one using a 3D wrapping approach for the deltoid muscle representation. The second phase, related to the clinical problem, aimed to assess the variability of the CSA on the biomechanics of the GHJ after NC-TSA and potential glenoid component loosening. In order to carry out the second phase of this thesis, the geometrical model of the deltoid muscle required improvement. Hence, the second phase also aimed at demonstrating the feasibility of using the model for clinical question related to the impact of scapula's morphology.

The findings related to the technical problem are described in the Chapter III and Chapter IV. Sins et al. (2015) implemented humeral head translation and contact calculations to the large-scale musculoskeletal model of the upper extremity from the Anybody Modeling System (Damsgaard et al., 2006). Starting from this model, the purpose of the work presented here was to improve the geometrical representation of the deltoid muscle. The lateral and posterior compartments of the deltoid muscle are attached to the scapula. Therefore, a correct geometric representation of the deltoid is essential in the analysis of the scapula morphology on the GHJ biomechanics. Two approaches were proposed and evaluated, namely a 2D-mesh approach (Chapter III) and a multi-ellipsoid wrapping approach (Chapter IV).

In Chapter III, we presented the 2D-mesh model implemented to the deltoid muscle. This solution is based on adding transvers constraints between muscles lines of action, which allow

to maintain deltoid muscle shape and removed previously used via-points. The 2D-mesh model showed improvements in reproducing deltoid muscle geometry. In fact, by integrating transverse constrains into the deltoid model, the rounded contour of deltoid muscle fibers overlying humeral head was maintained, whereas in the via-point model anterior fibers adopt a V-shape around 45° of arm elevation and lateral fibers adopt a V-shape around 90° . The 2D-mesh largely solves the problem of non-physiological fibers trajectories and misleading anterior deltoid function related to the moment arms. The 2D-mesh model leads to more consistent muscle activation patterns and GHJ-contact force estimation during scapular plane abduction than previously used via-point model.

Chapter IV described our multi-ellipsoid wrapping approach. This solution allows to place wrapping surfaces in a systematic way and control the deltoid muscle shape due to the use of one longitudinal ellipsoid for each muscle fiber. The multi-ellipsoid approach was implemented directly to the full body model and has been made available to the larger modeling community through Anybody modelling repository (Lund et al., 2019), which represents a valuable knowledge translation. One main advantage of this approach is that scaling is possible due to the connection of the control surface to the anatomical landmarks. In brief, the multi-ellipsoid model solves the problem of non-anatomical fibres trajectories and non-physiological anterior deltoid muscle function that was still present in the 2D-mesh model. The deltoid muscle moment arms are consistent with the literature. The improvement is especially notable for the anterior deltoid. The multi-wrapping ellipsoid approach restores abduction moment arm of anterior deltoid during abduction. This approach is also reasonable in terms of computational time compared to the 3D-volumetric mesh representation (Blemker & Delp, 2005; M. Hoffmann, Begon, Lafon, & Duprey, 2020; Webb et al., 2014), that are known to be computationally expensive.

In Chapter V, we highlighted the usefulness of the model in a clinical application. The study described in Chapter III aimed at exploring the impact of the morphological parameter called the critical shoulder angel on the biomechanics of the GHJ after TSA and potential glenoid loosening. The CSA in the model was modified by varying the acromion length and the glenoid

inclination independently to better understand their respective role on glenoid loosening process. Results show that a large CSA causes more superior position of the COP compared to a normal CSA. Reducing lateral acromion extension or superior glenoid tilt lowers the COP position. An increased glenoid inclination augments GHJ reaction force while acromion lengthening reduced GHJ contact force despite the CSA size. GHJ contact force and muscle forces are not particularly sensitive to the size of the CSA, but rather to the glenoid inclination and the acromion extension alone. GHJ contact force and muscle forces increases with superior glenoid inclination and decrease with lateral extension of acromion. The superior position of COP might cause extensive superior edge loading, which can support glenoid component loosening. Additionally, more superior position of the humeral head can cause subacromial impingement and contribute to rotator cuff tears. While this study was exploratory, it provides an important insight to the effect of the CSA on glenoid component loosening and can help surgeons to better understand the biomechanical consequences of the large CSA. Whether and when the great CSA should be corrected remains an open question and should be the subject of further investigation.

6.2 Limitations and Recommendations for Future Research

Limitations of presented work are listed and discussed below. With these limitations recommendations for the future research are proposed.

Compared to the via-point approach, the 2D-mesh model leads to more consistent predictions in terms of muscle moment arms and internal forces. However, it increases the computation time and requires additional constraints to be able to simulate more complex movements. In search of a solution to the latter drawback, the multi-ellipsoid wrapping approach was developed. However, some limitations remain to be solved in this approach, which might be the motivation for further research.

The first limitation is that the size, position and orientation of the wrapping ellipsoids is estimated based on the bone geometry from the model. Possibly a more accurate solution

would be to fit control surfaces to the reconstructed images of the deltoid muscle. The use of diffusion tensor imaging would be particularly interesting since it has a capacity to capture muscle fiber orientation. Hence, diffusion tensor imaging may improve the development of the multi-ellipsoid approach and ensure its validity. Nonetheless, it has to be noted that the aim of Chapter IV was to present an alternative and more structured approach for the deltoid muscle wrapping and to show its additional advantage over the previously used via-point model. Scaling and more extensive validation of this approach should be the aim of the future research. Another limitation comes from the representation of the muscle model as one-dimensional massless strings. The muscle volume, shape and deformation are basically neglected in this approach. Volumetric models based on MRI are developed alternatively to the string models (Blemker & Delp, 2005; Webb et al., 2014). They are not yet suitable for the static optimization, but in the future, they can give the possibility to account of the complex behavior of muscle tissue.

The Chapter V focused on the one morphological measurement, namely the critical shoulder angle. The morphology of the scapula is very complex and presents considerable inter-individual variability. Adding more morphological measurements and performing a parametric analysis based on the prospective cohort design would allow to evaluate the impact of each measurement on the GHJ biomechanics and to deliver recommendations for clinical practitioners about the relevance of each measurement.

The methodological limitation of the Chapter V is the use of a generic model, which is based on one cadaveric specimen. Medical technology tends to move towards personalized solutions. This trend is also visible in musculoskeletal modelling. Terms as ‘patient-’ or ‘subject-specific’ are generally used to describe models in which bone geometry was modified to match the specific subject. Bone geometry can be personalized using different methods from different scaling methods (Lund, Andersen, de Zee, & Rasmussen, 2015) to bone morphing based on reconstructed medical images (Marra et al., 2015). However, model personalization not only required specific data, which sometimes is difficult to obtain, but it is also time consuming with the use of current techniques. In addition, there is still no clear evidence for advantages

of the subject-specific models over generic ones. For many musculoskeletal studies which aim to answer the ‘what if’ question, the solutions could be to create parametric models that cover morphological variability in the population. Therefore, combining multibody musculoskeletal modelling with statistical shape models (Casier et al., 2018; Mutsvangwa, Burdin, Schwartz, & Roux, 2015) could be a useful approach in many clinically related applications. Statistical shape models allow capturing the natural variability of bone geometry. Yet, this approach necessitates access to large data sets of medical images to create accurate and representative model. Furthermore, to make a model truly ‘subject-specific’ not only subject morphology should be taken into account but also musculotendon properties. For many models, cadaveric specimens are used to obtain musculotendon properties. However, there are not necessarily representative for the entire population, especially when shoulder injuries are present. Scaling optimization algorithms (Manal & Buchanan, 2004; Modenese, Ceseracciu, Reggiani, & Lloyd, 2016) are used to estimate musculotendon properties such as a muscle and tendon slack lengths and maximum isometric force. However, it has been found that these parameters are not directly dependent on the subject anthropometry (Winby, Lloyd, & Kirk, 2008). The Hill-type model is particularly sensible to the tendon slack length (Ackland et al., 2012). Thus, it seems to be important to include this variation into the musculoskeletal models. The progress in the medical imaging can be promising to do so. Especially diffusion tensor imaging can be an interesting tool to discover more about muscle architecture and incorporate inter-individual variability into the musculoskeletal models (Charles, Grant, D’Août, & Bates, 2020). Then, the predicted muscle force with parameters obtained from diffusion tensor imaging could be validated with the use of experimental tools such as an isokinetic dynamometer (Karabay, Yesilyaprak, & Sahiner Picak, 2020).

On another topic, it must be pointed out that in this work only abduction in the scapular plane was simulated. The choice of this movement comes from the fact that most of the available data in the literature that can be used for model validation is limited to simple movements, especially scapular plane abduction. This is usually justified by the fact that according to the clinical studies most of daily-life movements occur below 45° of abduction. However, movements that occur above the neck are also very common in daily life and they are often

related to pain and/or impairments. Studying more realistic movements would be undoubtedly beneficial for clinical applications of musculoskeletal models. The common practice is to drive model kinematics with the data from optical markers, inertial sensors or fluoroscopy. However, the data collection is time consuming and requires special equipment. Kinematical data collection is rare in clinical practice. The development of statistical models of human kinematics is a promising approach to drive musculoskeletal models. The construction of this approach requires an extensive amount of kinematic data. Yet, once a model is created, kinematics can be personalized based on *e.g.* subjects anthropometry, sex or disorders. Presently, statistical models are created mostly for running and gait analysis. Creation of this type of model for upper-limb movements may strengthen predictive capacities of the musculoskeletal shoulder modelling.

Model validation remains an important issue in musculoskeletal modeling. The presented model was validated only with the use of data from literature, which allows mostly for qualitative and indirect validation. For example the in-vivo GHJ reaction force from Bergmann et al. (2011) does not contain patients' kinematics, which limits the relevance of its use in validation. More efforts should be put into the development of the new validation methods based on experimental data. In addition, more studies should focus on data collection for musculoskeletal model validation purposes. Raw data should be published, and collection process should be precisely described to make it possible to repeat the experiment if necessary. Comprehensive and coherent data sets would also be very useful for the model validation and development. A good example of excellent data set for the musculoskeletal model validation is the Grand Challenge Competition to Predict in Vivo Knee Loads (Fregly et al., 2012). Unfortunately, the data is only available for the knee joint. Similar data sets for the shoulder joint would definitely strengthen shoulder models' development and make them more valuable in clinical practice.

CONCLUSION

The first objective behind this thesis was to address a drawback in musculoskeletal shoulder modeling by improving the geometrical representation of the deltoid muscle. The new geometrical model aimed at eliminating non-physiological muscle fibers trajectories and permitting investigation of larger range-of-motion. The second objective aimed at assessing the variability of scapular morphology on GHJ biomechanics and potential glenoid component loosening with previously established model. Two solutions were proposed and assessed to overcome the limitation associated with the geometric representation of the deltoid muscle. Both solutions are intended to remove via-points that cause a non-physiological muscle path in high abduction angle. The first proposition is based on a 2D-mesh model, which contains transverse constraints between muscle fibers. The 2D-mesh model was evaluated against experimental data resulting in more realistic deltoid muscle moment arms and prediction of muscle and joint reaction forces. The second proposition contains creating muscle wrapping approach, called multi-ellipsoid wrapping. This solution also improved the deltoid muscle moment arms and prediction of the internal forces. Additionally, the multi-ellipsoid wrapping is less computationally expensive and suitable for the simulation of daily-life activities in comparison to the 2D-mesh model. Subsequently, established musculoskeletal model was used to study the effect of large CSA on the prosthetic GHJ biomechanics to better understand the influence of the shoulder morphology on the potential glenoid component loosening. Findings of this study shows that a large CSA causes more superior position of the COP compared to a normal CSA. The superior position of COP might result in extensive superior edge loads. GHJ contact force and muscle forces are not particularly sensitive to the size of the CSA.

BIBLIOGRAPHY

- Ackland, D. C., Lin, Y. C., & Pandy, M. G. (2012). Sensitivity of model predictions of muscle function to changes in moment arms and muscle-tendon properties: A Monte-Carlo analysis. *Journal of Biomechanics*, 45(8). <https://doi.org/10.1016/j.jbiomech.2012.02.023>
- Ackland, D. C., Pak, P., Richardson, M., & Pandy, M. G. (2008). Moment arms of the muscles crossing the anatomical shoulder. *Journal of Anatomy*, 213(4), 383–390. <https://doi.org/10.1111/j.1469-7580.2008.00965.x>
- Alpert, S. W., Pink, M. M., Jobe, F. W., McMahon, P. J., & Mathiyakom, W. (2000). Electromyographic analysis of deltoid and rotator cuff function under varying loads and speeds. *Journal of Shoulder and Elbow Surgery*, 9(1), 47–58. <https://doi.org/10.1103/PhysRevE.77.031608>
- Andersen, M. S., De Zee, M., Damsgaard, M., Nolte, D., & Rasmussen, J. (2017). Introduction to force-dependent kinematics: Theory and application to mandible modeling. *Journal of Biomechanical Engineering*, 139(9), 091001. <https://doi.org/10.1115/1.4037100>
- Anderson, F. C., & Pandy, M. G. (2001). Dynamic optimization of human walking. *Journal of Biomechanical Engineering*, 123(5). <https://doi.org/10.1115/1.1392310>
- Anglin, C., Wyss, U. P., & Pichora, D. R. (2000). Mechanical testing of shoulder prostheses and recommendations for glenoid design. *Journal of Shoulder and Elbow Surgery*, 9(4). <https://doi.org/10.1067/mse.2000.105451>
- Arden, N., & Nevitt, M. C. (2006). Osteoarthritis: Epidemiology. *Best Practice and Research: Clinical Rheumatology*. <https://doi.org/10.1016/j.berh.2005.09.007>
- ASME. (2006). Guide for Verification and Validation in Computational Solid Mechanics. *American Society of Mechanical Engineers*, (March).
- Balke, M., Schmidt, C., Dedy, N., Banerjee, M., Bouillon, B., & Liem, D. (2013). Correlation of acromial morphology with impingement syndrome and rotator cuff tears. *Acta Orthopaedica*, 84(2). <https://doi.org/10.3109/17453674.2013.773413>
- Baumgartner, D., Tomas, D., Gossweiler, L., Siegl, W., Osterhoff, G., & Heinlein, B. (2014). Towards the development of a novel experimental shoulder simulator with rotating scapula and individually controlled muscle forces simulating the rotator cuff. *Medical and Biological Engineering and Computing*, 52(3). <https://doi.org/10.1007/s11517-013-1120-z>
- Bergmann, G., Graichen, F., Bender, A., Rohlmann, A., Halder, A., Beier, A., & Westerhoff,

- P. (2011). In vivo gleno-humeral joint loads during forward flexion and abduction. *Journal of Biomechanics*, 44(8), 1543–1552. <https://doi.org/10.1016/j.jbiomech.2011.02.142>
- Bigliani, L. U., Morrison, D. S., & April, E. W. (1986a). The morphology of the acromion and its relationship to rotator cuff tears. *Ortho Trans*, 10.
- Bigliani, L. U., Morrison, D. S., & April, E. W. (1986b). The morphology of the acromion and its relationship to rotator cuff tears. *Ortho Trans*, 10, 228.
- Billuart, F., Devun, L., Skalli, W., Mitton, D., & Gagey, O. (2008). Role of deltoid and passives elements in stabilization during abduction motion (0 degrees-40 degrees): an ex vivo study. *Surgical & Radiologic Anatomy*, 30(7).
- Bishop, J. L., Kline, S. K., Aalderink, K. J., Zuel, R., & Bey, M. J. (2009). Glenoid inclination: In vivo measures in rotator cuff tear patients and associations with superior glenohumeral joint translation. *Journal of Shoulder and Elbow Surgery*, 18(2). <https://doi.org/10.1016/j.jse.2008.08.002>
- Blache, Y., Begon, M., Michaud, B., Desmoulins, L., Allard, P., & Maso, F. D. (2017). Muscle function in glenohumeral joint stability during lifting task. *PLoS ONE*. <https://doi.org/10.1371/journal.pone.0189406>
- Blemker, S. S., & Delp, S. L. (2005). Three-dimensional representation of complex muscle architectures and geometries. *Annals of Biomedical Engineering*, 33(5), 661–673. <https://doi.org/10.1007/s10439-005-1433-7>
- Blonna, D., Giani, A., Bellato, E., Mattei, L., Caló, M., Rossi, R., & Castoldi, F. (2016). Predominance of the critical shoulder angle in the pathogenesis of degenerative diseases of the shoulder. *Journal of Shoulder and Elbow Surgery*. <https://doi.org/10.1016/j.jse.2015.11.059>
- Bohsali, K. I., Bois, A. J., & Wirth, M. A. (2017). Complications of shoulder arthroplasty. *Journal of Bone and Joint Surgery - American Volume*. <https://doi.org/10.2106/JBJS.16.00935>
- Bolsterlee, B., Veeger, D. H. E. J., & Chadwick, E. K. (2013). Clinical applications of musculoskeletal modelling for the shoulder and upper limb. *Medical and Biological Engineering and Computing*. <https://doi.org/10.1007/s11517-013-1099-5>
- Bright, A. S., Torpey, B., Magid, D., Codd, T., & McFarland, E. G. (1997). Reliability of radiographic evaluation for acromial morphology. *Skeletal Radiology*, 26(12). <https://doi.org/10.1007/s002560050317>
- Brown, J. M. M., & Wickham, J. (2006). Neuromotor coordination of multisegmental muscle

- during a change in movement direction. *Journal of Musculoskeletal Research*, 10(2). <https://doi.org/10.1142/S0218957706001716>
- Buchanan, T. S., Moniz, M. J., Dewald, J. P. A., & Rymer, W. Z. (1993). Estimation of muscle forces about the wrist joint during isometric tasks using an EMG coefficient method. *Journal of Biomechanics*, 26(4–5). [https://doi.org/10.1016/0021-9290\(93\)90016-8](https://doi.org/10.1016/0021-9290(93)90016-8)
- Casier, S. J., Van den Broecke, R., Van Houcke, J., Audenaert, E., De Wilde, L. F., & Van Tongel, A. (2018). Morphologic variations of the scapula in 3-dimensions: a statistical shape model approach. *Journal of Shoulder and Elbow Surgery*, 27(12). <https://doi.org/10.1016/j.jse.2018.06.001>
- Castro, M. N., Rasmussen, J., Andersen, M. S., & Bai, S. (2019). A compact 3-DOF shoulder mechanism constructed with scissors linkages for exoskeleton applications. *Mechanism and Machine Theory*, 132. <https://doi.org/10.1016/j.mechmachtheory.2018.11.007>
- Charles, J. P., Grant, B., D’Août, K., & Bates, K. T. (2020). Subject-specific muscle properties from diffusion tensor imaging significantly improve the accuracy of musculoskeletal models. *Journal of Anatomy*, 237(5). <https://doi.org/10.1111/joa.13261>
- Charlton, I. W., & Johnson, G. R. (2006). A model for the prediction of the forces at the glenohumeral joint. *Proceedings of the Institution of Mechanical Engineers, Part H: Journal of Engineering in Medicine*, 220(8). <https://doi.org/10.1243/09544119JEIM147>
- Charlton, Iain W., & Johnson, G. R. (2001). Application of spherical and cylindrical wrapping algorithms in a musculoskeletal model of the upper limb. *Journal of Biomechanics*, 34(9). [https://doi.org/10.1016/S0021-9290\(01\)00074-4](https://doi.org/10.1016/S0021-9290(01)00074-4)
- Cherchi, L., Ciornohac, J. F., Godet, J., Clavert, P., & Kempf, J. F. (2016). Critical shoulder angle: Measurement reproducibility and correlation with rotator cuff tendon tears. *Orthopaedics and Traumatology: Surgery and Research*. <https://doi.org/10.1016/j.otsr.2016.03.017>
- Churchill, R. S., Brems, J. J., & Kotschi, H. (2001). Glenoid size, inclination, and version: An anatomic study. *Journal of Shoulder and Elbow Surgery*, 10(4). <https://doi.org/10.1067/mse.2001.115269>
- Cil, A., Veillette, C. J. H., Sanchez-Sotelo, J., Sperling, J. W., Schleck, C. D., & Cofield, R. H. (2010). Survivorship of the humeral component in shoulder arthroplasty. *Journal of Shoulder and Elbow Surgery*, 19(1). <https://doi.org/10.1016/j.jse.2009.04.011>
- Codman, E. (1934). Tendinitis of the short rotators. In: The shoulder rupture of the supraspinatus tendon and other lesions in or about the subacromial bursa. *The Shoulder*. Boston: Thomas Todd.

- Collins, D., Tencer, A., Sidles, J., & Matsen, F. (1992). Edge displacement and deformation of glenoid components in response to eccentric loading. The effect of preparation of the glenoid bone. *Journal of Bone and Joint Surgery - Series A*, 74(4). <https://doi.org/10.2106/00004623-199274040-00005>
- Culham, E., & Peat, M. (1993). Functional anatomy of the shoulder complex. *Journal of Orthopaedic and Sports Physical Therapy*. <https://doi.org/10.2519/jospt.1993.18.1.342>
- Damsgaard, M., Rasmussen, J., Christensen, S. T., Surma, E., & de Zee, M. (2006). Analysis of musculoskeletal systems in the AnyBody Modeling System. *Simulation Modelling Practice and Theory*, 14(8), 1100–1111. <https://doi.org/10.1016/j.simpat.2006.09.001>
- Dawson, P. A., Adamson, G. J., Pink, M. M., Kornswiet, M., Lin, S., Shankwiler, J. A., & Lee, T. Q. (2009). Relative contribution of acromioclavicular joint capsule and coracoclavicular ligaments to acromioclavicular stability. *Journal of Shoulder and Elbow Surgery*, 18(2). <https://doi.org/10.1016/j.jse.2008.08.003>
- De Groot, J. H., & Brand, R. (2001). A three-dimensional regression model of the shoulder rhythm. *Clinical Biomechanics*, 16(9), 735–743. [https://doi.org/10.1016/S0268-0033\(01\)00065-1](https://doi.org/10.1016/S0268-0033(01)00065-1)
- De Wilde, L., Audenaert, E., Barbaix, E., Audenaert, A., & Soudan, K. (2002). Consequences of deltoid muscle elongation on deltoid muscle performance: A computerised study. *Clinical Biomechanics*, 17(7), 499–505. [https://doi.org/10.1016/S0268-0033\(02\)00065-7](https://doi.org/10.1016/S0268-0033(02)00065-7)
- Delp, S. L., & Loan, J. P. (1995). A graphics-based software system to develop and analyze models of musculoskeletal structures. *Computers in Biology and Medicine*, 25(1). [https://doi.org/10.1016/0010-4825\(95\)98882-E](https://doi.org/10.1016/0010-4825(95)98882-E)
- Desailly, E., Sardain, P., Khouri, N., Yepremian, D., & Lacouture, P. (2010). The convex wrapping algorithm: A method for identifying muscle paths using the underlying bone mesh. *Journal of Biomechanics*, 43(13). <https://doi.org/10.1016/j.jbiomech.2010.05.005>
- Deshmukh, A. V., Koris, M., Zurakowski, D., & Thornhill, T. S. (2005). Total shoulder arthroplasty: Long-term survivorship, functional outcome, and quality of life. *Journal of Shoulder and Elbow Surgery*, 14(5). <https://doi.org/10.1016/j.jse.2005.02.009>
- Díaz, Á. C., de Soto, P. C. M., & Uroz, N. Z. (2020). The anatomy in shoulder instability. In *360° Around Shoulder Instability*. https://doi.org/10.1007/978-3-662-61074-9_2
- Dickerson, C. R., Hughes, R. E., & Chaffin, D. B. (2008). Experimental evaluation of a computational shoulder musculoskeletal model. *Clinical Biomechanics*, 23(7), 886–894. <https://doi.org/10.1016/j.clinbiomech.2008.04.004>
- Engelhardt, C., Farron, A., Becce, F., Place, N., Pioletti, D. P., & Terrier, A. (2017). Effects of

- glenoid inclination and acromion index on humeral head translation and glenoid articular cartilage strain. *Journal of Shoulder and Elbow Surgery*. <https://doi.org/10.1016/j.jse.2016.05.031>
- Erdemir, A., McLean, S., Herzog, W., & van den Bogert, A. J. (2007). Model-based estimation of muscle forces exerted during movements. *Clinical Biomechanics*. <https://doi.org/10.1016/j.clinbiomech.2006.09.005>
- Farron, A., Terrier, A., & Büchler, P. (2006). Risks of loosening of a prosthetic glenoid implanted in retroversion. *Journal of Shoulder and Elbow Surgery*, 15(4). <https://doi.org/10.1016/j.jse.2005.10.003>
- Favre, P., Gerber, C., & Snedeker, J. G. (2010). Automated muscle wrapping using finite element contact detection. *Journal of Biomechanics*, 43(10). <https://doi.org/10.1016/j.jbiomech.2010.03.018>
- Favre, P., Senteler, M., Hipp, J., Scherrer, S., Gerber, C., & Snedeker, J. G. (2012). An integrated model of active glenohumeral stability. *Journal of Biomechanics*, 45(13). <https://doi.org/10.1016/j.jbiomech.2012.06.010>
- Favre, P., Snedeker, J. G., & Gerber, C. (2009). Numerical modelling of the shoulder for clinical applications. *Philosophical Transactions of the Royal Society A: Mathematical, Physical and Engineering Sciences*. <https://doi.org/10.1098/rsta.2008.0282>
- Felli, L., Biglieni, L., Fiore, M., Coviello, M., Borri, R., & Cutulo, M. (2012). Functional study of glenohumeral ligaments. *Journal of Orthopaedic Science*, 17(5). <https://doi.org/10.1007/s00776-012-0261-5>
- Forster, E., Simon, U., Augat, P., & Claes, L. (2004). Extension of a state-of-the-art optimization criterion to predict co-contraction. *Journal of Biomechanics*, 37(4), 577–581. <https://doi.org/10.1016/j.jbiomech.2003.09.003>
- Fox, T. J., Cil, A., Sperling, J. W., Sanchez-Sotelo, J., Schleck, C. D., & Cofield, R. H. (2009). Survival of the glenoid component in shoulder arthroplasty. *Journal of Shoulder and Elbow Surgery*, 18(6). <https://doi.org/10.1016/j.jse.2008.11.020>
- Franklin, J. L., Barrett, W. P., Jackins, S. E., & Matsen, F. A. (1988). Glenoid loosening in total shoulder arthroplasty. *The Journal of Arthroplasty*, 3(1). [https://doi.org/10.1016/s0883-5403\(88\)80051-2](https://doi.org/10.1016/s0883-5403(88)80051-2)
- Fregly, B. J., Besier, T. F., Lloyd, D. G., Delp, S. L., Banks, S. A., Pandy, M. G., & D'Lima, D. D. (2012). Grand challenge competition to predict in vivo knee loads. *Journal of Orthopaedic Research*. <https://doi.org/10.1002/jor.22023>
- Gao, F., Damsgaard, M., Rasmussen, J., & Tørholm Christensen, S. (2002). Computational

method for muscle-path representation in musculoskeletal models. *Biological Cybernetics*, 87(3). <https://doi.org/10.1007/s00422-002-0326-1>

Garner, B. A., & Pandy, M. G. (2000). The obstacle-set method for representing muscle paths in musculoskeletal models. *Computer Methods in Biomechanics and Biomedical Engineering*, 3(1). <https://doi.org/10.1080/10255840008915251>

Gartsman, G. M., Roddey, T. S., & Hammerman, S. M. (2000). Shoulder arthroplasty with or without resurfacing of the glenoid in patients who have osteoarthritis. *Journal of Bone and Joint Surgery - Series A*, 82(1). <https://doi.org/10.2106/00004623-200001000-00004>

Gerber, C., Snedeker, J. G., Baumgartner, D., & Viehöfer, A. F. (2014). Supraspinatus tendon load during abduction is dependent on the size of the critical shoulder angle: A biomechanical analysis. *Journal of Orthopaedic Research*. <https://doi.org/10.1002/jor.22621>

Habermeyer, P., Magosch, P., Luz, V., & Lichtenberg, S. (2006). Three-dimensional glenoid deformity in patients with osteoarthritis: A radiographic analysis. *Journal of Bone and Joint Surgery - Series A*, 88(6). <https://doi.org/10.2106/JBJS.E.00622>

Habermeyer, Peter, Schuller, U., & Wiedemann, E. (1992). The intra-articular pressure of the shoulder: An experimental study on the role of the glenoid labrum in stabilizing the joint. *Arthroscopy: The Journal of Arthroscopic and Related Surgery*, 8(2). [https://doi.org/10.1016/0749-8063\(92\)90031-6](https://doi.org/10.1016/0749-8063(92)90031-6)

Hawkes, D. H., Khaiyat, O. A., Howard, A. J., Kemp, G. J., & Frostick, S. P. (2019). Patterns of muscle coordination during dynamic glenohumeral joint elevation: An EMG study. *PLoS ONE*, 14(2). <https://doi.org/10.1371/journal.pone.0211800>

Hecker, A., Aguirre, J., Eichenberger, U., Rosner, J., Schubert, M., Sutter, R., ... Bouaicha, S. (2021). Deltoid muscle contribution to shoulder flexion and abduction strength: an experimental approach. *Journal of Shoulder and Elbow Surgery*, 30(2). <https://doi.org/10.1016/j.jse.2020.05.023>

Hicks, J. L., Uchida, T. K., Seth, A., Rajagopal, A., & Delp, S. L. (2015). Is My Model Good Enough? Best Practices for Verification and Validation of Musculoskeletal Models and Simulations of Movement. *Journal of Biomechanical Engineering*. <https://doi.org/10.1115/1.4029304>

Hik, F., & Ackland, D. C. (2019). The moment arms of the muscles spanning the glenohumeral joint: a systematic review. *Journal of Anatomy*, 234(1), 1–15. <https://doi.org/10.1111/joa.12903>

Hill, A. V. (1938). The heat of shortening and the dynamic constants of muscle. *Proceedings of the Royal Society of London. Series B - Biological Sciences*, 126(843), 136–195.

<https://doi.org/10.1098/rspb.1938.0050>

- Hoffmann, M., Begon, M., Lafon, Y., & Duprey, S. (2020). Influence of glenohumeral joint muscle insertion on moment arms using a finite element model. *Computer Methods in Biomechanics and Biomedical Engineering*. <https://doi.org/10.1080/10255842.2020.1789606>
- Hoffmann, Marion, Haering, D., & Begon, M. (2017). Comparison between line and surface mesh models to represent the rotator cuff muscle geometry in musculoskeletal models. *Computer Methods in Biomechanics and Biomedical Engineering*, 20(11), 1175–1181. <https://doi.org/10.1080/10255842.2017.1340463>
- Hölscher, T., Weber, T., Lazarev, I., Englert, C., & Dendorfer, S. (2016). Influence of rotator cuff tears on glenohumeral stability during abduction tasks. *Journal of Orthopaedic Research*, 34(9). <https://doi.org/10.1002/jor.23161>
- Holzbour, K. R. S., Murray, W. M., & Delp, S. L. (2005). A model of the upper extremity for simulating musculoskeletal surgery and analyzing neuromuscular control. *Annals of Biomedical Engineering*, 33(6). <https://doi.org/10.1007/s10439-005-3320-7>
- Hsu, H. C., Luo, Z. P., Cofield, R. H., & An, K. N. (1997). Influence of rotator cuff tearing on glenohumeral stability. *Journal of Shoulder and Elbow Surgery / American Shoulder and Elbow Surgeons ... [et Al.]*, 6(5). [https://doi.org/10.1016/S1058-2746\(97\)70047-8](https://doi.org/10.1016/S1058-2746(97)70047-8)
- Hughes, R. E., Bryant, C. R., Hall, J. M., Wening, J., Huston, L. J., Kuhn, J. E., ... Blasler, R. B. (2003). Glenoid inclination is associated with full-thickness rotator cuff tears. *Clinical Orthopaedics and Related Research*, (407). <https://doi.org/10.1097/00003086-200302000-00016>
- Ibounig, T., Simons, T., Launonen, A., & Paavola, M. (2020). Glenohumeral Osteoarthritis: An Overview of Etiology and Diagnostics. *Scandinavian Journal of Surgery*. <https://doi.org/10.1177/1457496920935018>
- Itoigawa, Y., & Itoi, E. (2016). Anatomy of the capsulolabral complex and rotator interval related to glenohumeral instability. *Knee Surgery, Sports Traumatology, Arthroscopy*. <https://doi.org/10.1007/s00167-015-3892-1>
- Izquierdo, R., Voloshin, I., Edwards, S., Freehill, M. Q., Stanwood, W., Michael Wiater, J., ... Sluka, P. (2010). Treatment of glenohumeral osteoarthritis. *Journal of the American Academy of Orthopaedic Surgeons*, 18(6). <https://doi.org/10.5435/00124635-201006000-00010>
- Jackins, S. E., Barrett, W. P., & Matsen, F. A. (1988). Glenoid loosening in total shoulder arthroplasty: Association with rotator cuff deficiency. *Journal of Arthroplasty*, 3(1). [https://doi.org/10.1016/S0883-5403\(88\)80051-2](https://doi.org/10.1016/S0883-5403(88)80051-2)

- Jensen, E. F., Raunsbæk, J., Lund, J. N., Rahman, T., Rasmussen, J., & Castro, M. N. (2018). Development and simulation of a passive upper extremity orthosis for amyoplasia. *Journal of Rehabilitation and Assistive Technologies Engineering*, 5. <https://doi.org/10.1177/2055668318761525>
- Jensen, R. H., & Davy, D. T. (1975). An investigation of muscle lines of action about the hip: A centroid line approach vs the straight line approach. *Journal of Biomechanics*, 8(2). [https://doi.org/10.1016/0021-9290\(75\)90090-1](https://doi.org/10.1016/0021-9290(75)90090-1)
- Kandemir, U., Allaire, R. B., Jolly, J. T., Debski, R. E., & McMahon, P. J. (2006). The relationship between the orientation of the glenoid and tears of the rotator cuff. *Journal of Bone and Joint Surgery - Series B*, 88(8). <https://doi.org/10.1302/0301-620X.88B8.17732>
- Karabay, D., Yesilyaprak, S. S., & Sahiner Picak, G. (2020). Reliability and validity of eccentric strength measurement of the shoulder abductor muscles using a hand-held dynamometer. *Physical Therapy in Sport*, 43. <https://doi.org/10.1016/j.ptsp.2020.02.002>
- Kelly, B. T., Williams, R. J., Cordasco, F. A., Backus, S. I., Otis, J. C., Weiland, D. E., ... Warren, R. F. (2005). Differential patterns of muscle activation in patients with symptomatic and asymptomatic rotator cuff tears. *Journal of Shoulder and Elbow Surgery*, 14(2). <https://doi.org/10.1016/j.jse.2004.06.010>
- Kobayashi, Y., & Tanaka, K. (2018). Evaluation of a Competition Wheelchair Based on Estimation of Muscle Activity for Forward Linear Operation by Using Inverse Dynamics Analysis. *Proceedings*, 2(6). <https://doi.org/10.3390/proceedings2060259>
- Kuechle, D. K., Newman, S. R., Itoi, E., Morrey, B. F., & An, K. N. (1997). Shoulder muscle moment arms during horizontal flexion and elevation. *Journal of Shoulder and Elbow Surgery / American Shoulder and Elbow Surgeons ... [et Al.]*, 6(5), 429–439. [https://doi.org/10.1016/S1058-2746\(97\)70049-1](https://doi.org/10.1016/S1058-2746(97)70049-1)
- Lee, J. T., Campbell, K. J., Michalski, M. P., Wilson, K. J., Spiegl, U. J. A., Wijdicks, C. A., & Millett, P. J. (2014). Surgical anatomy of the sternoclavicular joint: A qualitative and quantitative anatomical study. *Journal of Bone and Joint Surgery - American Volume*, 96(19). <https://doi.org/10.2106/JBJS.M.01451>
- Li, X., Xu, W., Hu, N., Liang, X., Huang, W., Jiang, D., & Chen, H. (2017). Relationship between acromial morphological variation and subacromial impingement: A three-dimensional analysis. *PLoS ONE*, 12(4). <https://doi.org/10.1371/journal.pone.0176193>
- Lin, M. C., & Otaduy, M. A. (2008). *Haptic rendering: Foundations, algorithms, and applications*. *Haptic Rendering: Foundations, Algorithms, and Applications*.

- Liu, F., Galvin, A., Jin, Z., & Fisher, J. (2011). A new formulation for the prediction of polyethylene wear in artificial hip joints. *Proceedings of the Institution of Mechanical Engineers, Part H: Journal of Engineering in Medicine*, 225(1). <https://doi.org/10.1243/09544119JEIM819>
- Liu, J., Hughes, R., Smutz, W., Niebur, G., & Nan-An, K. (1997). Roles of deltoid and rotator cuff muscles in shoulder elevation. *Clinical Biomechanics*, 12(1), 32–38. [https://doi.org/10.1016/S0268-0033\(96\)00047-2](https://doi.org/10.1016/S0268-0033(96)00047-2)
- Lloyd, J. E., Roewer-Despres, F., & Stavness, I. (2021). Muscle Path Wrapping on Arbitrary Surfaces. *IEEE Transactions on Biomedical Engineering*, 68(2). <https://doi.org/10.1109/TBME.2020.3009922>
- Lo, I. K. Y., Litchfield, R. B., Griffin, S., Faber, K., Patterson, S. D., & Kirkley, A. (2005). Quality-of-life outcome following hemiarthroplasty or total shoulder arthroplasty in patients with osteoarthritis: A prospective, randomized trial. *Journal of Bone and Joint Surgery - Series A*, 87(10). <https://doi.org/10.2106/JBJS.D.02198>
- Lund, M. E., Andersen, M. S., de Zee, M., & Rasmussen, J. (2015). Scaling of musculoskeletal models from static and dynamic trials. *International Biomechanics*, 2(1), 1–11. <https://doi.org/10.1080/23335432.2014.993706>
- Lund, M. E., De Zee, M., Andersen, M. S., & Rasmussen, J. (2012). On validation of multibody musculoskeletal models. In *Proceedings of the Institution of Mechanical Engineers, Part H: Journal of Engineering in Medicine* (Vol. 226). <https://doi.org/10.1177/0954411911431516>
- Lund, M. E., Tørholm, S., Dzialo, C. M., & Jensen, B. K. (2019, April 3). The AnyBody Managed Model Repository (AMMR). <https://doi.org/10.5281/ZENODO.1481635>
- MacDonald, P., McRae, S., Leiter, J., Mascarenhas, R., & Lapner, P. (2011). Arthroscopic rotator cuff repair with and without acromioplasty in the treatment of full-thickness rotator cuff tears: A multicenter, randomized controlled trial. *Journal of Bone and Joint Surgery - Series A*, 93(21). <https://doi.org/10.2106/JBJS.K.00488>
- Manal, K., & Buchanan, T. S. (2004). Subject-specific estimates of tendon slack length: A numerical method. *Journal of Applied Biomechanics*, 20(2). <https://doi.org/10.1123/jab.20.2.195>
- Marra, M. A., Vanheule, V., Fluit, R., Koopman, B. H. F. J. M., Rasmussen, J., Verdonchot, N., & Andersen, M. S. (2015). A Subject-Specific Musculoskeletal Modeling Framework to Predict in Vivo Mechanics of Total Knee Arthroplasty. *Journal of Biomechanical Engineering*, 137(2). <https://doi.org/10.1115/1.4029258>
- Marsden, S. P., Swailes, D. C., & Johnson, G. R. (2008). Algorithms for exact multi-object

muscle wrapping and application to the deltoid muscle wrapping around the humerus. *Proceedings of the Institution of Mechanical Engineers, Part H: Journal of Engineering in Medicine*, 222(7), 1081–1095. <https://doi.org/10.1243/09544119JEIM378>

Marsden, SP. (2010). Muscle wrapping techniques applied to the shoulder. The University of Newcastle Upon Tyne., 1965(November).

Marsden, Stuart. (2010). *Muscle Wrapping Techniques Applied to the Shoulder*. University of Newcastle upon Tyne.

Modenese, L., Ceseracciu, E., Reggiani, M., & Lloyd, D. G. (2016). Estimation of musculotendon parameters for scaled and subject specific musculoskeletal models using an optimization technique. *Journal of Biomechanics*, 49(2). <https://doi.org/10.1016/j.jbiomech.2015.11.006>

Møller, S. P., Brauer, C., Mikkelsen, S., Alkjær, T., Koblauch, H., Pedersen, E. B., ... Thygesen, L. C. (2018). Risk of subacromial shoulder disorder in airport baggage handlers: combining duration and intensity of musculoskeletal shoulder loads. *Ergonomics*, 61(4). <https://doi.org/10.1080/00140139.2017.1382721>

Moor, B. K., Bouaicha, S., Rothenfluh, D. A., Sukthankar, A., & Gerber, C. (2013). Is there an association between the individual anatomy of the scapula and the development of rotator cuff tears or osteoarthritis of the glenohumeral joint? A radiological study of the critical shoulder angle. *Bone and Joint Journal*. <https://doi.org/10.1302/0301-620X.95B7.31028>

Moor, B. K., Kuster, R., Osterhoff, G., Baumgartner, D., Werner, C. M. L., Zumstein, M. A., & Bouaicha, S. (2016). Inclination-dependent changes of the critical shoulder angle significantly influence superior glenohumeral joint stability. *Clinical Biomechanics*. <https://doi.org/10.1016/j.clinbiomech.2015.10.013>

Moor, Beat K., Wieser, K., Slankamenac, K., Gerber, C., & Bouaicha, S. (2014). Relationship of individual scapular anatomy and degenerative rotator cuff tears. *Journal of Shoulder and Elbow Surgery*, 23(4). <https://doi.org/10.1016/j.jse.2013.11.008>

Morgan, S. J., Furry, K., Parekh, A. A., Agudelo, J. F., & Smith, W. R. (2006). The deltoid muscle: An anatomic description of the deltoid insertion to the proximal humerus. *Journal of Orthopaedic Trauma*, 20(1). <https://doi.org/10.1097/01.bot.0000187063.43267.18>

Morrow, D. A., Haut Donahue, T. L., Odegard, G. M., & Kaufman, K. R. (2010). Transversely isotropic tensile material properties of skeletal muscle tissue. *Journal of the Mechanical Behavior of Biomedical Materials*, 3(1), 124–129. <https://doi.org/10.1016/j.jmbbm.2009.03.004>

Mutsvangwa, T., Burdin, V., Schwartz, C., & Roux, C. (2015). An Automated Statistical Shape

- Model Developmental Pipeline: Application to the Human Scapula and Humerus. *IEEE Transactions on Biomedical Engineering*, 62(4). <https://doi.org/10.1109/TBME.2014.2368362>
- Neer, C. S. (1972). Anterior acromioplasty for the chronic impingement syndrome in the shoulder: a preliminary report. *The Journal of Bone and Joint Surgery. American Volume*, 54(1). <https://doi.org/10.2106/00004623-197254010-00003>
- Nicholson, G. P., Goodman, D. A., Flatow, E. L., & Bigliani, L. U. (1996). The acromion: morphologic condition and age-related changes. A study of 420 scapulas. *Journal of Shoulder and Elbow Surgery / American Shoulder and Elbow Surgeons ... [et Al.]*, 5(1). [https://doi.org/10.1016/S1058-2746\(96\)80024-3](https://doi.org/10.1016/S1058-2746(96)80024-3)
- Nyffeler, R. W., & Meyer, D. C. (2017). Acromion and glenoid shape: Why are they important predictive factors for the future of our shoulders? *EFORT Open Reviews*. <https://doi.org/10.1302/2058-5241.2.160076>
- Nyffeler, R. W., Werner, C. M. L., Sukthankar, A., Schmid, M. R., & Gerber, C. (2006a). Association of a large lateral extension of the acromion with rotator cuff tears. *Journal of Bone and Joint Surgery - Series A*. <https://doi.org/10.2106/JBJS.D.03042>
- Nyffeler, R. W., Werner, C. M. L., Sukthankar, A., Schmid, M. R., & Gerber, C. (2006b). Association of a large lateral extension of the acromion with rotator cuff tears. *Journal of Bone and Joint Surgery - Series A*, 88(4). <https://doi.org/10.2106/JBJS.D.03042>
- Ohlsson, M. L., Danvind, J., & Joakim Holmberg, L. (2018). Shoulder and lower back joint reaction forces in seated double poling. *Journal of Applied Biomechanics*, 34(5). <https://doi.org/10.1123/jab.2017-0281>
- Orfaly, R. M., Rockwood, C. A., Esenyel, C. Z., & Wirth, M. A. (2003). A prospective functional outcome study of shoulder arthroplasty for osteoarthritis with an intact rotator cuff. *Journal of Shoulder and Elbow Surgery*, 12(3). [https://doi.org/10.1016/S1058-2746\(02\)86882-3](https://doi.org/10.1016/S1058-2746(02)86882-3)
- Pandey, V., & Jaap Willems, W. (2015). Rotator cuff tear: A detailed update. *Asia-Pacific Journal of Sports Medicine, Arthroscopy, Rehabilitation and Technology*. <https://doi.org/10.1016/j.asmart.2014.11.003>
- Pandy, M. G. (1999). Moment arm of a muscle force. *Exercise and Sport Sciences Reviews*, 27.
- Paraskevas, G., Tzaveas, A., Papaziogas, B., Kitsoulis, P., Natsis, K., & Spanidou, S. (2008). Morphological parameters of the acromion. *Folia Morphologica*, 67(4).
- Poppen, N. K., & Walker, P. S. (1978). Forces at the glenohumeral joint in abduction. *Clinical*

Orthopaedics and Related Research. <https://doi.org/10.1097/00003086-197809000-00035>

Pouliart, N., & Gagey, O. (2006). The effect of isolated labrum resection on shoulder stability. *Knee Surgery, Sports Traumatology, Arthroscopy*, 14(3). <https://doi.org/10.1007/s00167-005-0666-1>

Quental, C., Folgado, J., Ambrósio, J., & Monteiro, J. (2016). A new shoulder model with a biologically inspired glenohumeral joint. *Medical Engineering and Physics*, 38(9), 969–977. <https://doi.org/10.1016/j.medengphy.2016.06.012>

Quental, Carlos, Folgado, J., Ambrósio, J., & Monteiro, J. (2015a). Critical analysis of musculoskeletal modelling complexity in multibody biomechanical models of the upper limb. *Computer Methods in Biomechanics and Biomedical Engineering*, 18(7), 749–759. <https://doi.org/10.1080/10255842.2013.845879>

Quental, Carlos, Folgado, J., Ambrósio, J., & Monteiro, J. (2015b). Critical analysis of musculoskeletal modelling complexity in multibody biomechanical models of the upper limb. *Computer Methods in Biomechanics and Biomedical Engineering*, 18(7), 749–759. <https://doi.org/10.1080/10255842.2013.845879>

Rahme, H., Mattsson, P., & Larsson, S. (2004). Stability of cemented all-polyethylene keeled glenoid components. A radiostereometric study with a two-year follow-up. *Journal of Bone and Joint Surgery - Series B*, 86(6). <https://doi.org/10.1302/0301-620X.86B6.14882>

Reddy, A. S., Mohr, K. J., Pink, M. M., & Jobe, F. W. (2000). Electromyographic analysis of the deltoid and rotator cuff muscles in persons with subacromial impingement. *Journal of Shoulder and Elbow Surgery*, 9(6), 519–523. <https://doi.org/10.1067/mse.2000.109410>

Reinold, M. M., Macrina, L. C., Wilk, K. E., Fleisig, G. S., Dun, S., Barrentine, S. W., ... Andrews, J. R. (2007). Electromyographic analysis of the supraspinatus and deltoid muscles during 3 common rehabilitation exercises. *Journal of Athletic Training*, 42(4). [https://doi.org/10.1016/s0162-0908\(08\)79368-1](https://doi.org/10.1016/s0162-0908(08)79368-1)

Rispoli, D. M., Athwal, G. S., Sperling, J. W., & Cofield, R. H. (2009). The anatomy of the deltoid insertion. *Journal of Shoulder and Elbow Surgery*, 18(3). <https://doi.org/10.1016/j.jse.2008.10.012>

Rugg, C. M., Hettrich, C. M., Ortiz, S., Wolf, B. R., Baumgarten, K. M., Bishop, J. Y., ... Zhang, A. L. (2018). Surgical stabilization for first-time shoulder dislocators: a multicenter analysis. *Journal of Shoulder and Elbow Surgery*, 27(4). <https://doi.org/10.1016/j.jse.2017.10.041>

Sakoma, Y., Sano, H., Shinozaki, N., Itoigawa, Y., Yamamoto, N., Ozaki, T., & Itoi, E. (2011). Anatomical and functional segments of the deltoid muscle. *Journal of Anatomy*, 218(2).

<https://doi.org/10.1111/j.1469-7580.2010.01325.x>

- Sanchez-Sotelo, J., Cofield, R. H., & Rowland, C. M. (2001). Shoulder hemiarthroplasty for glenohumeral arthritis associated with severe rotator cuff deficiency. *Journal of Bone and Joint Surgery - Series A*, 83(12), 1814–1822. <https://doi.org/10.2106/00004623-200112000-00008>
- Sankaranarayanan, S., Saks, B. R., Holtzman, A. J., Tabeayo, E., Cuomo, F., & Gruson, K. I. (2020). The critical shoulder angle (CSA) in glenohumeral osteoarthritis: Does observer experience affect measurement reliability on plain radiographs? *Journal of Orthopaedics*, 22. <https://doi.org/10.1016/j.jor.2020.04.004>
- Scholz, A., Sherman, M., Stavness, I., Delp, S., & Kecskeméthy, A. (2016). A fast multi-obstacle muscle wrapping method using natural geodesic variations. *Multibody System Dynamics*, 36(2), 195–219. <https://doi.org/10.1007/s11044-015-9451-1>
- Schrumpf, M., Maak, T., Hammoud, S., & Craig, E. V. (2011). The glenoid in total shoulder arthroplasty. *Current Reviews in Musculoskeletal Medicine*, 4(4). <https://doi.org/10.1007/s12178-011-9096-5>
- Schultz, A. B., Faulkner, J. A., & Kadhiresan, V. A. (1991). A simple Hill element-nonlinear spring model of muscle contraction biomechanics. *Journal of Applied Physiology*, 70(2). <https://doi.org/10.1152/jappl.1991.70.2.803>
- Schwartz, D. G., Kang, S. H., Lynch, T. S., Edwards, S., Nuber, G., Zhang, L. Q., & Saltzman, M. (2013). The anterior deltoid's importance in reverse shoulder arthroplasty: A cadaveric biomechanical study. *Journal of Shoulder and Elbow Surgery*. <https://doi.org/10.1016/j.jse.2012.02.002>
- Shah, N. N., Bayliss, N. C., & Malcolm, A. (2001). Shape of the acromion: Congenital or acquired - A macroscopic, radiographic, and microscopic study of acromion. *Journal of Shoulder and Elbow Surgery*, 10(4). <https://doi.org/10.1067/mse.2001.114681>
- Silva, M. P. T., & Ambrósio, J. A. C. (2002). Kinematic data consistency in the inverse dynamic analysis of biomechanical systems. *Multibody System Dynamics*, 8(2). <https://doi.org/10.1023/A:1019545530737>
- Sins, L., Tétreault, P., Hagemester, N., & Nuño, N. (2015). Adaptation of the AnyBody™ Musculoskeletal Shoulder Model to the Nonconforming Total Shoulder Arthroplasty Context. *Journal of Biomechanical Engineering*, 137(10), 101006. <https://doi.org/10.1115/1.4031330>
- Sins, L., Tétreault, P., Nuño, N., & Hagemester, N. (2016). Effects of Prosthetic Mismatch and Subscapularis Tear on Glenohumeral Contact Patterns in Total Shoulder Arthroplasty: A Numerical Musculoskeletal Analysis. *Journal of Biomechanical*

Engineering, 138(12). <https://doi.org/10.1115/1.4034654>

Terrier, A., Reist, A., & Nyffeler, R. W. (2006). Influence of the shape of the acromion on joint reaction force and humeral head translation during abduction in the scapular plane. *Journal of Biomechanics*. [https://doi.org/10.1016/s0021-9290\(06\)83218-5](https://doi.org/10.1016/s0021-9290(06)83218-5)

Terrier, Alexandre, Vogel, A., Capezzali, M., & Farron, A. (2008). An algorithm to allow humerus translation in the indeterminate problem of shoulder abduction. *Medical Engineering and Physics*, 30(6). <https://doi.org/10.1016/j.medengphy.2007.07.011>

Torchia, M. E., Cofield, R. H., & Settegren, C. R. (1997). Total shoulder arthroplasty with the Neer prosthesis: Long-term results. *Journal of Shoulder and Elbow Surgery*, 6(6). [https://doi.org/10.1016/S1058-2746\(97\)90081-1](https://doi.org/10.1016/S1058-2746(97)90081-1)

Torpey, B. M., Ikeda, K., Wang, M., van der Heeden, D., Chao, E. Y. S., & McFarland, E. G. (1998). The Deltoid Muscle Origin. *The American Journal of Sports Medicine*, 26(3). <https://doi.org/10.1177/03635465980260030601>

Townsend, H., Jobe, F. W., Pink, M., & Perry, J. (1991). Electromyographic analysis of the glenohumeral muscles during a baseball rehabilitation program. *The American Journal of Sports Medicine*, 19(3), 264–272. <https://doi.org/10.1177/036354659101900309>

Tsuang, Y. H., Novak, G. J., Schipplein, O. D., Hafezi, A., Trafimow, J. H., & Andersson, G. B. J. (1993). Trunk muscle geometry and centroid location when twisting. *Journal of Biomechanics*, 26(4–5). [https://doi.org/10.1016/0021-9290\(93\)90015-7](https://doi.org/10.1016/0021-9290(93)90015-7)

Turkel, S. J., Panio, M. W., Marshall, J. L., & Girgis, F. G. (1981). Stabilizing mechanisms preventing anterior dislocation of the glenohumeral joint. *Journal of Bone and Joint Surgery - Series A*, 63(8). <https://doi.org/10.2106/00004623-198163080-00002>

van der Helm, F. C. T. (1994a). A finite element musculoskeletal model of the shoulder mechanism. *Journal of Biomechanics*, 27(5), 551–569. [https://doi.org/10.1016/0021-9290\(94\)90065-5](https://doi.org/10.1016/0021-9290(94)90065-5)

van der Helm, F. C. T. (1994b). Analysis of the kinematic and dynamic behavior of the shoulder mechanism. *Journal of Biomechanics*, 27(5). [https://doi.org/10.1016/0021-9290\(94\)90064-7](https://doi.org/10.1016/0021-9290(94)90064-7)

Van der Helm, F. C. T., Veeger, H. E. J., Pronk, G. M., Van der Woude, L. H. V., & Rozendal, R. H. (1992). Geometry parameters for musculoskeletal modelling of the shoulder system. *Journal of Biomechanics*, 25(2), 129–144. [https://doi.org/10.1016/0021-9290\(92\)90270-B](https://doi.org/10.1016/0021-9290(92)90270-B)

Viehöfer, A. F., Gerber, C., Favre, P., Bachmann, E., & Snedeker, J. G. (2016). A larger critical shoulder angle requires more rotator cuff activity to preserve joint stability. *Journal of*

Orthopaedic Research, 34(6). <https://doi.org/10.1002/jor.23104>

- Viehöfer, A. F., Snedeker, J. G., Baumgartner, D., & Gerber, C. (2016). Glenohumeral joint reaction forces increase with critical shoulder angles representative of osteoarthritis - A biomechanical analysis. *Journal of Orthopaedic Research*, 34(6). <https://doi.org/10.1002/jor.23122>
- Villatte, G., van der Kruk, E., Bhuta, A. I., Zumstein, M. A., Moor, B. K., Emery, R. J. H., ... Reilly, P. (2020). A biomechanical confirmation of the relationship between critical shoulder angle (CSA) and articular joint loading. *Journal of Shoulder and Elbow Surgery*, 29(10). <https://doi.org/10.1016/j.jse.2020.03.002>
- Waite, D. L., Brookham, R. L., & Dickerson, C. R. (2010). On the suitability of using surface electrode placements to estimate muscle activity of the rotator cuff as recorded by intramuscular electrodes. *Journal of Electromyography and Kinesiology*, 20(5). <https://doi.org/10.1016/j.jelekin.2009.10.003>
- Walch, G., Edwards, T. B., Boulahia, A., Boileau, P., Molé, D., & Adeleine, P. (2002). The influence of glenohumeral prosthetic mismatch on glenoid radiolucent lines: Results of a multicenter study. *Journal of Bone and Joint Surgery - Series A*, 84(12). <https://doi.org/10.2106/00004623-200212000-00010>
- Walker, D. R., Struk, A. M., Matsuki, K., Wright, T. W., & Banks, S. A. (2016). How do deltoid muscle moment arms change after reverse total shoulder arthroplasty? *Journal of Shoulder and Elbow Surgery*. <https://doi.org/10.1016/j.jse.2015.09.015>
- Watling, J. P., Sanchez, J. E., Heilbroner, S. P., Levine, W. N., Bigliani, L. U., & Jobin, C. M. (2018). Glenoid component loosening associated with increased critical shoulder angle at midterm follow-up. *Journal of Shoulder and Elbow Surgery*, 27(3). <https://doi.org/10.1016/j.jse.2017.10.002>
- Watson, M. (1978). The refractory painful arc syndrome. *Journal of Bone and Joint Surgery - Series B*, 60 B(4). <https://doi.org/10.1302/0301-620x.60b4.711806>
- Webb, J., Blemker, S., & Delp, S. (2014). 3D finite element models of shoulder muscles for computing lines of actions and moment arms. *Computer Methods in Biomechanics and Biomedical Engineering*. Taylor & Francis. <https://doi.org/10.1080/10255842.2012.719605>
- Weinstein, D. M., Bucchieri, J. S., Pollock, R. G., Flatow, E. L., & Bigliani, L. U. (2000). Arthroscopic debridement of the shoulder for osteoarthritis. *Arthroscopy*, 16(5). <https://doi.org/10.1053/jars.2000.5042>
- Winby, C. R., Lloyd, D. G., & Kirk, T. B. (2008). Evaluation of different analytical methods for subject-specific scaling of musculotendon parameters. *Journal of Biomechanics*,

41(8). <https://doi.org/10.1016/j.jbiomech.2008.03.008>

Wirth, M. A., & Rockwood, C. A. (1996). Complications of total shoulder-replacement arthroplasty. *Journal of Bone and Joint Surgery - Series A*. <https://doi.org/10.2106/00004623-199604000-00018>

Wong, M., & Kiel, J. (2018). *Anatomy, Shoulder and Upper Limb, Acromioclavicular Joint. StatPearls*.

Yamamoto, N., Itoi, E., Tuoheti, Y., Seki, N., Abe, H., Minagawa, H., ... Okada, K. (2006). The effect of the inferior capsular shift on shoulder intra-articular pressure: A cadaveric study. *American Journal of Sports Medicine*, 34(6). <https://doi.org/10.1177/0363546505283834>

Yang, J. (James), Feng, X., Xiang, Y., Kim, J. H., & Rajulu, S. (2009). Determining the three-dimensional relation between the skeletal elements of the human shoulder complex. *Journal of Biomechanics*, 42(11). <https://doi.org/10.1016/j.jbiomech.2009.04.048>

Yelin, E., Weinstein, S., & King, T. (2016). The burden of musculoskeletal diseases in the United States. *Seminars in Arthritis and Rheumatism*. <https://doi.org/10.1016/j.semarthrit.2016.07.013>

Zajac, F. E. (1989). Muscle and tendon: properties, models, scaling, and application to biomechanics and motor control. *Critical Reviews in Biomedical Engineering*.

Zheng, M., Zou, Z., Bartolo, P. jorge D. silva, Peach, C., & Ren, L. (2017). Finite element models of the human shoulder complex: a review of their clinical implications and modelling techniques. *International Journal for Numerical Methods in Biomedical Engineering*, 33(2). <https://doi.org/10.1002/cnm.2777>

